ENVIRONMENTAL GAS ANALYSIS OF FLUID INCLUSIONS IN CALCIUM CARBONATES FROM NEW MEXICO INCLUDING VEIN CALCITES FROM LOS ALAMOS NATIONAL LABORATORY, USING QUADRUPOLE MASS SPECTROMETER

By

Madhukar Gundimeda

Submitted in Partial Fulfillment of the
Requirement for the Degree of Master of Science
in Geochemistry

New Mexico Institute of Mining and Technology
Socorro, New Mexico
May 4, 1995

ABSTRACT

Our principal objective of this study is to determine the genesis of the carbonate fracture fillings present at shallow depths at Los Alamos National Laboratory (LANL) and at other hazardous and environmentally sensitive waste sites. To determine the genesis of the carbonate fracture fillings we analyzed volatiles included within the 100 samples of non-marine calcites including pedogenic calcites (non-indurated and indurated), ancient travertines, travertines deposited by active springs, calcretes, calcite concretions in sand, and hydrothermal vein calcites. We also analyzed 29 vein calcite samples from fracture fillings in tuffs at LANL and 3 travertine samples from Nevada Test Site (NTS). Volatile species in fluid inclusions contained within these minerals were measured by means of a Balzers Q.M.420 quadrupole mass spectrometer. Volatiles within the fluid inclusions were released by the thermally decrepitation and mechanical crushing of the fluid inclusions within different carbonates. The principal gaseous species measured during thermal decrepitation of the fluid inclusions were H_2, He, CO, CH_4, H_2O, Ne, N_2, O_2, Ar, CO_2 and the lower chain hydrocarbons (C_{2-6}). The gaseous species analyzed by mechanical crushing were He, CH_4, H_2O, N_2, O_2, Ar and CO_2. The analyses of split samples by the two methods are different; analyses of thermally decrepitated carbonates indicate greater amounts of CO_2, N_2 and H_2. Carbon-dioxide, N_2 and H_2 are

products of pyrolysis of organic material; hence, analyses by thermal decrepitation were not considered in the interpretation of the results.

Results from crushing indicate that the volatiles in the carbonates can be used to distinguish calcium carbonate formed in the vadose zone from the calcium carbonate deposited ground water. Cluster analysis separated the 126 analyses into two groups based on the H_2O content. The mean concentration of H_2O in group I and group II carbonates are 97.5% and 48.7%. The principal volatile present in the analysis of group II carbonates was CH_4. We used ternary diagrams to distinguish group II carbonates from group I carbonates. Ternary diagrams such as $100Ar\text{-}CH_4\text{-}CO_2$, $0.01H_2O\text{-}CH_4\text{+}CO_2\text{-}N_2$, $0.01H_2O\text{-}CH_4\text{-}CO_2$ and $0.001H_2O\text{-}CH_4\text{-}100He$ show clear separation of group II carbonates from group I carbonates. LANL vein calcites yielded analyses similar to group II carbonates indicating a similar genesis. The CH_4-rich vapor in group II carbonates suggests formation in a O_2 depleted (micro-reducing) environment.

TABLE OF CONTENTS

LIST OF FIGURES

LIST OF TABLES

LIST OF FIGURES IN APPENDICES

LIST OF TABLES IN APPENDICES

ACKNOWLEDGEMENTS

I would like to thank the members of my thesis committee David I. Norman, Peter S. Mozley, Bruce Harrison, Thomas J. Kieft and John W. Hawley, for their helpful advice, guidance and critical review of this thesis. I found a mentor and friend in each of them. Many thanks are due to my advisor, David Norman, for writing the proposal for the project, proposing the research problem, and providing support during this project. Also, I sincerely thank David Norman, who took me under his wing and introduced me to the concept of the gas analysis of fluid inclusions using quadrupole mass spectrometry. I also thank the many colleagues and friends who shared their knowledge of geochemistry with me: Philip Kyle, Andrew Campbell, Robert Bowman, Ingar Walder, William Chavez, Grazna Zreda, Kurt Panter, and Brent Newman. I also thank Schon Levy of Los Alamos National Laboratory and Chris Wilkowske for sample collection. Also, I thank John Groff, Pat Mills and Renitha Mazumdar for undertaking the painful task of going through my thesis for technical and grammatical errors.

I appreciate generous support from the Waste-Management Educational and Research Consortium (WERC) for partly supporting my study at New Mexico Tech. Also, I acknowledge the help provided by the department secretaries, Pat Mills, Connie Apache and Nancy Weiss during my stay at New

Mexico Tech. Ofcourse, how can I forget the love, affection and warm hospitality shown by the Mishra family, Sony (Pranathi), Anil and Harsha.

A final note of thanks to those special people without whom this thesis would not have been completed. The love and affection shown by Sandhya, Ramana, Ravi, Anu and Sagar cannot be measured. Lastly, I graciously thank my parents for their unending support throughout my entire academic career, and I dedicate this thesis to them.

INTRODUCTION

Ground waters, geothermal waters, and pedogenic processes deposit calcium carbonate. In environmentally sensitive areas, such as the Los Alamos National Laboratory (LANL) and the Nevada Test Site (NTS), calcium carbonate occurs in fracture fillings (Fisher, 1986; Syzmanski, 1989). This suggests the possibility of future ground water flow in those areas unless there is strong evidence that the calcium carbonate has formed in the vadose zone. This has prompted study of carbonate mineralization to find a means of determining the genesis of the fracture fillings. Research into the genesis of vein calcites formed at shallow depths has used trace-element geochemistry, stable and radiogenic isotopic studies, and/or petrographic methods. These approaches have not, however, clearly differentiated carbonates deposited in the phreatic zone versus carbonates deposited in the vadose zone (Winograd and Doty, 1980; Butler, 1985; Warner et al., 1986).

As part of this thesis, a geochemical method for determining the depositional environments of calcium carbonate were developed. Trapping of the volatile species takes place in fluid inclusions within a precipitating carbonate mineral during its formation. Analysis of inclusion volatiles may indicate the depositional environment. To test this hypothesis, trapped volatiles in inclusions within various carbonates were analyzed. Samples of different

calcium carbonates formed near surface or at depth were collected and analyzed. Gas analysis was done using quadrupole mass spectrometry. Cleaned samples were split and included gases were extracted by mechanical crushing and by thermal decrepitation methods to determine the more appropriate method of measurement. Different samples such as pedogenic calcites (non-indurated and indurated), calcretes, calcite concretions in sand, hydrothermal vein calcites, ancient travertines and travertines being deposited by active spring were analyzed. Thirty-two vein calcites from tuffs and fracture fillings from LANL trenches and travertines from NTS were also analyzed.

GASES CONTAINED WITHIN MINERALS

During the precipitation of minerals, fluid inclusions develop as parent fluid is trapped in minute amounts. Fracturing of the host mineral may create multiple generations of fluid inclusions. Thus, we may deduce from the chemistry of different generations of fluid inclusions the history of a mineral. The fluid chemistry and the pressure-temperature conditions during the trapping of fluid inclusions may be determined from micro-thermometric measurements, (Roedder, 1984). We can determine from the analyses of gases in these fluid inclusions the partial pressure of the gases and their fugacities. From the partial pressure and fugacities of the gases, we calculate the depth of trapping of the fluid inclusions (Roedder, 1984).

Fluid inclusions may range in size from sub-micron to those that are visible to the naked eye (Roedder, 1984). Primary fluid inclusions contain material trapped during crystallization. These fluid inclusions may contain trapped liquid, vapor and solid phases. Solid phases may be accidentally trapped or may be daughter minerals precipitated from the trapped fluids. Two-phase inclusions with trapped liquid and vapor phases are more common. We can extract volatile species contained in fluid inclusions by bulk analyses using the quadrupole mass spectrometer (Norman and Sawkins, 1987). If we heat the host mineral to a temperature equivalent to the trapping temperature then the gas analyses are most representative of the environment of formation (Norman et al., 1991).

Secondary fluid inclusions are liquid and vapor trapped within minerals after formation of the host mineral. These may result from fracturing of the host mineral. Because the grain size is too small to observe any fluid inclusions in pedogenic calcite (non-indurated and indurated), calcrete or travertine, it is not known whether secondary inclusions exist or not. Fluid inclusions may occur, however, in overgrowths and coatings that formed much later than the original carbonate mineral. Because we analyzed samples in bulk in the quadrupole mass spectrometer, we do not know whether the volatiles released included gases from secondary fluid inclusions and inclusions contained in overgrowths.

Shallow ground water and geothermal water dissolve gaseous species mostly in the range of 1 to 2 % (Heneley et al., 1984). At the time of infiltration, air saturates meteoric water. Air has a composition of 78.09 mole % N_2, 20.95 mole % O_2, 0.93 mole % Ar, 350 ppm v/v CO_2, 18 ppm v/v Ne, 14 ppm v/v CH_4 and 5.24 ppm v/v He (Rose et al., 1979). As air saturated meteoric waters descend and interact with the bedrock, the concentrations of Ar, Ne and N_2 do not change appreciably (Mazor and Bosch, 1987). Additions of CO_2, CH_4 and H_2S can alter the composition of the subsurface waters by decreasing the amount of dissolved O_2 (Rose, 1987). Eventually, CO_2 accumulates as O_2 decreases (Rose, 1987). Similarly, radiogenic He can accumulate in ground water due to the radioactive decay of U and Th in the crust and result in fluids that have high concentrations of He (Balderer and Lehmann, 1989; Heaton, 1984; Mazor and Bosch, 1987). Literature shows that using the radiogenic He contained within these fluids, we can date ground waters and geothermal waters (Elliot, 1990; Marrin, 1987; Mazor, 1975; Mazor, 1988; Stute et al., 1992). We can illustrate changes in the gas composition of meteoric waters that reside in the crust and interact with rocks with ternary diagrams. The shaded region in **Figure 1** indicates the gaseous composition of meteoric water and changes in the gaseous composition as meteoric water resides in the crust and exchanges volatiles with the host rocks. On ternary diagrams, stars represent air and air-saturated water (ASW).

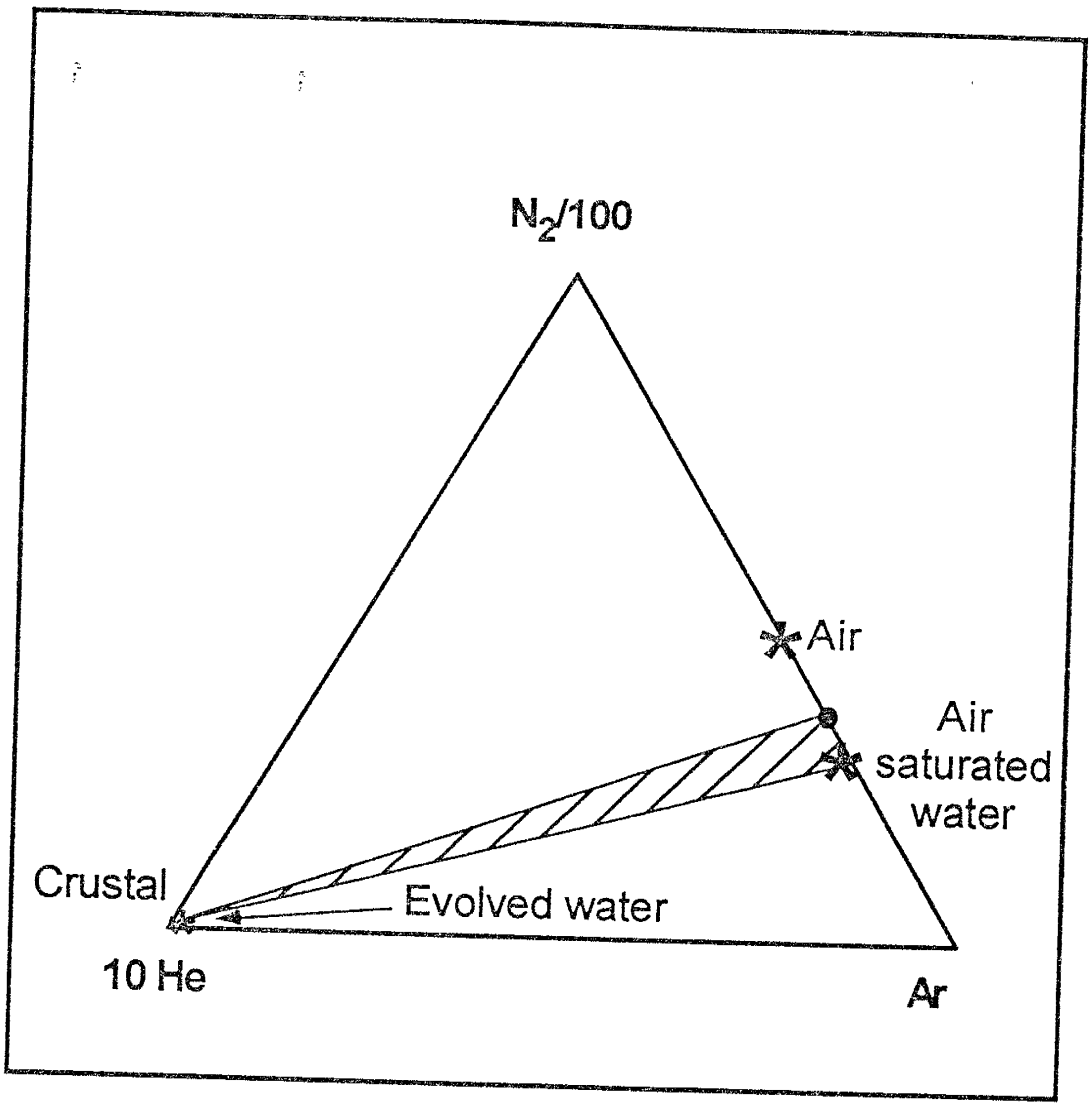

FIGURE 1: A N_2-He-Ar diagram after Norman and Musgrave (1994). The shaded area illustrates the region occupied by ground water. Air and air saturated water (star symbols) have little He. With time, groundwater accumulates radiogenic He from crustal rocks and the composition moves towards the He apex, whereas N_2 and Ar are conserved.

MATERIALS and METHODS

Gas analyses of fluid inclusions yield quantitative and qualitative information about the different volatiles dissolved in the fluid at the time of trapping. In the following section we discuss sample preparation, experimental setup, different analytical techniques used in gas analysis, analytical problems, and data processing.

SAMPLE PREPARATION

We prepared samples in the following manner for conducting analysis by heating or by mechanical crushing:

1) We crushed the samples to mesh size -10 to +40.
2) We washed the sample with water until we removed all dirt, organic matter and twigs.
3) We warmed the sample in a solution of 10% sodium hydroxide (NaOH) for 2 to 3 hours to remove any adsorbed oils and later rinsed it with distilled water.
4) We reacted the sample with a 10% hydrochloric acid (HCl) solution.
5) We boiled the sample in distilled water for 3 to 4 hours.
6) We baked the sample in an oven at 80 °C, overnight, and
7) We wrapped the cooled sample in an aluminum foil to prevent exposure of the cleaned sample to atmospheric moisture.

We modified the sample preparation because we analyzed carbonate minerals with different physical morphologies. In the case of hydrothermal vein calcites, calcretes, active and ancient travertines, we prepared the samples according to the procedure outlined above.

In the case of pedogenic calcite (non-indurated and indurated), calcite concretions in sand, travertines from Riley and fracture-filled vein calcites from Los Alamos National Laboratory, we omitted the intermediate stages of warming with a 10% NaOH, reacting with a 10% HCl, boiling in ultrapure demineralized water, and drying in oven. Nonetheless, we sieved these samples to remove fine dust and visible organic material before sealing in air-tight containers. In case of samples of basalts from White Rock, first we crushed the samples and then we scrapped off the coatings of pedogenic calcites (non-indurated) on the pieces of basalts.

EXPERIMENTAL SETUP

Gas analyses were performed on a Balzers Q.M.420 quadrupole mass spectrometer housed at New Mexico Tech. The quadrupole mass spectrometer we used is preferred over other mass spectrometers because of its fast scanning capability and high sensitivity. Through the computer we monitored the quadrupole mass spectrometer. Samples were heated and/or mechanically crushed to release gases contained in fluid inclusions (Musgrave and Norman, 1995).

Analysis by Thermal Decrepitation

Figure 2 schematically shows the essential components of the gas extraction line. We analyzed mixtures of gases contained in fluid inclusions, quantitatively, using a quadrupole mass spectrometer and a high-vacuum extraction line. The metal surfaces in the extraction line are kept to a minimum to prevent surface reactions with released volatiles such as the sulfur species. The experimental setup for analysis of a sample in the quadrupole mass spectrometer by thermal decrepitation involve the following components: (1) an extraction line made of Pyrex glass tubing with glass-body bellow-seal-type intervening valves, (2) a quartz oven to heat the sample to temperatures appropriate to decrepitate fluid inclusions, (3) a capacitance manometer to

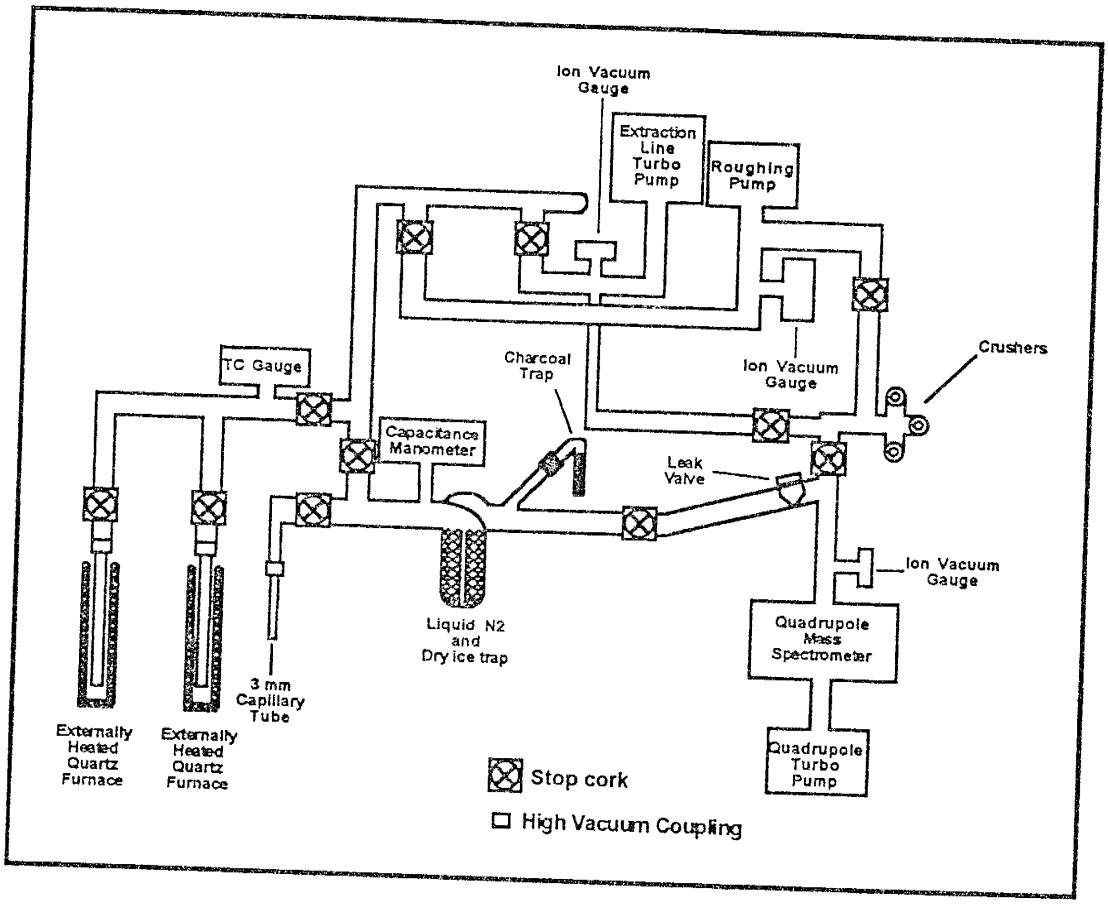

FIGURE 2: Schematic diagram of the quadrupole gas analysis facility at New Mexico Tech. The vacuum extraction line is constructed of Pyrex glass to minimize gas adsorption. The stopcorks are all of the bellow seal type and pressures as low as 10^{-8} mbars can be attained.

measure the pressure of the volatile species in the extraction line, (4) a leak valve in the extraction line, made of sapphire, to regulate the volatile gases into the quadrupole mass spectrometer, and (5) two turbo vacuum pumps to pump away gases during the degassing of the sample and after analyzing the sample.

Gas analysis by thermal decrepitation involved decrepitation of fluid inclusions by heating, followed by cryogenic separation of the released gases into non-condensable, condensable, and water fractions (Norman and Sawkins, 1987). Gases that do not condense below the temperature of liquid N_2 (that is -196 °C) represents the non-condensable gases. The non-condensable gas fraction consists of hydrogen (H_2), helium (He), carbon-monoxide (CO), methane (CH_4), neon (Ne), nitrogen (N_2), oxygen (O_2), and argon (Ar). The condensable gas fraction consists of carbon-dioxide (CO_2), hydrogen sulfide (H_2S), sulfur-dioxide (SO_2), and the lower chain hydrocarbons (C_{1-6}). We separated the condensable gas fraction from the water vapor fraction using a dry ice-alcohol trap at a temperature of -78 °C. We analyzed each gas fraction discussed above and measured each gas fraction separately in the quadrupole mass spectrometer using the scan-bargraph mode. We converted volatiles in each gaseous fraction into mole percentages for individual gas species (Musgrave and Norman, 1995; and Ruff, 1993).

Analysis by Mechanical Crushing

Analysis of a sample by mechanical crushing involves the following procedures: (1) heating the sample under vacuum to degas the sample, (2) selecting specific gaseous species to be analyzed by the quadrupole mass spectrometer operating in a mid-intensity diagram mode, (3) crushing the sample mechanically to release gases, contained in fluid inclusions, directly into the quadrupole mass spectrometer, and (4) modifying the parameters in the mid-intensity diagram mode and measuring only those gases during crushing (Norman and Sawkins, 1987; and Ruff, 1993).

During the analysis by crushing we analyzed collectively the non-condensable, the condensable, and the water fractions. The gaseous species released during mechanical crushing of fluid inclusions contained in different carbonate minerals include helium (He), methane (CH_4), water (H_2O), nitrogen (N_2), oxygen (O_2), argon (Ar), and carbon-dioxide (CO_2). We analyzed NH_3 in travertine inclusions deposited by active springs (Norman et al., 1994). We detected NH_3 in only one travertine sample actively deposited by spring. We did not analyze NH_3 in other carbonate minerals because the water peaks obscured the NH_3 mass peaks.

ANALYTICAL PROCEDURE

The basic procedure of analyzing inclusions by heating and crushing is discussed in detail by Musgrave (1992); Norman and Musgrave (1995); Norman and Sawkins (1986). **Figure 3** shows an analysis of a sample that has undergone thermal decrepitation. **Figure 3(a)** shows the spectra given by non-condensable volatiles analyzed between mass 1 to 50, while **Figure 3(b)** shows the spectra given by condensable volatiles analyzed between mass 10 to 100.

For crushing, we loaded a small lump of a cleaned and dried sample, say 0.5 to 1.0 grams, into the crushers. We degassed all adsorbed gases by heating the sample to 100 °C while under high vacuum. Once the optimum pressure in the crushers reaches 10^{-7} mbar, we stop pumping and opened the sample to the mass spectrometer. During the analysis, we crushed the sample repeatedly to obtain multiple analysis. We removed trapped air within the micro-fractures in the sample by first crushing the sample in high vacuum. We performed blank crushes by crushing a chip of quartz rod to check whether we released any gases during the crushing process. The amount of gases evolved was minor; we did not, hence, do any blank corrections to the analyses. **Figure 4** shows an analysis of a sample that has undergone crushing and the spectra given the volatiles being analyzed for 300 cycles. The Y-axis in **Figure 4(a)** is shown in logarithmic scale, while in **Figure 4(b)** the Y-axis is shown linearly.

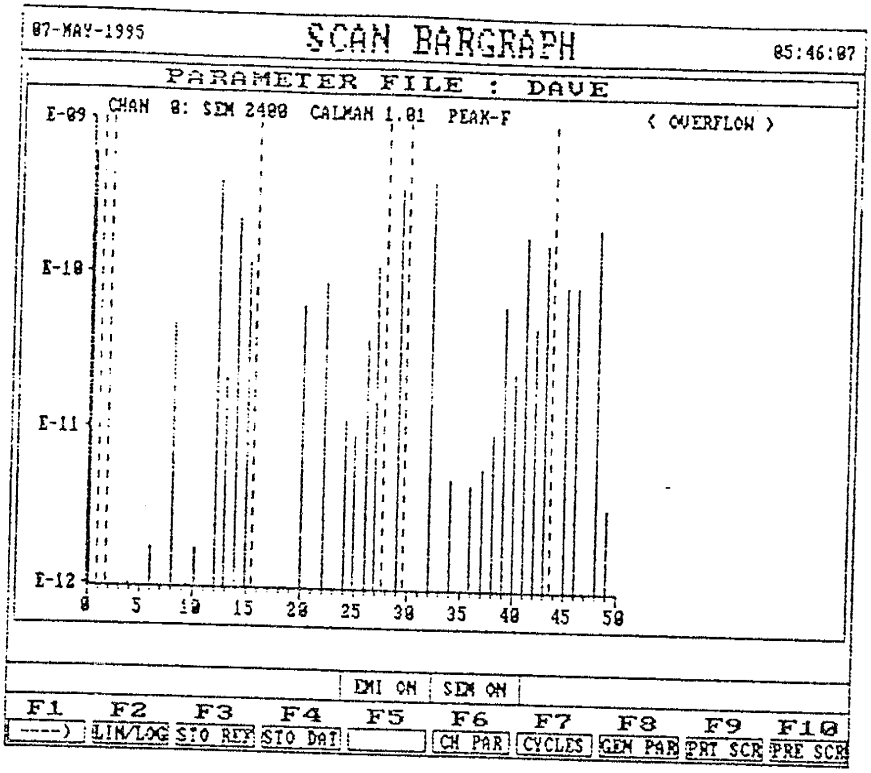

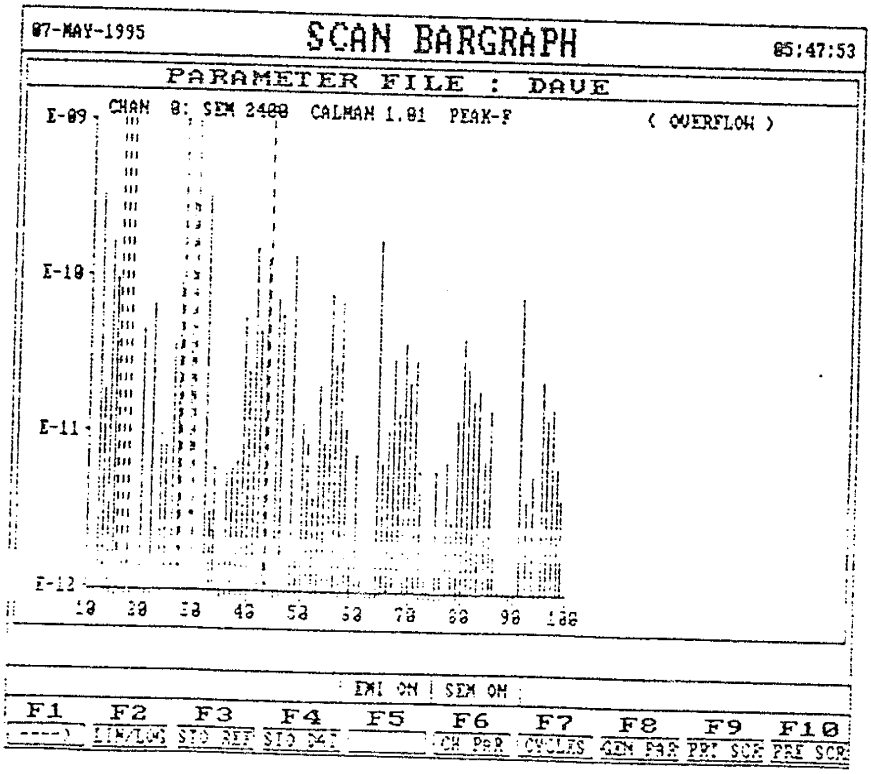

FIGURE 3: Computer display of analysis from heating for non-condensable gases and condensable gases.

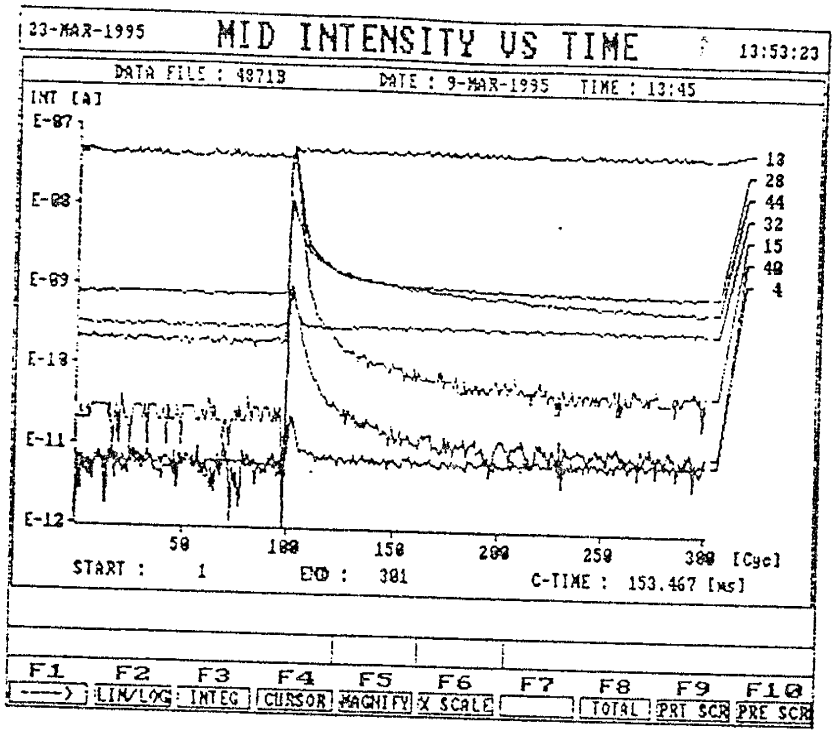

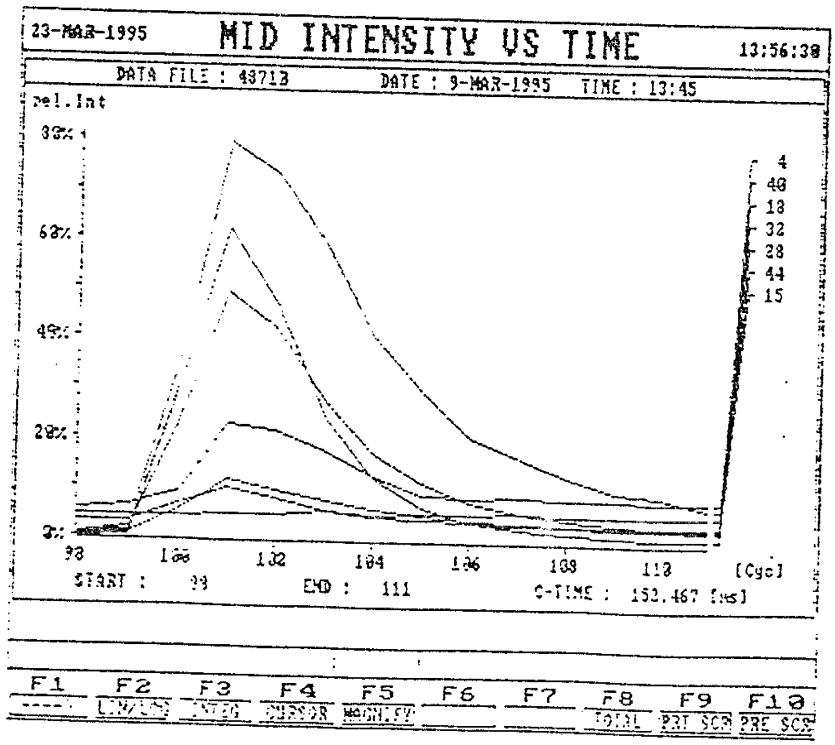

FIGURE 4: Computer display of analysis from crushing(MID) mode. Y-axis is in Log-scale and in linear scale.

ANALYTICAL PROBLEMS

We encountered few analytical problems during the measurement of gases in different carbonate minerals. Gases such as N_2, Ar, and He are non-reactive. We did not observe significant absorption of these gases by surfaces within the vacuum line during analysis by thermal decrepitation or by mechanical crushing. NH_3 may, however, break down to N_2 in samples that are being analyzed by thermal decrepitation (Norman and Musgrave, 1994). Although the principal mass peak for CO and N_2 is at 28, the relative proportions of these two gases did not affect the accuracy of the measurements because we can determine the individual concentrations of these gases with the help of a matrix solution. Also, the principal gaseous specie in the non-condensable gas fraction is generally N_2, hence, we cannot detect low concentrations of CO (Norman and Musgrave, 1994).

Another principal analytical difficulty faced during an analysis is the presence of He and Ar at concentrations of less than 10 ppm v/v in fluid inclusion gases. During such low concentrations, these gases may be difficult to detect if the sample contained a small number of the fluid inclusions or if fluid inclusions contain low concentrations of these gaseous species. The quadrupole mass spectrometer that we used for these analyses had a detection limit of 10^{-15}

moles and a measurement limit of 1 ppm v/v. The measurement limit of 1 ppm v/v hence affects the detection of He (Norman and Musgrave, 1994).

DATA PROCESSING

We obtained a quantitative determination of each gas fraction by measuring the pressure of each gas fraction within a known volume of the extraction line for samples that underwent thermal decrepitation. We determined the amount of water contained in the fluid inclusions by measuring the pressure in the extraction line or by freezing the H_2O into a capillary tube and then weighing the tube. We calibrated the mass spectrometer using commercial gas mixtures and an in-house fluid inclusion standard HF-1 (Norman and Musgrave, 1994). We did the calibrations for water measurements by thermal decrepitation of hydrous minerals such as gypsum and muscovite followed by freezing the liberated water into a capillary tube. Then we weighed a number of capillary tubes that contained water from a known amount of dehydrated gypsum or muscovite and later we formulated an equation for the water correction.

We recorded the data in the binary form in the computer and later converted the data to the ASCII form. We reduced the converted files for samples that have undergone thermal decrepitation using the program "REDUCEN". We wrote the program in the Basic language; and the output of the

program gives the relative concentrations of analyzed gases with background values. Then we processed the reduced file in a spreadsheet to determine the mole percentages of different gaseous species. The program also calculates the molar percentages of different gaseous species in a water-free environment.

In the case of samples that underwent mechanical crushing, we determined areas under individual peaks by integrating the peaks. Then we multiplied the integrated areas with a 7x7 matrix to determine the mole percentage of each gas. Data in the 7x7 matrix includes the sensitivity factors for the analyzed gases. **Table B1** in Appendix includes data contained in the 7x7 matrix used in the calculations.

SAMPLE LOCATIONS

We collected 130 samples of carbonate minerals around the Rio Grande rift, in New Mexico. These were forty-one pedogenic calcites (thirty non-indurated and eleven indurated), eighteen travertines from active springs, fifteen ancient travertines, fifteen hydrothermal vein calcites, six calcretes, two calcite concretions in sand and thirty-two vein calcites from trenches and tuffs from LANL and NTS.

PEDOGENIC CALCITES (NON-INDURATED)

Pedogenic calcites (non-indurated) is the equivalent of stage I and II of calcic horizon development of McGrath and Hawley (1987). We collected thirty samples of pedogenic calcites (non-indurated) principally from four locations around the Rio Grande river. These include samples collected from Puye Quadrangle near White Rock, from locations within the Belen and Luis Lopez Quadrangles, from road cuts along the I-25 and from localities in the Loma De Las Cañas and San Antonio Quadrangles. We collected most of the samples from thin 10cm to 15cm horizons just beneath the land surface or from thin, discontinuous coatings on pebbles and basalts (Machette, 1985). **Figure 5** gives the location of pedogenic calcites (non-indurated) collected in New Mexico

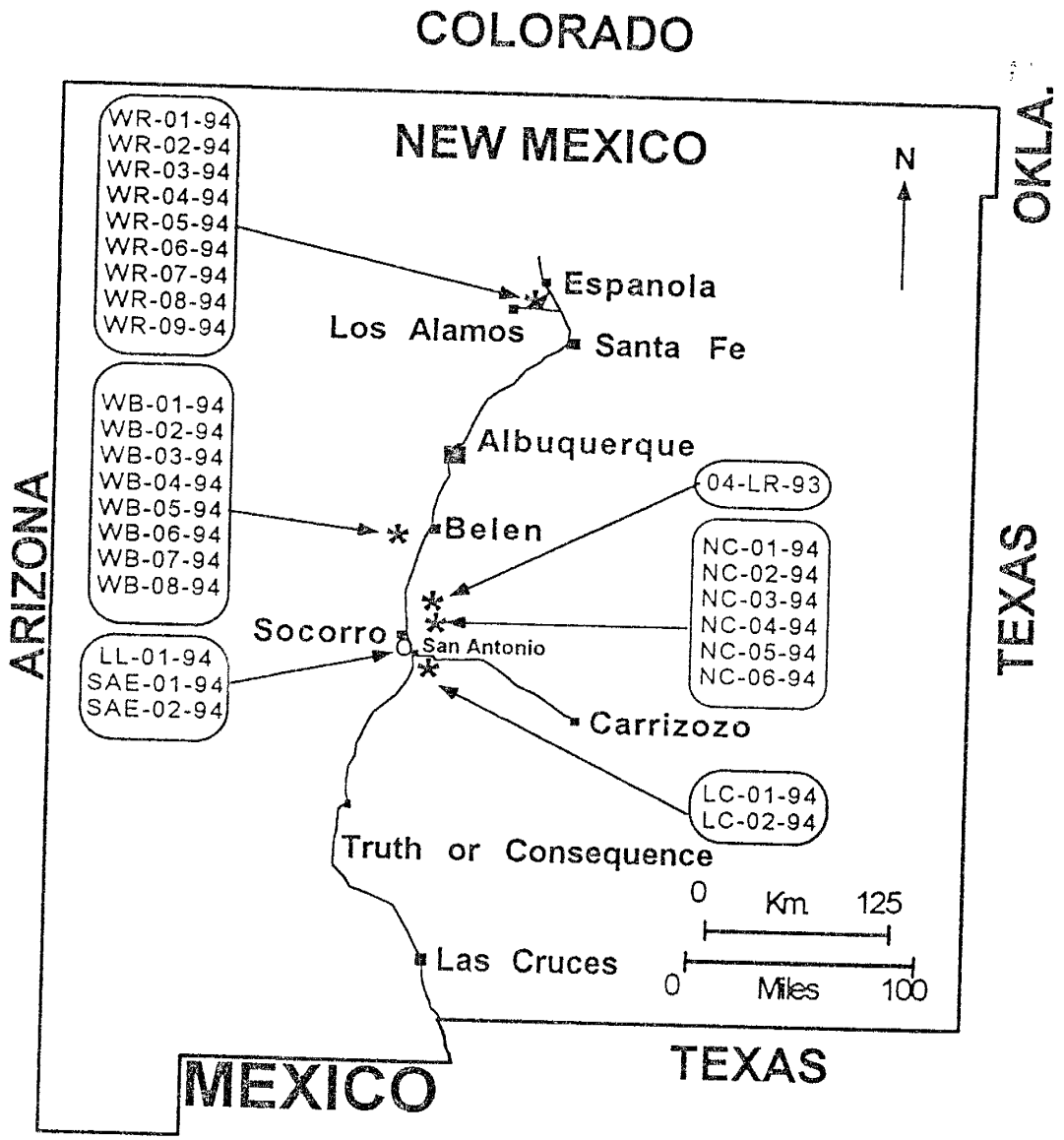

FIGURE 5: Location map of pedogenic calcites (non-pedogenic) collected in New Mexico. Samples WB-01-94 to WB-08-94 were collected from Belen Quadrangle. Samples WR-01-94 to WR-09-94 were collected from Puye Quadrangle, near White Rock. Samples NC-01-94 to NC-04-94 and 04-LR-93 were collected from Loma De Las Canas Quadrangle, while NC-05-94, NC-06-94, LC-01-94 and LC-02-94 were collected from San Antonio Quadrangle. Samples LL-01-94, SAE-01-94 and SAE-01-94 were collected from Luis Lopez Quadrangle, near Socorro, New Mexico.

We collected five samples, NC-01-94 to NC-04-94 and 04-LR-93, from the Loma De Las Cañas Quadrangle, while we collected samples NC-05-94, NC-06-94, LC-01-94 and LC-02-94 from the San Antonio Quadrangle. We collected all these samples along the road cut and these samples represent the remnant of the "Las Cañas" geomorphic surface. Thick continuous coating of carbonate cover samples from Las Cañas geomorphic surface along with some loose carbonate in the matrix. **Figure A1 to A6** in appendix illustrates the individual locations of the above samples (Hawley et al., 1987). **Figure 6** shows the author collecting sample LC-02-94 in the field.

We collected nine samples, WR-01-94 to WR-09-94, along highway NM4 in the Puye Quadrangle near the White Rock. Samples, WR-01-94 to WR-06-94, were all basalts with thin, discontinuous to continuous coatings of carbonate. We collected sample WR-01-94 near the water tower talus slope formed near a road cut. We collected samples WR-02-94 and WR-03-94 from the "Ripple Mark" area, within the same outcrop as sample WR-01-94. We collected samples, WR-04-94 to WR-06-94, from a fracture within the lower unwelded Bandalier ash fall tuff. The fracture, which was near a road cut, was 5 to 10cm in width, and approximately 10 meters in height. We collected samples WR-08-94 and WR-09-94 in proximity to the surface. In contrast, we collected sample WR-07-94 at a greater depth. **Figure A7** in appendix illustrates the individual locations of the above samples.

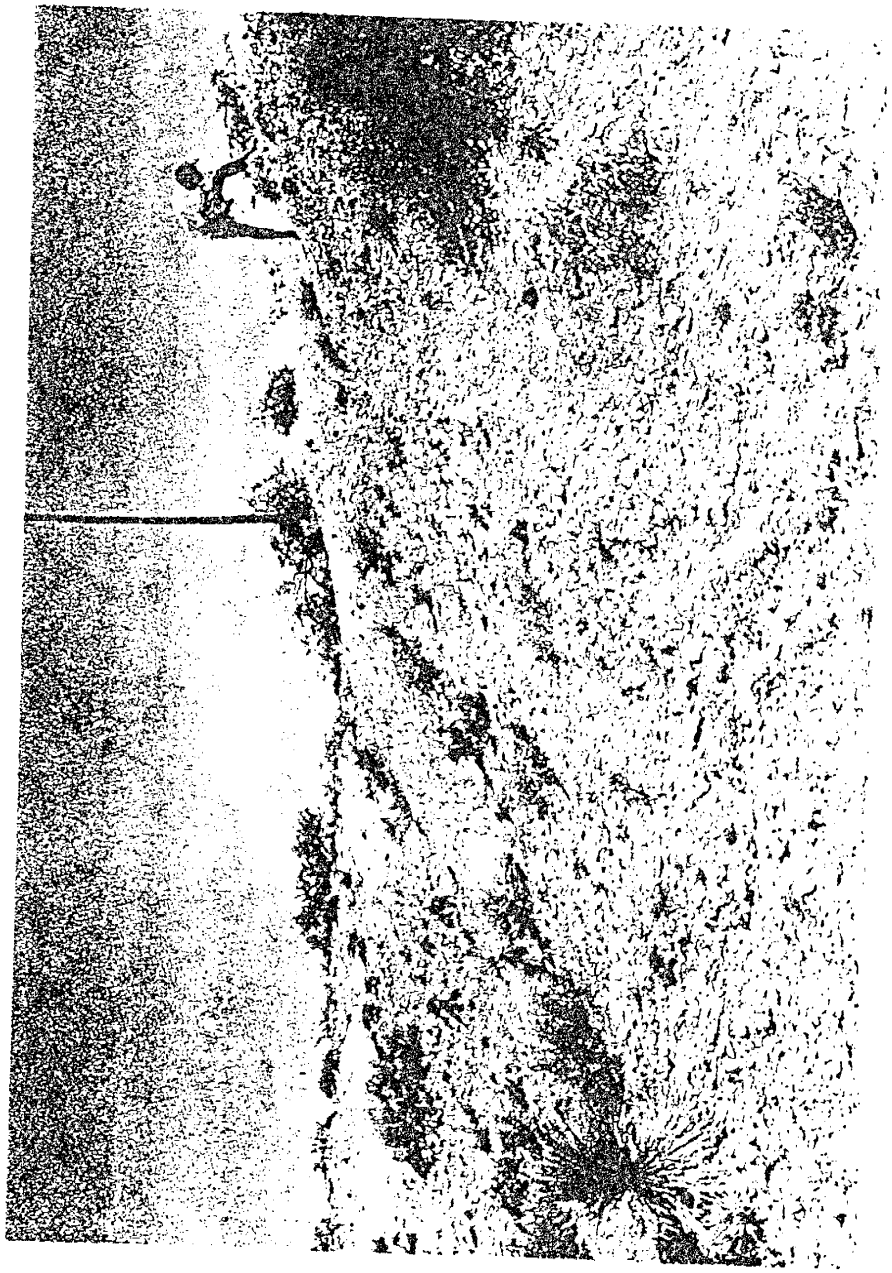

FIGURE 6: Picture showing pedogenic calcite (non-indurated) sample "LC-02-94" at San Antonio Quadrangle, New Mexico.

We collected eight samples, WB-01-94 to WB-08-94, in the Belen Quadrangle and **Figure A8** in appendix gives the sample locations. We located the eight samples near the flat-topped hills, west of I-25, near Belen. We collected the samples from the top of a 10cm to 15cm horizon composed of massive accumulations of calcium carbonate. **Figure 7** displays a pedogenic calcite (non-indurated) block, west of I-25 near Belen, in an advanced stage of weathering. Sample WB-05-94, WB-07-94 and WB-08-94 represent soft calcic nodules, 4 cm to 6 cm in diameter and found in the K horizon (Machette, 1985). **Figure 8** shows pedogenic calcite (non-indurated) with a nodular appearance.

From the Luis Lopez Quadrangle we collected three samples of non-indurated pedogenic calcite. We collected sample LL-01-94 along the road cut of highway US-85. We collected the samples from the top 2 cm to 5 cm of a discontinuous horizon composed of a thin accumulation of carbonate minerals. We collected samples, SAE-01-94 and SAE-02-94, at 0.5 and 1 mile from the San Antonio exit, on I-25 towards Socorro. We collected the samples along the I-25 and calcic carbonate occurs as a thin coating of carbonate horizon on weathered pebbles (Machette, 1985). **Figure A9 and A10** in appendix give the location of these samples.

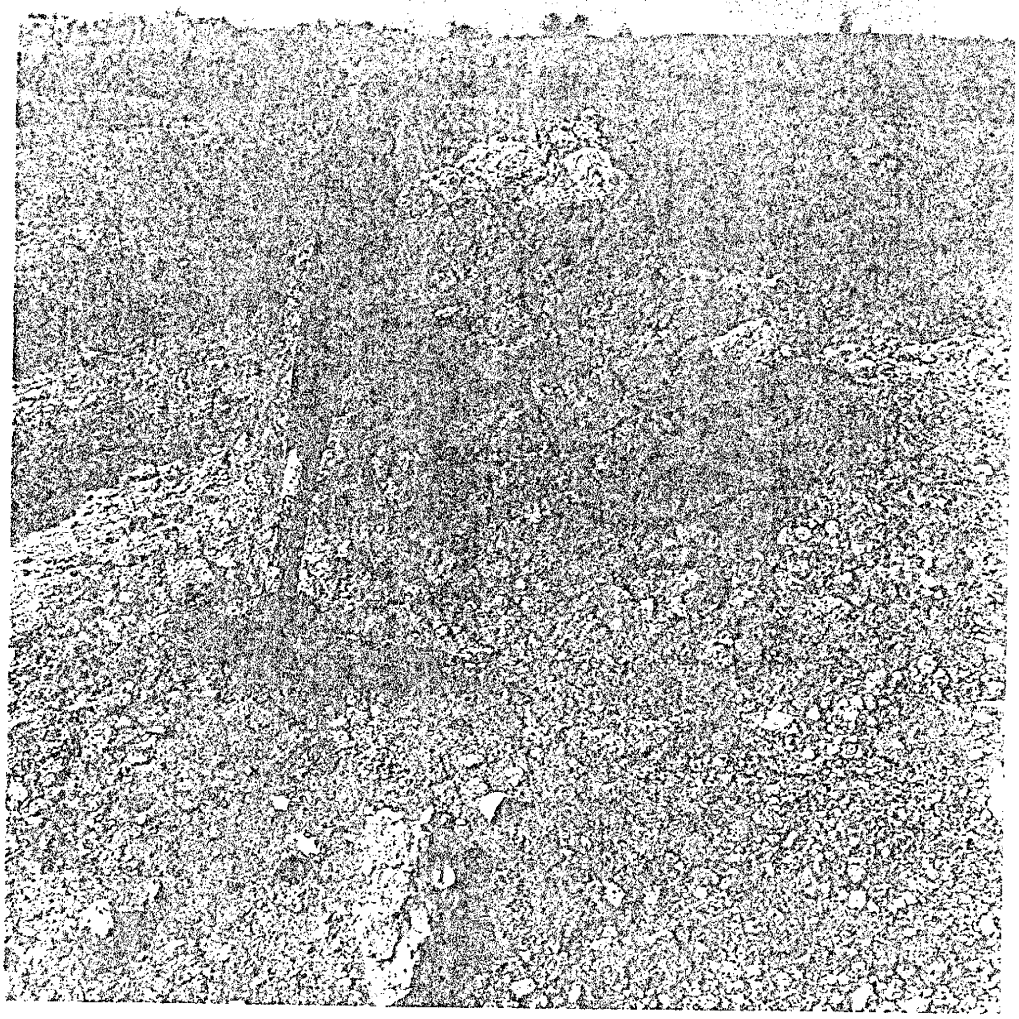

FIGURE 7: Picture showing an outcrop of a pedogenic calcite (non-indurated) located West of I-25, near Belen, New Mexico.

FIGURE 8: Picture of nodular pedogenic calcite (non-indurated) at an outcrop West of I-25, near Belen, New Mexico. The sample that was collected was "WB-08-94".

TRAVERTINES

We collected fifteen samples of ancient travertines around New Mexico these were samples collected from the Mesas Mojinas and the Belen Quadrangles. **Figure 9** gives the location of the ancient travertines collected in New Mexico. We collected four samples, 01-AM-93 to 04-AM-93, from section 12 of the Mesas Mojinas Quadrangle, while we collected sample 05-AM-93 at section 25 near a stream. All the samples are of Desert Gold variety; these samples are part of the Aparejo Mesa. The samples contain color banding, with colors that ranged from white to pink to yellow brown. **Figure A11 and A12** in appendix give the location of the samples. **Figure 10** shows an ancient travertine bed at Aparejo Mesa in Mesas Mojinas Quadrangle.

We collected seven ancient travertine samples, NMT-01-94 to NMT-07-94, from the Scheherazade quarry, (New Mexico Travertine Inc.), located near West of Belen. The samples from the Aparejo Mesa formation exhibited banding, contained void spaces, and ranged in color from pale cream to pink and brown. **Figure 11** shows a network of veinlets in an ancient travertine from Scheherazade quarry, while **Figure 12** shows quarrying operations in progress at the same locality. **Figure A13** in appendix give the location of the NMT samples. We collected three samples, RY-01-94 to RY-03-94, along the western

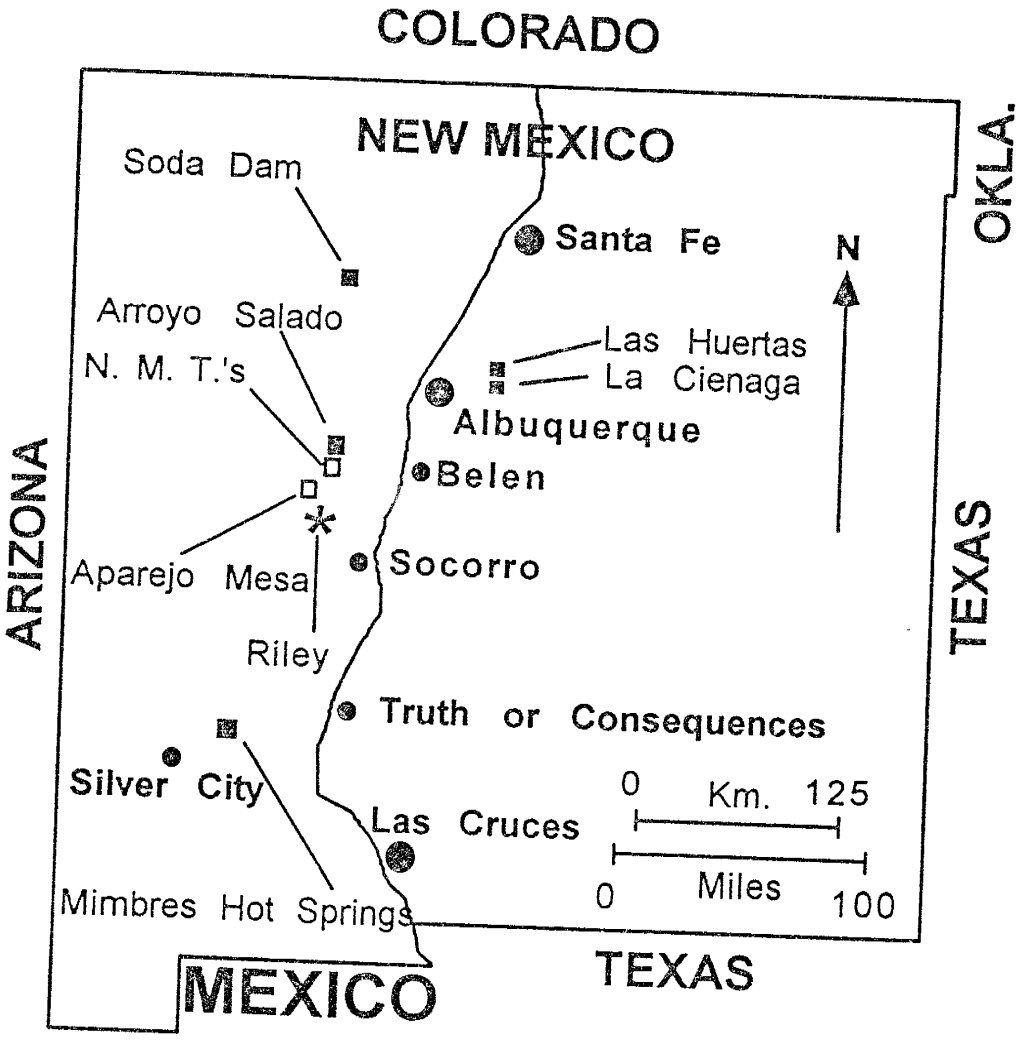

FIGURE 9: Location map of Travertines collected in New Mexico. Arroyo Salado, La Cienage, Las Huertas, Mimbres Hot Springs and Soda Dam are sites of recent travertines from active travertine depositing springs (closed square symbols). Ancient travertines (open square symbols) were collected from Aparejo Mesa and at New Mexico Travertine Quarry near Belen. Travertines from Riley (star symbol) are grouped separately.

Fig. 10

Fig. 11

FIGURE 10: Picture of an ancient travertine bed at Aparejo Mesa, NM.

FIGURE 11: Picture showing veinlets in ancient travertine from New Mexico Travertine Inc., near Belen, NM.

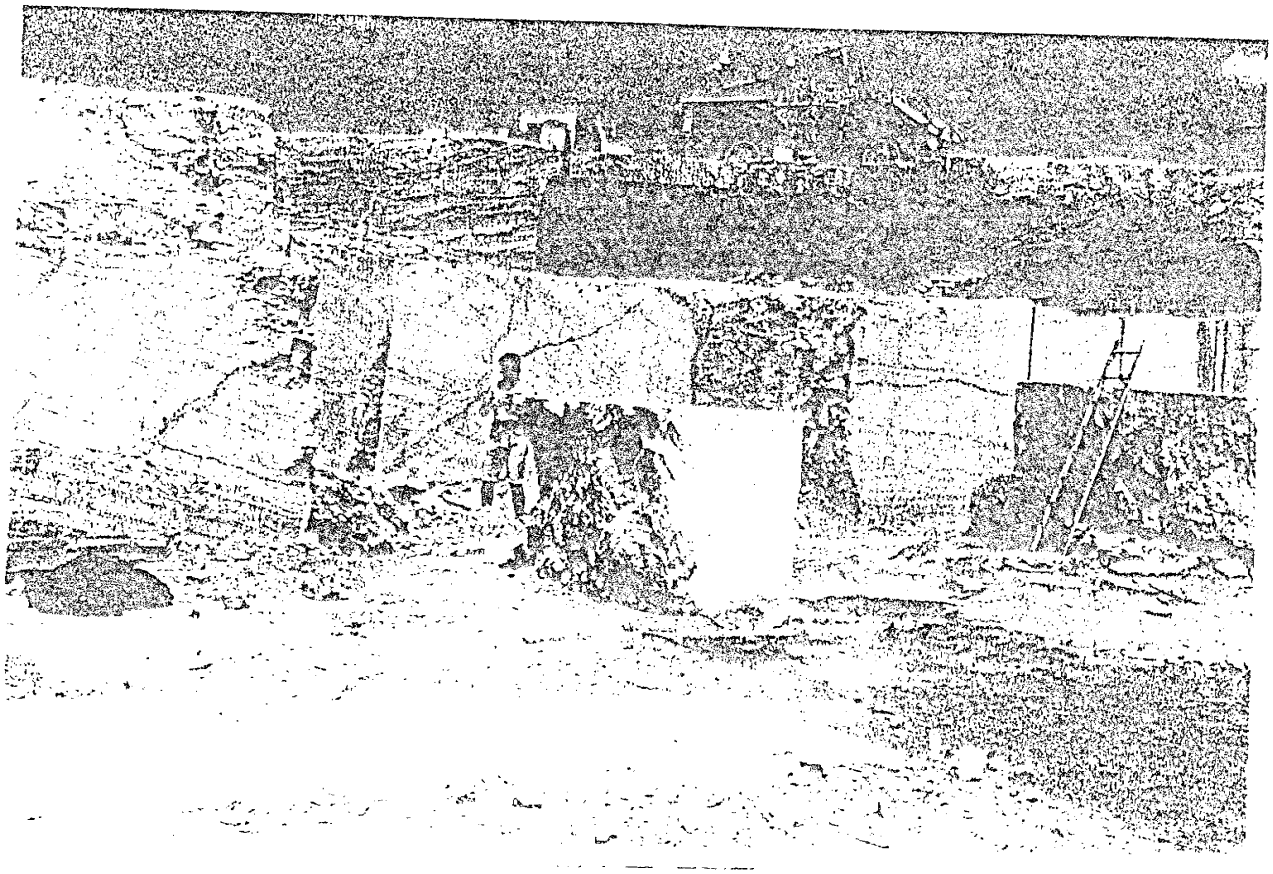

FIGURE 12: Picture of ancient travertine being quarried at New Mexico Travertine Inc., near Belen, New Mexico.

flank of the Ladron peak (Norman et al., 1994). We believe that these ancient travertines have multiple origins (Barker, 1983).

We believe that the travertines at Aparejo Mesa are of Quaternary age. Furthermore, the Pennsylvanian Madera limestone is assumed to be the primary source rock for the carbonate-rich water that formed these travertines (Austin and Barker, 1990). Evaporation of water, or loss of carbon dioxide (CO_2) due to degassing by pressure release, turbulence, photosynthesis, and/or bacterial metabolism may result in the formation of waters saturated with carbonate. These carbonate-saturated waters could then deposit calcium carbonate in a spring system. Coloration of travertines is due to the impurities in them (Austin and Barker, 1990).

We collected eighteen samples of travertines from active springs at different locations in New Mexico along with waters from some of those springs (Norman et al., 1994). **Figure 9** gives the location of all travertines deposited by active springs in New Mexico. We collected three samples, designated AS-01-94 to AS-03-94, from a spring that deposits travertine actively and forms ledges and mounds in the Arroyo Salado. **Figure 13** shows water sample being collected at Arroyo Salado where active travertine is being deposited as layers in the spring. We believe that the source for the carbonate-rich spring water is the Pennsylvanian Madera limestone. The process of travertine precipitation here

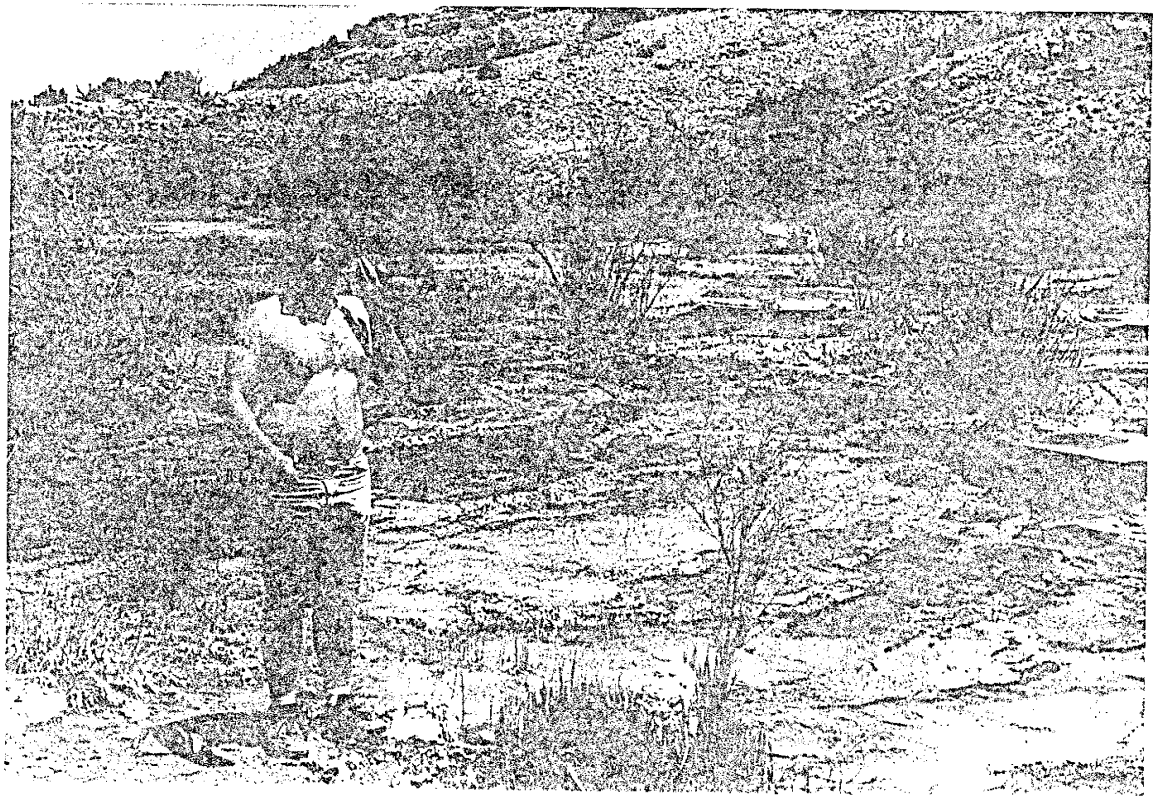

FIGURE 13: Picture showing collection of water sample from an active spring at Arroyo Salado, New Mexico. Precipitation of the travertines by active springs can be seen in the background.

illustrates a way that ancient travertines from Aparejo Mesa may have formed (Austin and Barker, 1990).

We collected three samples, LC-01-94, LC-02-94 and LC-04-94, at the La Cienaga picnic area in the wilderness of Sandia Mountains. Here, travertine is being deposited as coatings, on rocks and logs in the stream, that results in the formation of resistant ledges and rapids. Similarly, we collected two samples, LH-01-94 and LH-02-94, at the Las Huertas picnic area, where travertine precipitates from active springs. Also, two samples MHS-01-94 and MHS-02-94 were collected at the Mimbres Hot Springs, where travertine is being deposited on pipes and water collection boxes. We collected eight travertine samples, SD2-01-94 to SD2-06-94 and SD-01-94 and SD-02-94, from the Soda Dam hot springs, where travertine form large mounds and dams the Jemez river. Chris Wilkowske collected all travertine samples actively deposited by springs (Norman et al., 1994).

PEDOGENIC CALCITES (INDURATED)

Pedogenic calcites (indurated) are the equivalent of stage III to stage VI of calcic horizon development of McGrath and Hawley (1987), and we collected eleven samples of the pedogenic calcites (indurated) from the Loma De Las Cañas Quadrangle (**Figure 14**). Hawley et al., (1987) give the descriptions for some of the samples collected in the Loma De Las Canas Quadrangle. We collected most of the samples from horizons up to 10 feet in thickness. We collected samples, 01-94-PC to 07-94-PC, from a petrocalcic horizon that exhibits well-developed stage IV to incipient stage V carbonate morphology, with thick laminae and case-hardened surfaces (Machette, 1985). **Figure 15** shows a close up of a thick horizon of a pedogenic calcite (indurated) being sampled (Norman et al., 1994). We collected the samples at different levels to determine if the concentrations of the volatiles were consistent. Hence, **Figure 16** gives a detailed distribution of the samples collected at this locality (McGrath and Hawley, 1987). The samples may represent the remnant of the "Las Cañas" surface and are part of the youngest piedmont facies of the Sierra Ladrones Formation, which ranges in age from early to middle Pleistocene (Hawley et al., 1987). **Figure A14** in appendix give the locations of the samples.

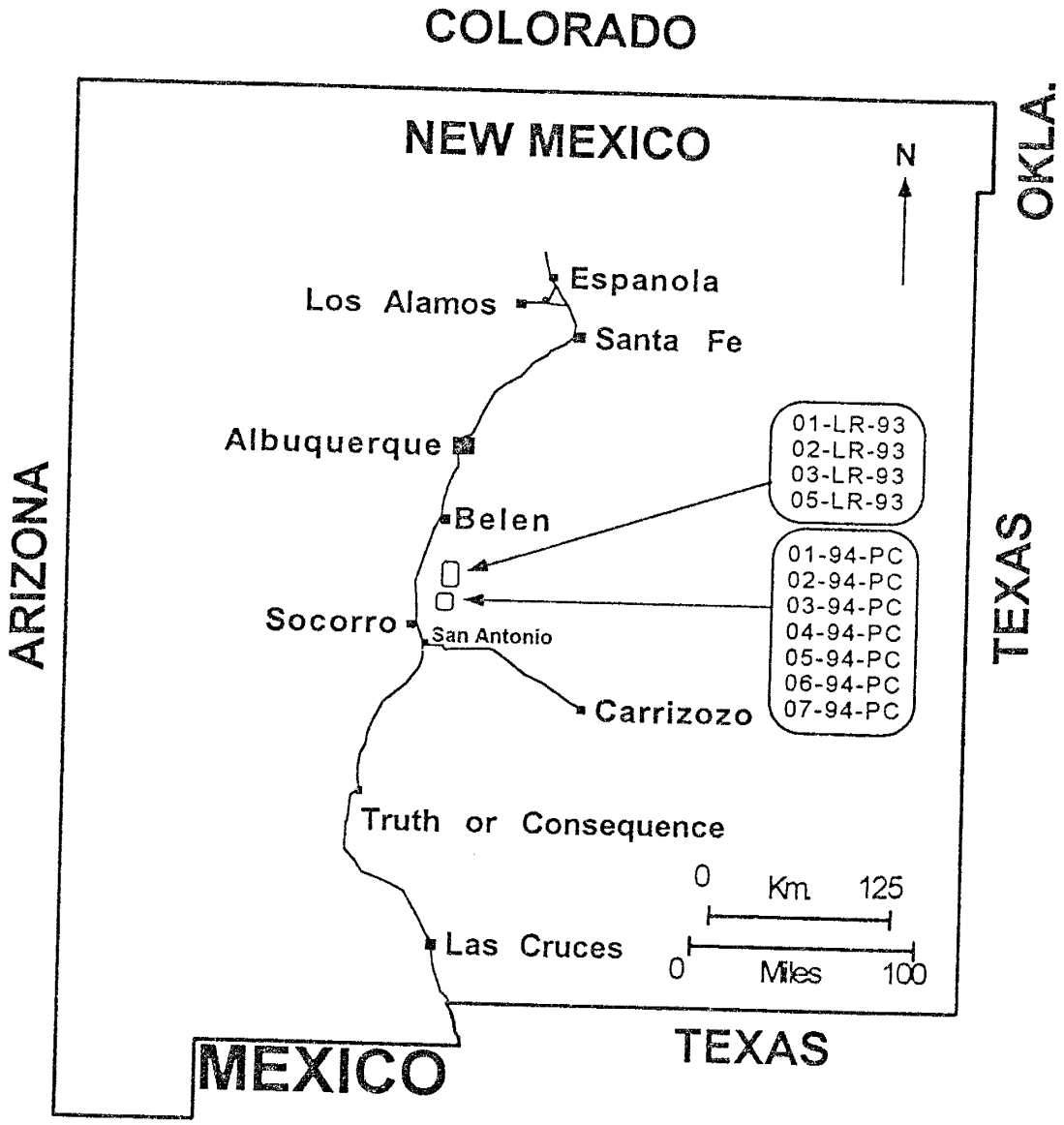

FIGURE 14: Location map of pedogenic calcites (indurated) collected in New Mexico. Samples 01-94-PC to 07-94-PC, 01-LR-93 to 03-LR-93 and 05-LR-93 were collected from Loma De Las Canas Quadrangle, East of Socorro, New Mexico.

Fig. 15

Fig. 16

FIGURE 15: Picture showing a pedogenic calcite (indurated) horizon at Loma De Las Canas Quadrangle.

FIGURE 16: Picture showing the same horizon where 7 pedogenic calcites (indurated) were collected.

We collected samples, 01-LR-93 to 03-LR-93 and 05-LR-93, along road cuts in the Loma De Las Cañas Quadrangle (**Figures A15, A16 and A17** in appendix). The horizon contains thin to moderately thick laminae in the upper part of the Km horizon and may represent stage IV accumulation. Thick continuous coatings of carbonate covered the samples from the Loma De Las Canas Quadrangle and in some places the samples were indurated (Machette, 1985). These samples represent the "Las Cañas" surface. **Figure 17** shows pedogenic calcite (indurated) sample, "LR-03-93", being collected of a layer at Loma De Las Cañas Quadrangle.

FIGURE 17: Picture showing pedogenic calcite (indurated) layer at Loma De Las Canas Quadrangle, near Socorro, New Mexico.

CALCRETES, HYDROTHERMAL VEIN CALCITES and CALCITE CONCRETIONS

"Calcretes are a conglomerate consisting of surficial sand and gravel cemented into a hard mass by calcium carbonate precipitated from solution by infiltrating waters, or deposited by the escape of CO_2 from vadose zone", (Bates and Jackson, 1984). Samples of calcretes, hydrothermal vein calcites and calcite concretions in sand were collected around the Rio Grande river and this includes fourteen hydrothermal vein calcites, six calcretes and two calcite concretions in sand (**Figure 18**). We collected eight of the fourteen hydrothermal vein calcite samples from the Luis Lopez Quadrangle and we designated these samples as UNK-01-93, UNK-02-93, MCA-01-94 to MCA-04-94, Tower-01-94 and Tower-02-94. **Figure 19** gives the location of the above samples in the Luis Lopez Quadrangle (Eggleston et al., 1983). **Figure 20** shows the San Luis manganese pit where we collected sample MCA-01-94.

We collected the remaining five hydrothermal vein calcites from the New Mexico Bureau of Mines and Geology Museum at Socorro. We designated these samples as "NMBMG", and the samples were from the following mines:

1) NMBMG-02 was collected from the Juantia mine, Magdelena district,
2) NMBMG-04 was collected from the San Pedro mine, Golden County,
3) NMBMG-05 was collected from the Mannie Baird mine, Otero County, and

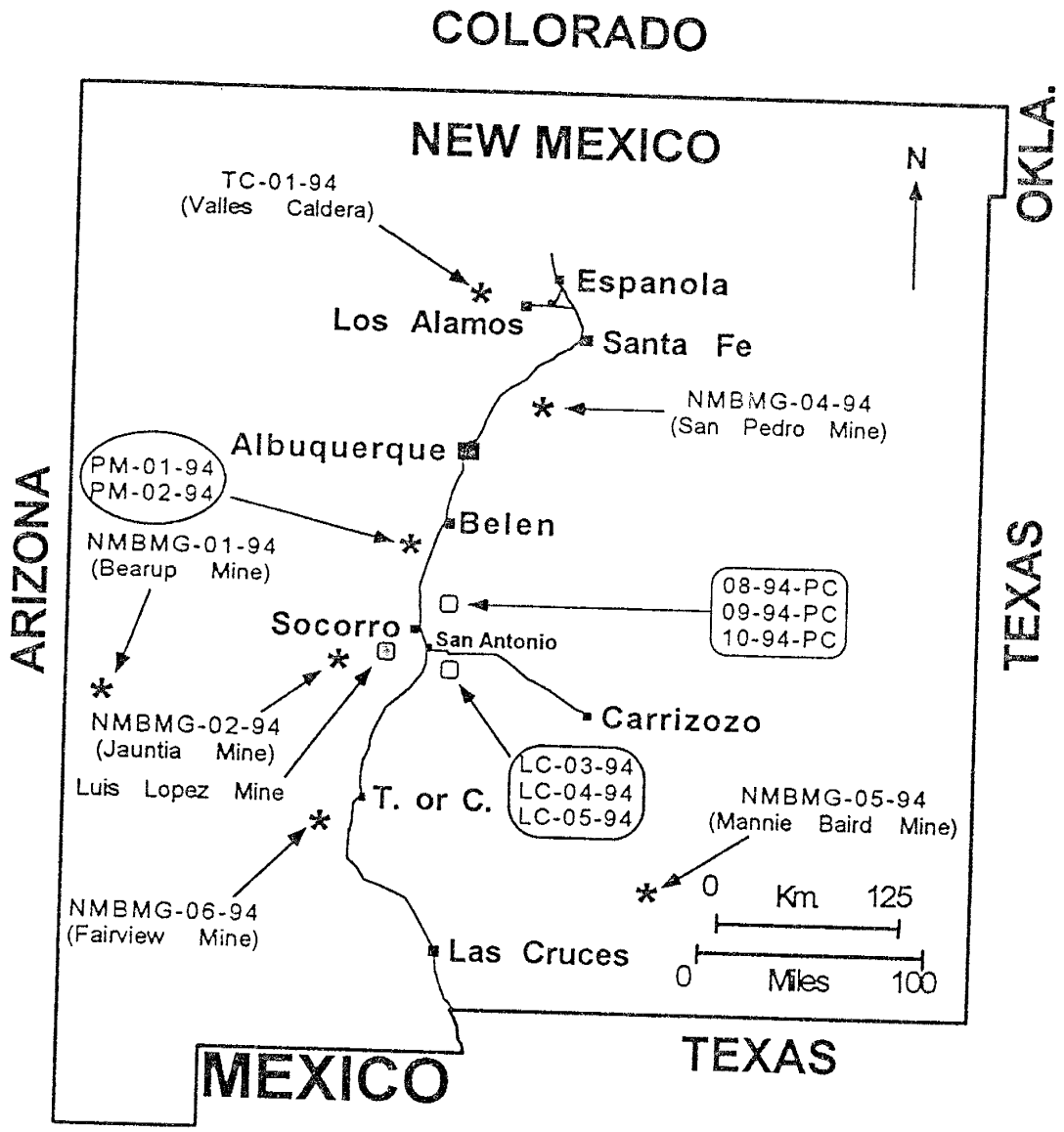

FIGURE 18: Location map of calcretes and hydrothermal vein calcites collected in New Mexico. Samples 08-94-PC to 10-94-PC and LC-03-94 to LC-03-94 are calcretes and were collected from Loma De Las Canas and San Antonio Quadrangle. Samples PM-01-94 and PM-02-94 are calcite concretions in sand and were collected from Veguita Quadrangle. Hydrothermal vein calcites were collected from Bearup mine, Fairview mine, Jauntia mine, Luis lopez mine, Mannie Baird mine and San Pedro mine. Sample TC-01-94 is a core sample from Valles Caldera collected at depth of 1929 feet, in New Mexico.

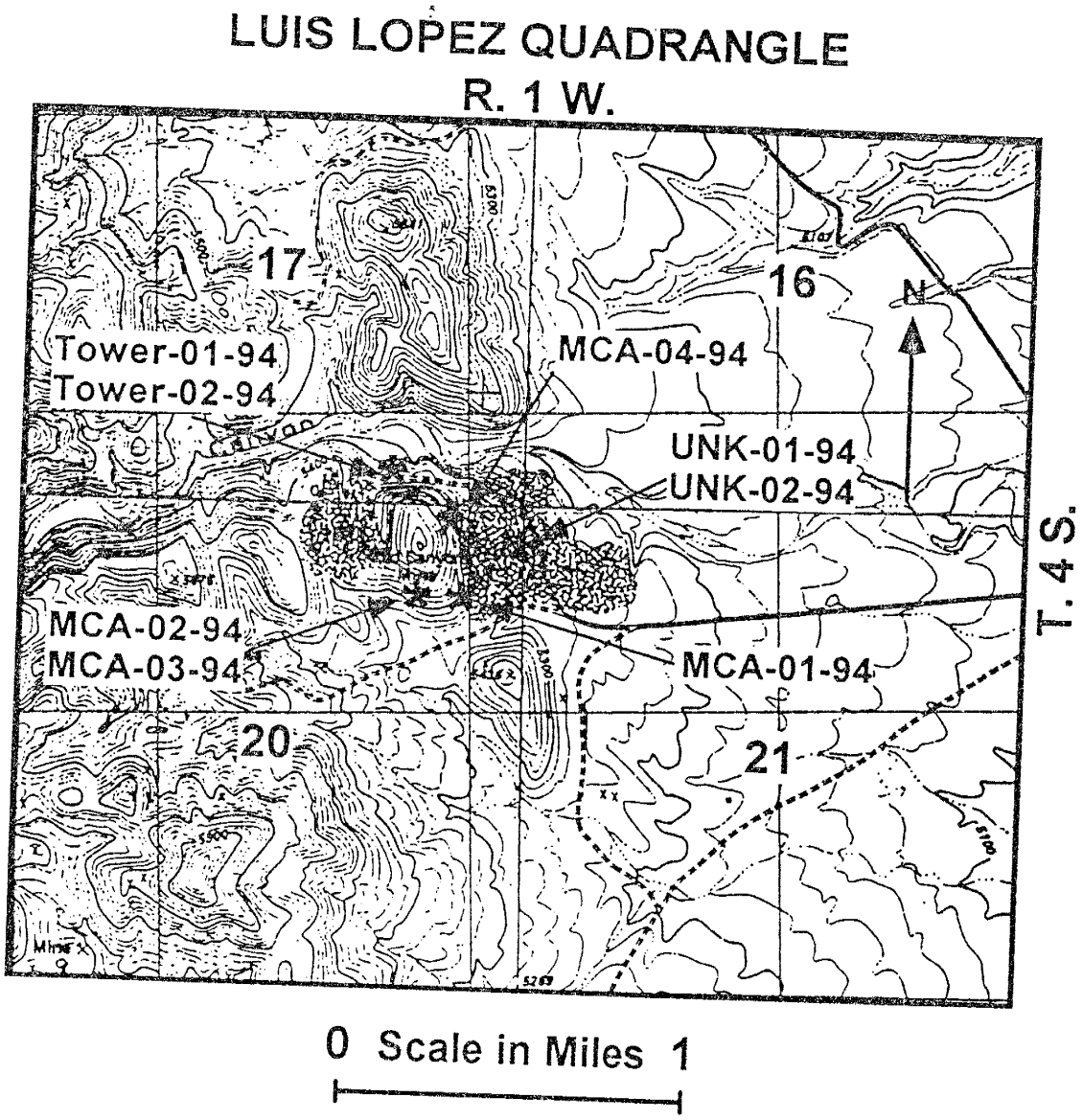

FIGURE 19: Location map of hydrothermal vein calcites collected from San Luis Manganese District, in Luis Lopez Quadrangle, South of Socorro, New Mexico.

FIGURE 20: Picture taken at Luis Lopez mining area, where 8 hydrothermal vein calcites were collected. The place is located South of Socorro, New Mexico.

4) NMBMG-06 was collected from the Circhillo Negro, Fairview mine, Sierra County.

5) Tim Callahan collected the sample TC-01-94 from the Continental Drilling Project, and taken at depth of 1929 feet at the Valles Caldera, New Mexico (VC-2B-1929`).

We collected six calcretes from sites described by Hawley et al. (1987). We collected three samples, designated 08-94-PC, 09-94-PC and 10-94-PC, from the Loma De Las Cañas Quadrangle, at the Arroyo Del Tajo interpretive site (**Figure 21**). We collected sample LC-03-94, LC-04-94 and LC-03-94 from the basal Sierra Ladrones conglomerate at sites located on the San Antonio Quadrangle (**Figures 22, 23 and 24**). Peter Mozley provided two samples of calcite concretions in sand. We designated these samples as PM-01-94 and PM-02-94 and these were from ancestral Rio Puerco river sands. The samples were collected in the Veguita Quadrangle, northwest of Bosque, New Mexico **(Figures A18, A19 and A20 in** appendix**)**.

FIGURE 21: Picture showing the place where a calcrete sample "08-94-PC" was collected. The sample was collected at Arroyo Del Tajo Interpretive site in Loma De Las Canas Quadrangle, New Mexico.

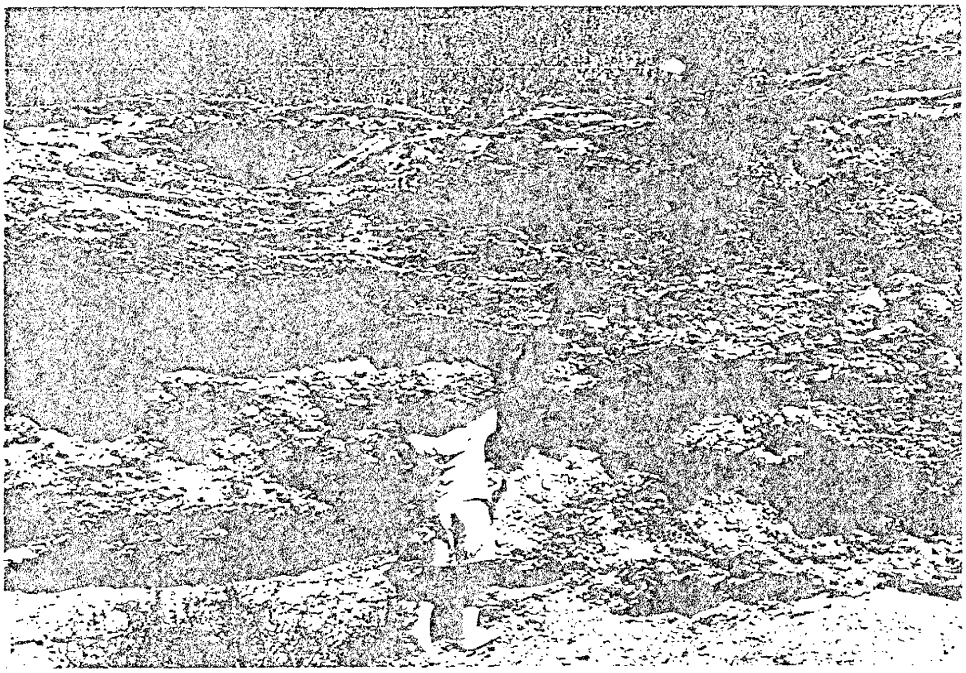

FIGURE 22: Picture showing calcrete sample at San Antonio Quadrangle.

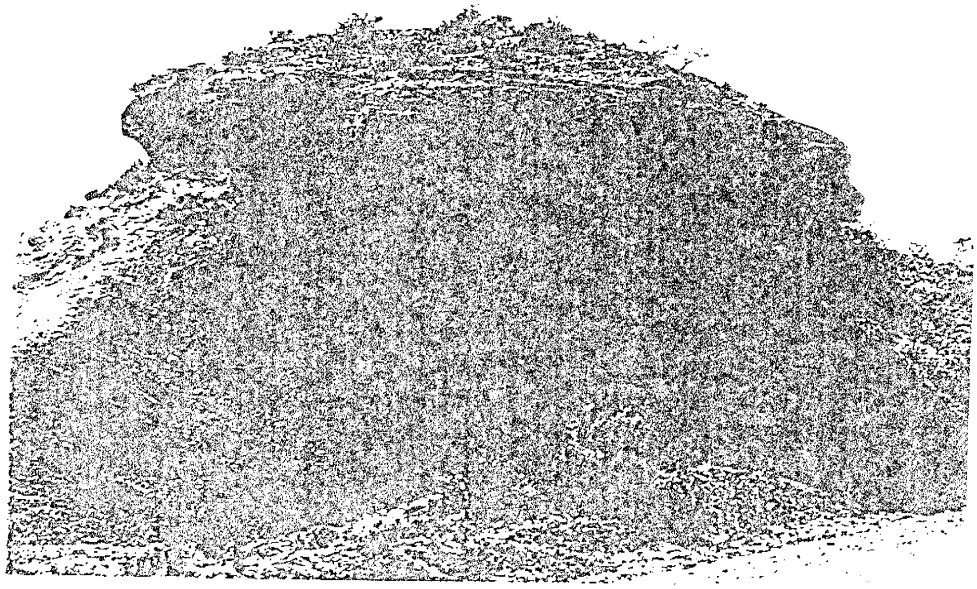

FIGURE 23: Unconformity between Sierra Ladrones and Gallop Sandstones, near San Antonio Quadrangle.

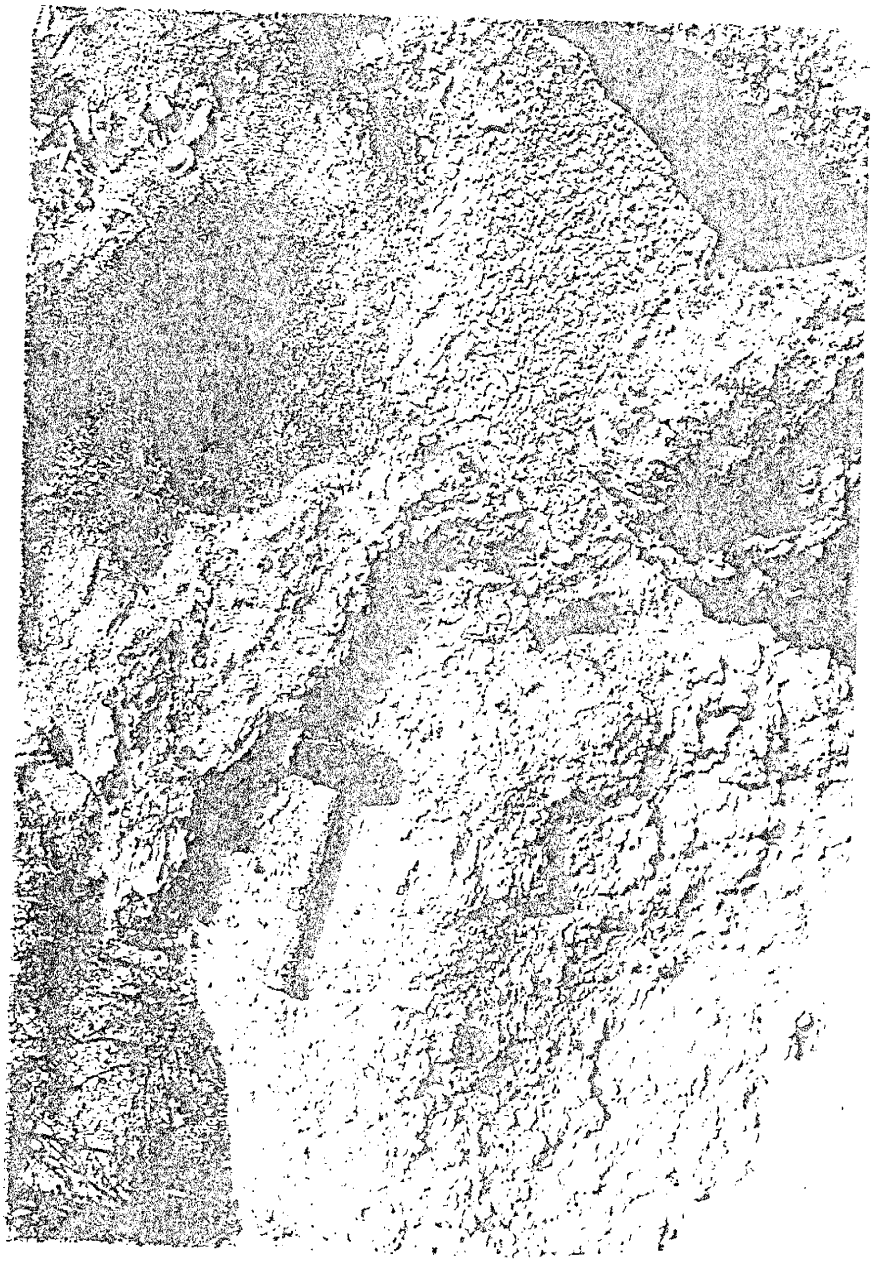

FIGURE 24: Picture showing a calcrete sample "LC-05-94" collected at San Antonio Quadrangle, New Mexico.

VEIN CALCITES from LANL

We collected thirty-two vein calcites from trenches in and around the LANL. Most of the samples were friable, powdery-white calcium carbonate that filled vertical to sub-horizontal fractures within volcanic tuff. The fractures range in thickness from 1 cm to 20 cm, are sub parallel, trend in an N-S direction, and extend to depths of greater than 2 meters. At some outcrops we collected samples from the top to the bottom of a fracture or laterally along the fracture to determine if gas concentrations were consistent.

David I. Norman and Ms. Schon S. Levy collected most of the trench samples. **Figure 25** gives an approximate location of the trench, designated "TA63" and the approximate location of trench "TA63" is within the Frijoles Quadrangle. Within this trench, we collected thirteen vein calcites and we designated these vein calcites as "TA-63's," "AL-93's" and "LA-93's". Cross sections for trenches illustrate the lateral and vertical distribution of samples (**Figures 26 and 27**).

During the investigation we collected nine additional samples of vein calcites within the city limits of Los Alamos. We designated these samples as "LANL". Except for sample LANL-06-94, we collected rest of the samples within

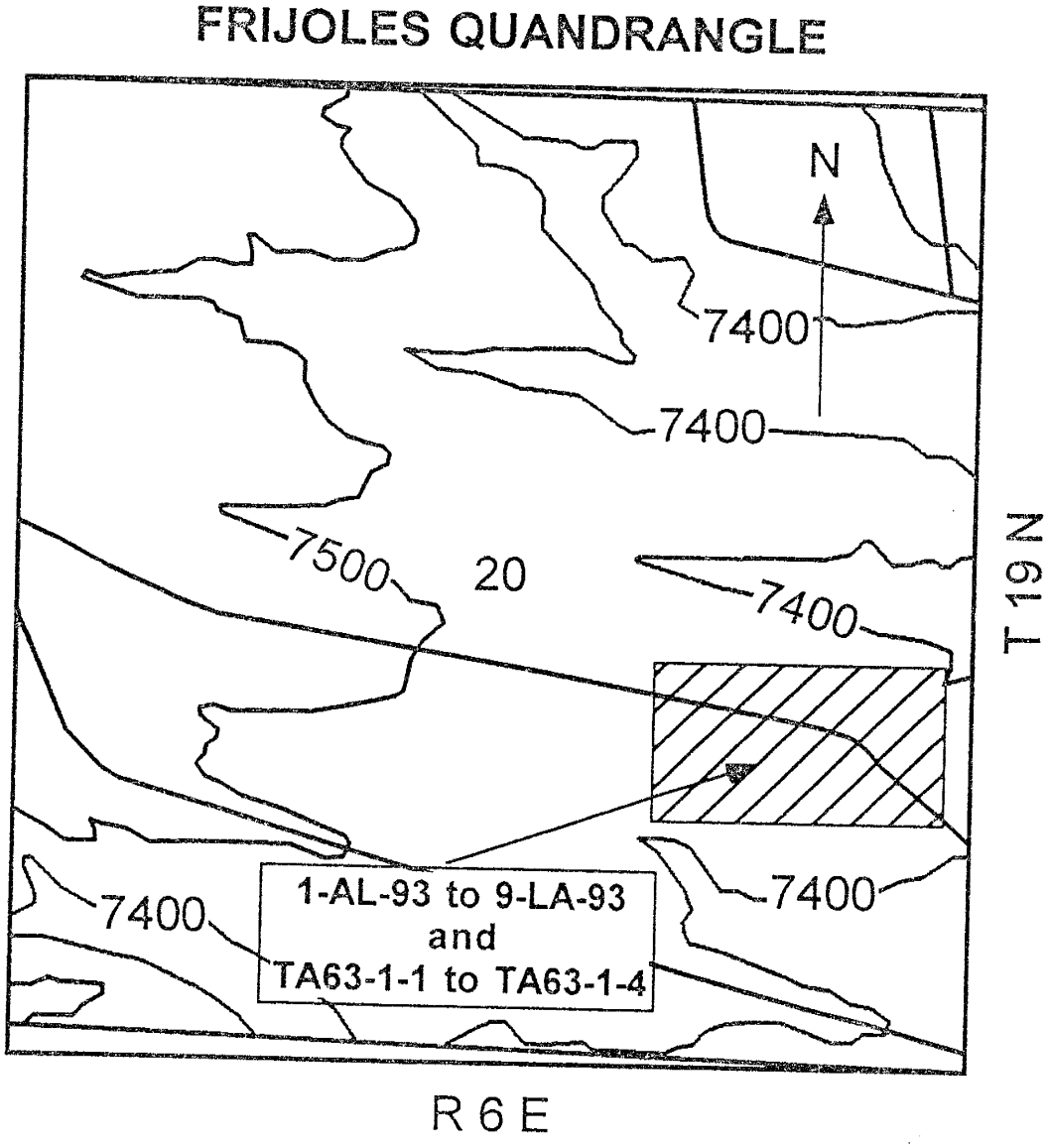

FIGURE 25: Location of Trench TA-63 in Frijoles Quadrangle where 13 vein calcites were sampled.

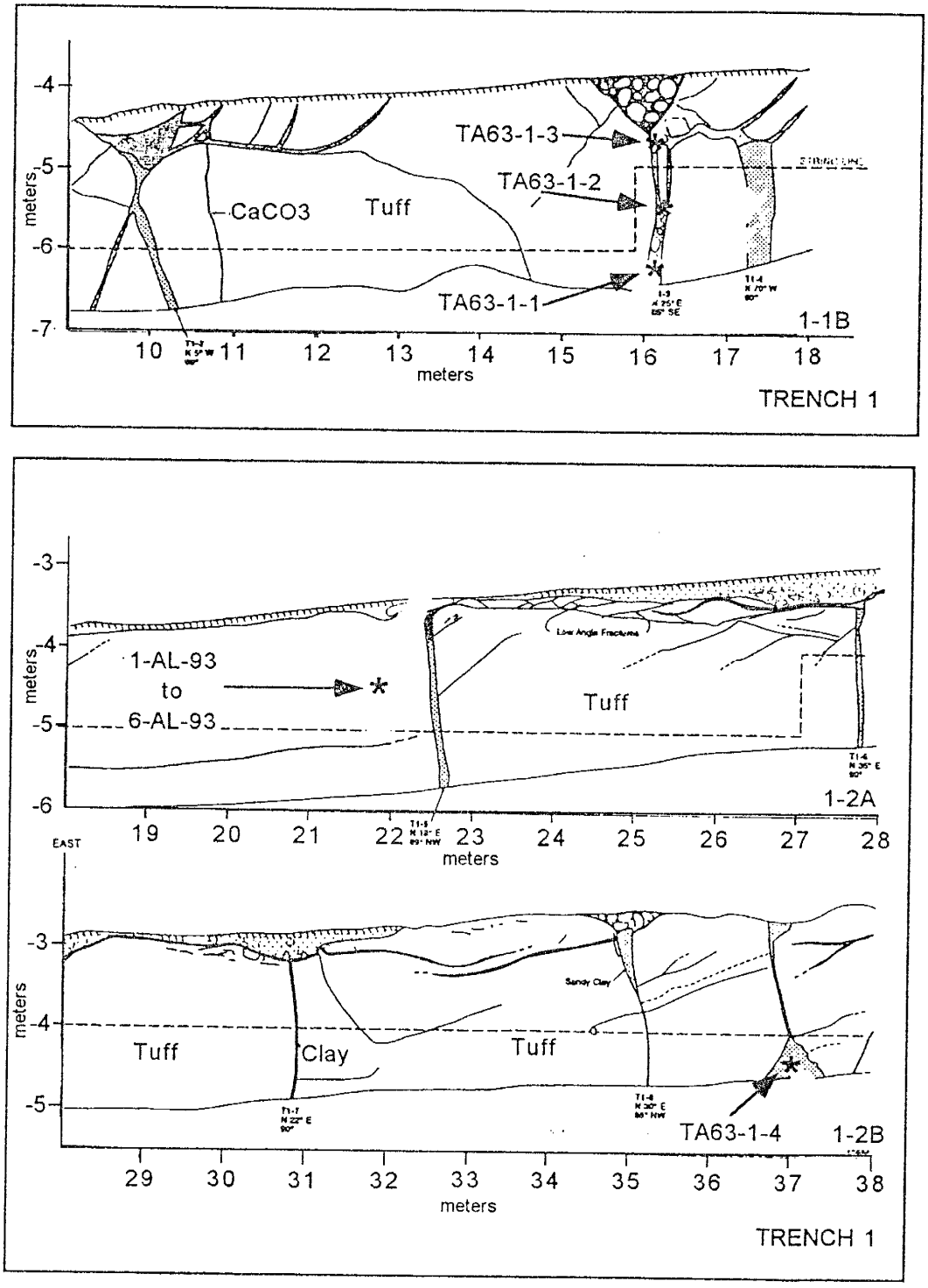

FIGURE 26: Location of 10 vein calcites from trench 1 at LANL. Modified from original figure by Woodward-clyde Consultants (Project No. 92C0774).

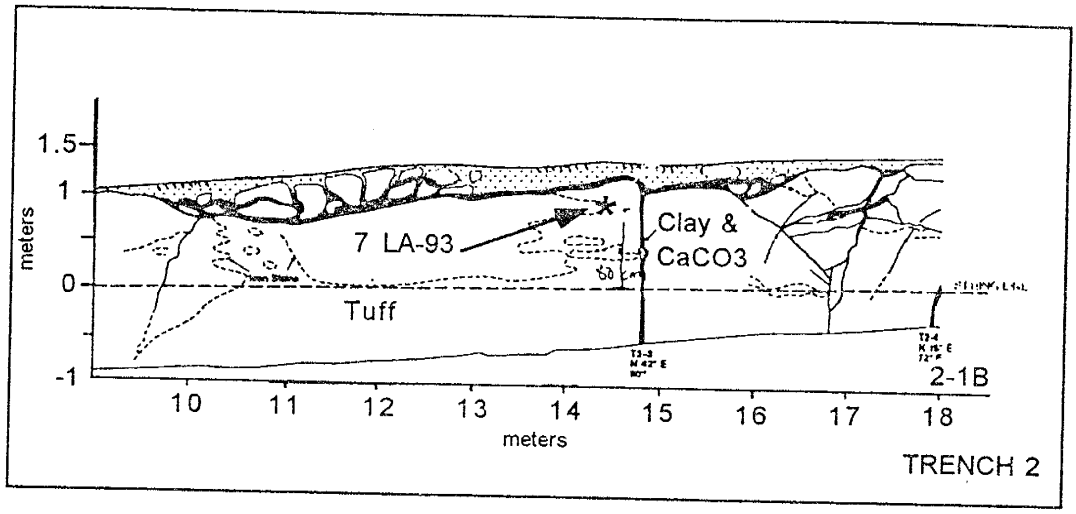

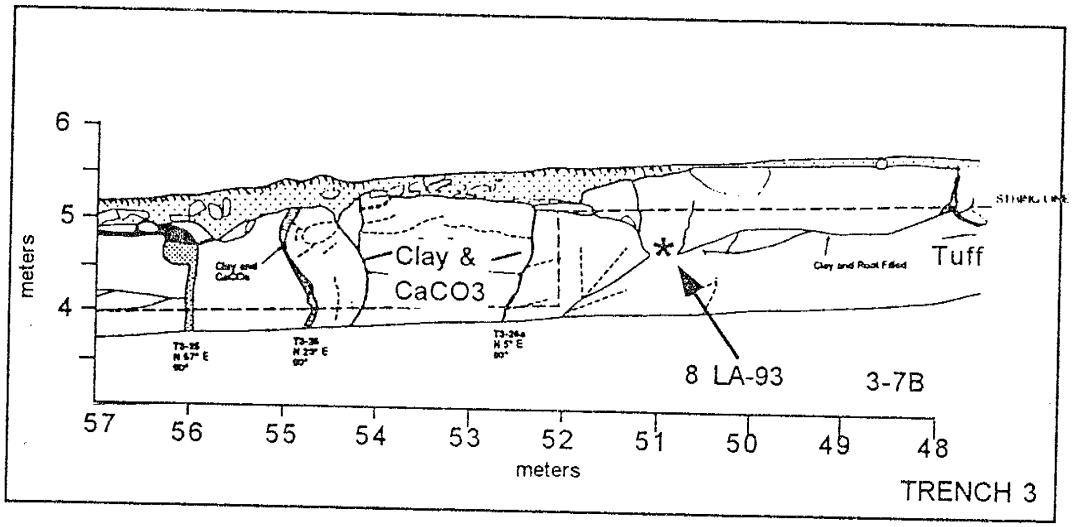

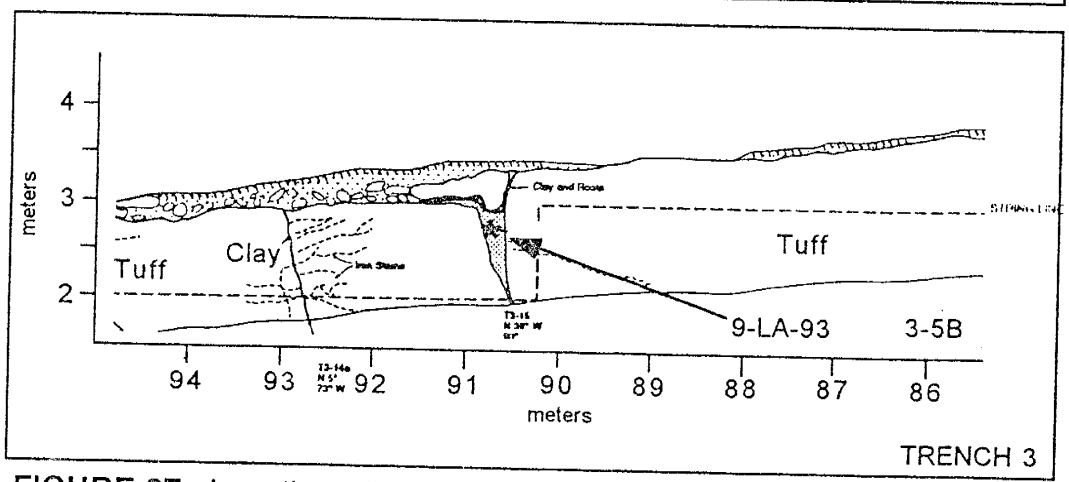

FIGURE 27: Location of 3 vein calcites from trench 2 and 3 at LANL. Modified from original figure by Woodward-clyde Consultants (Project No. 92C0774).

the Gauje Mountain Quadrangle. **Figure A21, A22, A23, A24 and A25** in appendix give the location of the nine samples.

Brent Newman, a graduate student at New Mexico Tech, provided seven more vein calcites, collected from trench TA54, within area J. We collected these samples to check the variation of volatile gases along vertical and horizontal traverses within the trench. We collected three samples, designated LAH-4-A to LAH-4-C, from a horizontal fracture filling, where we sampled LAH-4-A from the top of the fracture while we collected samples LAH-4-B and LAH-4-C from the middle and bottom of the same fracture. We collected three samples, LA1-8898-A to LA1-8898-C, from a vertical fracture at the same location as above, but sampled horizontally at depth of 88 cm to 98 cm. We collected sample LA1-8898-A from the West edge of the filling, while we collected samples LA1-8898-B and LA1-8898-C along the middle and East edge of the filling. Sample LA1-8898-300 is from the same vertical fracture but collected at the depth of 300 cm, and is a composite sample from the whole fracture width. **Figure 28** gives an approximate location of the trench "TA54, of area J".

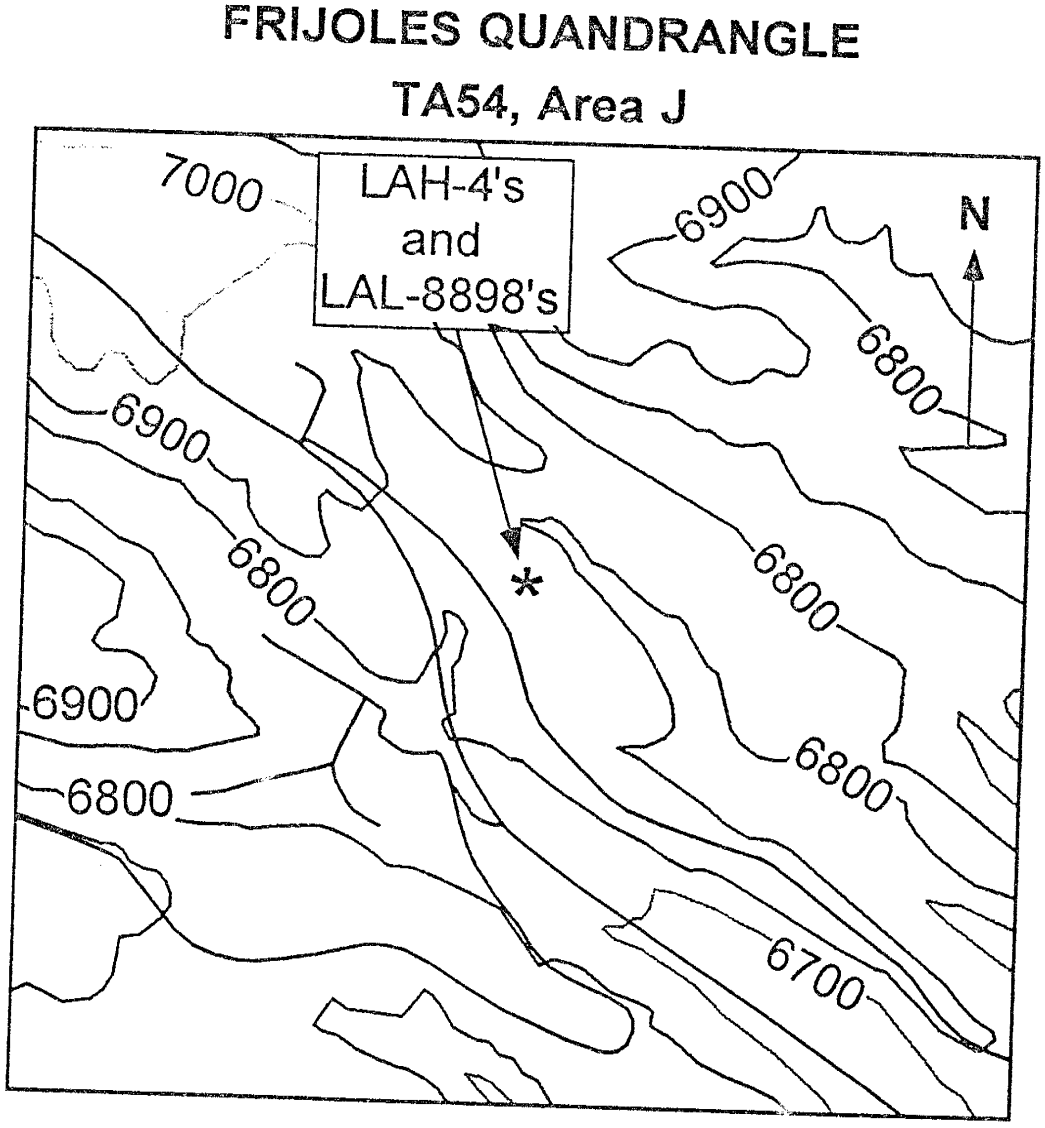

FIGURE 28: Approximate location of 7 vein calcite samples collected by Brent Newman at trench TA-54, near Los Alamos National Laboratories, New Mexico.

RESULTS

The principal gaseous species released during mechanical crushing of the fluid inclusions in different samples are H_2O, CH_4, CO_2, N_2, O_2, Ar and He. After preliminary crushing, we set the quadrupole mass spectrometer to measure these gaseous components. In the analysis of travertines from active springs, we checked the presence of NH_3 (Norman et al., 1994). We require significant concentrations of NH_3 for detecting this gas in the mass spectrometer, because mass peaks 17 and 16 given by NH_3 obscures the mass spectra given by H_2O, CH_4 and CO_2.

Samples that have undergone thermal decrepitation the gaseous species analyzed include H_2, He, CO, CH_4, H_2O, Ne, N_2, O_2, Ar, CO_2 and the lower chain hydrocarbons (C_{1-6}). In samples where the concentration of He released was low, we trapped the non-condensable gases within liquid N_2 dipped activated charcoal. During the analysis, after we noted the pressure of H_2O, we sealed the water vapor into a capillary tube. Then we weighed the sealed capillary tube to know the amount of H_2O released from the fluid inclusions after the sample was thermally decrepitated.

We observed maximum shift in the concentration of volatile gases within pedogenic calcite (non-indurated and indurated), travertines and hydrothermal vein calcites, when we carried out the analyses by mechanical crushing as well as by thermal decrepitation. **Table 1** and **Table 2** gives examples of the fluid inclusion analysis of split samples by crushing and by thermal decrepitation methods. **Table 3** shows changes in gas ratios within these two analytical methods. **Figure 29, 'a' to 'f'** shows different ternary plots illustrating the case that significant differences do exist when we carried out analyses by mechanical crushing and by thermal decrepitation. Therefore, thermal decrepitation of a sample yielded less CH_4, much less O_2 and higher concentrations of CO_2, and N_2 than those when crushed. During heating, the color of the sample changed except in the case of hydrothermal vein calcites.

Table 1: Analysis of samples that have undergone heating, water-free:

Sample #	He	CH_4	N_2	O_2	Ar	CO_2
MCA-01	3.8E-03	2.6E+00	5.0E+00	1.1E-02	2.4E-02	7.4E+01
NMT-01	1.8E-04	2.0E+00	6.6E-01	2.0E-03	2.3E-04	8.6E+01
WB-01-94	6.2E-05	1.5E+00	6.0.E-01	6.5E-03	2.9E-04	8.3E+01
02-94-PC	1.2E-04	2.1E-01	2.2E+00	3.5E-03	3.3E-05	8.0E+01

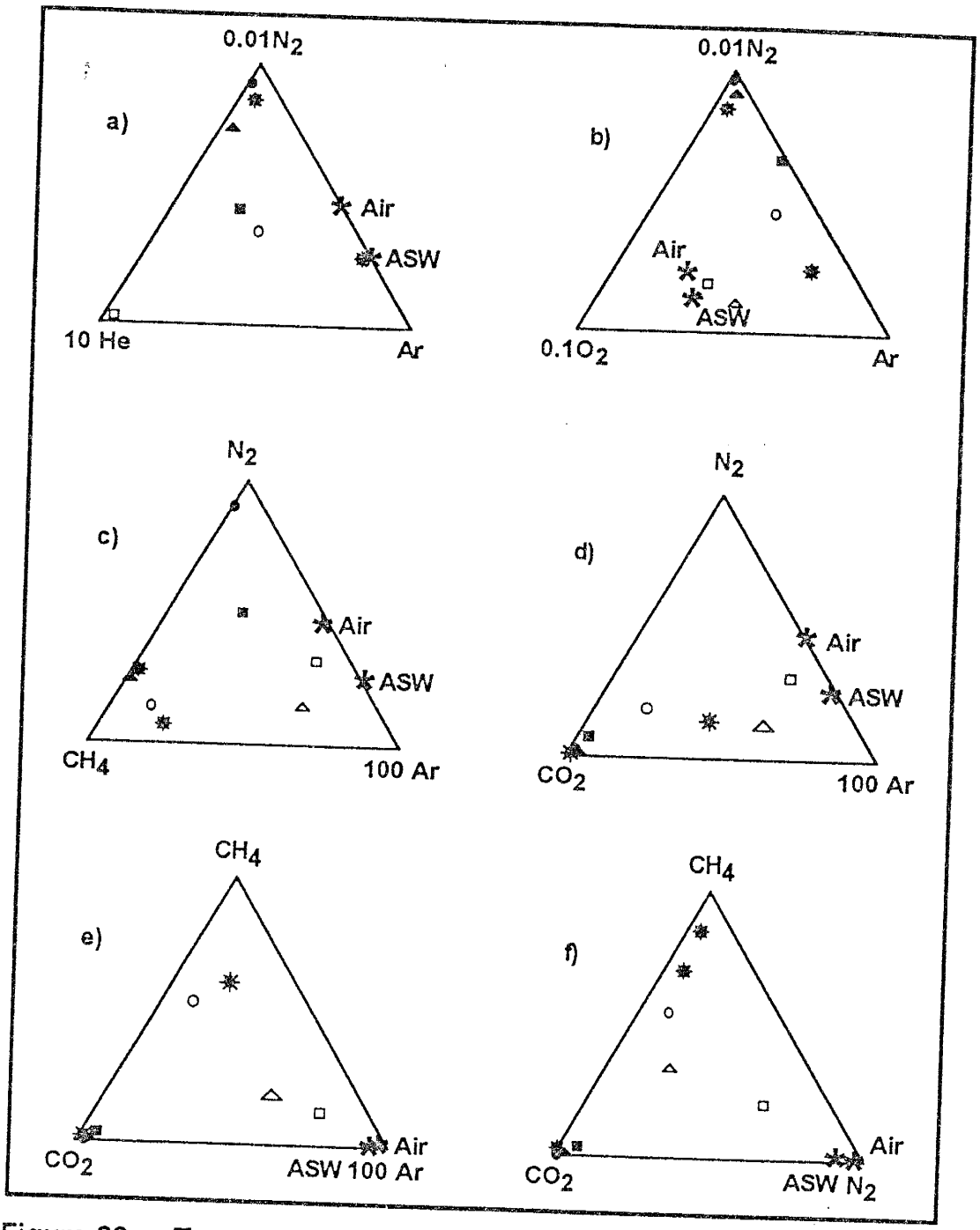

Figure 29: Ternary diagrams showing difference in analyses of split samples by the crushing (open symbols) and thermal decrepitation (closed symbols) methods. The 8 pointed star symbol is pedogenic calcite (non-indurated), the circle is pedogenic calcite (indurated), the triangle is travertine and the square is hydrothermal vein calcite.

Table 2: Analysis of samples that have undergone crushing, water-free:

Sample #	He	CH_4	N_2	O_2	Ar	CO_2
MCA-01	9.3E-01	1.6E+01	5.0E+01	1.4E+01	9.2E-01	1.9E+01
NMT-01	3.0E+00	2.8E+01	1.9E+01	7.5E+00	7.6E-01	4.2E+01
WB-01-94	9.4E-03	5.5E+01	9.7E+00	4.6E-01	3.0E-01	3.4E+01
02-94-PC	2.4E-04	1.1E+00	2.4E-01	5.7E-03	2.3E-03	9.4E-01

Table 3: Changes in gas ratios when we do analysis by heating and by crushing:

Sample	N_2/Ar	N_2/He	N_2/O_2	CO_2/CH_4	CO_2/N_2	Ar/He
PC(N-I)	inc. 1	inc. 1	inc. 1	inc. 2	inc. 2	no sig. inc.
PC(I)	inc. 2	inc. 1	inc. 1	inc. 2	inc. 1	no sig. inc.
Travertine	inc. 2	inc. 2	inc. 2	inc. 1	inc. 2	no sig. inc.
H. V. C.	inc. 1	inc. 2	inc. 2	inc. 1	inc. 1	no sig. inc.

"PC(N-I)" is Pedogenic calcite (non-indurated).

"PC(I)" is Pedogenic calcite (indurated).

"H. V. C." is Hydrothermal vein calcites.

"inc. 1" implies increased by one order of magnitude.

Table 3 shows that we cannot generate Ar and He during heating or during mechanical crushing. We plotted the data in **Table 1** on a ternary diagram. **Figure 29** shows the six plots where we observed differences in concentration of gases when we analyzed the in both the ways. **Table 4** shows the shift in volatiles when we do analysis by heating and by crushing. We termed

any gaseous species that increased its concentration when heated about its concentration when crushed as a positive shift in the concentration of that gas. We arranged the samples in the decreasing order of shift (that is, "+ve (4)" implies maximum positive shift; "-ve (4)" implies maximum negative shift).

Table 4: Shift in volatiles when we do analysis by heating and by crushing:

Sample	He	Ar	O_2	N_2	CH_4	CO_2
PC(N-I)	+ve (1)	-ve (3)	-ve (1)	+ve (2)	+ve (2)	+ve (2)
PC(I)	-ve (4)	-ve (4)	-ve (2)	+ve (1)	-ve (1)	+ve (1)
Travertine	-ve (3)	-ve (2)	-ve (3)	+ve (4)	+ve (4)	+ve (3)
H. V. C.	-ve (2)	+ve (1)	-ve (4)	+ve (3)	+ve (3)	+ve (4)

Abbreviations use in column "sample" are defined in **Table 3** in page 54.

With the help of equilibrium reactions between gaseous species, air trapped in micro-channels, and pyrolysis of the organic material, we explain the differences between analyses done by crushing and by thermal decrepitation methods. When we heated a sample, we released CO_2, CO and H_2 as CH_4 reacts with H_2O. Similarly, we released N_2 and H_2 as NH_3 reacts with H_2O at high temperatures (Norman et al., 1991; Musgrave and Norman, 1995). Equations 1 and 2 gives the reactions that might take place.

$$CH_4 + H_2O \text{ ======>} \quad H_2 + CO_2 + CO \quad \ldots\ldots\ldots\ldots (1)$$

$$NH_3 + H_2O \text{ ======>} \quad N_2 + H_2 \qquad \text{..... (2)}$$

The concentration of O_2 released during crushing is relatively greater than the amount released during heating (**Figure 29b**). Also, the O_2 content decreases during repeated crushing. This indicates that some of the trapped O_2 in the samples may occur in a manner different from other gaseous species. This trapped air may be present as adsorbed air onto micro-fractures, or air trapped by recent coatings. Since we degassed the samples at 100 °C to 125 °C under high vacuum, in either circumstances, we evacuated trapped air. During the analysis of the samples by thermal decrepitation, there was a change of color in the sample and a brown organic film condenses in the quartz furnaces. The coloration of the sample and the quartz furnace indicates that the organic material in the sample underwent pyrolysis.

The origin of C, H_2, N_2, and O_2 generated by the thermal decrepitation of a sample remained uncertain, as in the case of pedogenic calcite (non-indurated). Even though the decrepitation method yielded reliable analytical data for the rare gases, we cannot discriminate various calcium carbonates formed in different environments based on the concentration of He and Ar. On the other hand, when we crushed the samples, chemical reactions should not occur since we carried out the analyses at 25 °C. We did not generate gases such as CO_2 and H_2 because of the break down of heavier hydro-carbons, hence, analysis by

mechanical crushing provides better data for reactive gaseous species. Therefore, we discriminated various calcium carbonates formed in different environments based on the concentration of gaseous species released during crushing.

ANALYSES BY CRUSHING

Table B2 in appendix gives the concentration of gaseous species analyzed for various carbonates. We obtained similar, but not identical, ratios of gaseous species when we carried out multiple crushes on individual samples. Therefore, we crushed each sample atleast 3 to 4 times and we considered the mean of the concentration of the gases for the discrimination diagrams. Hydrothermal vein calcites showed the best repeatability of the analyses. **Table 5 a to d** gives the individual concentration of gaseous species analyzed and their means when we crushed repeatedly hydrothermal vein calcites, ancient travertines, pedogenic calcites (indurated and non-indurated).

Table 5a: Repeated analysis of hydrothermal vein calcite sample, "MCA-01-94".

Sample #	He	CH_4	N_2	O_2	Ar	CO_2
Crush A	6.4E-01	1.1E+01	6.1E+01	1.2E+01	1.0E+00	1.5E+01
Crush B	1.2E+00	2.1E+01	4.3E+01	1.4E+01	1.0E+00	2.0E+01
Crush C	8.6E-01	1.6E+01	4.9E+01	1.5E+01	8.4E-01	1.9E+01
Crush D	1.3E+00	1.9E+01	4.1E+01	1.5E+01	7.7E-01	2.3E+01
Mean	9.8E-01	1.7E+01	4.9E+01	1.4E+01	9.1E-01	1.9E+01

Table 5b: Repeated analysis of ancient travertine sample, "04-AM-93".

Sample #	He	CH_4	N_2	O_2	Ar	CO_2
Crush A	3.7E-01	1.0E+01	2.0E+01	6.8E+00	2.9E-01	6.2E+01
Crush B	3.4E-01	6.3E+00	1.2E+01	3.8E+00	2.3E-01	7.7E+01
Crush C	3.7E-01	5.7E+00	7.6E+00	3.0E+00	1.8E-01	8.3E+01
Crush D	5.4E-02	5.0E+00	1.7E+01	3.8E+00	2.3E-01	7.4E+01
Mean	2.8E-01	6.8E+00	1.4E+01	4.4E+00	2.3E-01	7.4E+01

Table 5c: Repeated analysis of pedogenic calcite (indurated) sample, "05-94-PC".

Sample #	He	CH_4	N_2	O_2	Ar	CO_2
Crush A	5.3E-03	7.3E+01	8.2E+00	3.2E-01	4.2E-02	1.8E+01
Crush B	1.3E-02	5.1E+01	7.2E+00	1.7E-01	4.3E-02	4.2E+01
Crush C	5.7E-03	4.7E+01	5.9E+00	2.7E-02	3.6E-02	4.7E+01
Crush D	3.5E-03	3.8E+01	1.1E+01	2.0E-01	4.5E-02	5.1E+01
Mean	6.8E-03	5.2E+01	7.9E+00	1.8E-01	4.6E-02	4.0E+01

Table 5d: Repeated analysis of pedogenic calcite (non-ind.) sample, "WB-02-94".

Sample #	He	CH_4	N_2	O_2	Ar	CO_2
Crush B	4.1E-02	5.4E+01	7.8E+01	3.5E-01	1.1E-01	3.8E+01
Crush C	2.3E-03	6.7E+01	1.1E+01	2.4E-01	8.0E-02	2.2E+01
Crush D	2.7E-02	6.8E+01	8.8E+01	1.7E+01	1.3E-01	6.0E+00
Crush E	1.7E-03	6.4E+01	3.3E+01	7.1E-01	2.4E-01	1.8E+00
Mean	1.8E-02	6.3E+01	1.5E+01	4.7E+00	1.4E-01	1.7E+01

When we plotted the data from the repeated crushes of hydrothermal vein calcites on ratio graphs, as shown in **Figure 30**, they all plotted on a straight line instead of exhibiting scattering. We show the analytical precision for any analysis from the width of the scattering, but in the case of ratio graphs, we do not relate crush to crush variation with the width of the scattering for analytical precision. The crush to crush variation suggests that we opened different assemblages of fluid inclusions during analysis that systematically vary in the composition. Also, each successive crush yielded lesser amounts of O_2.

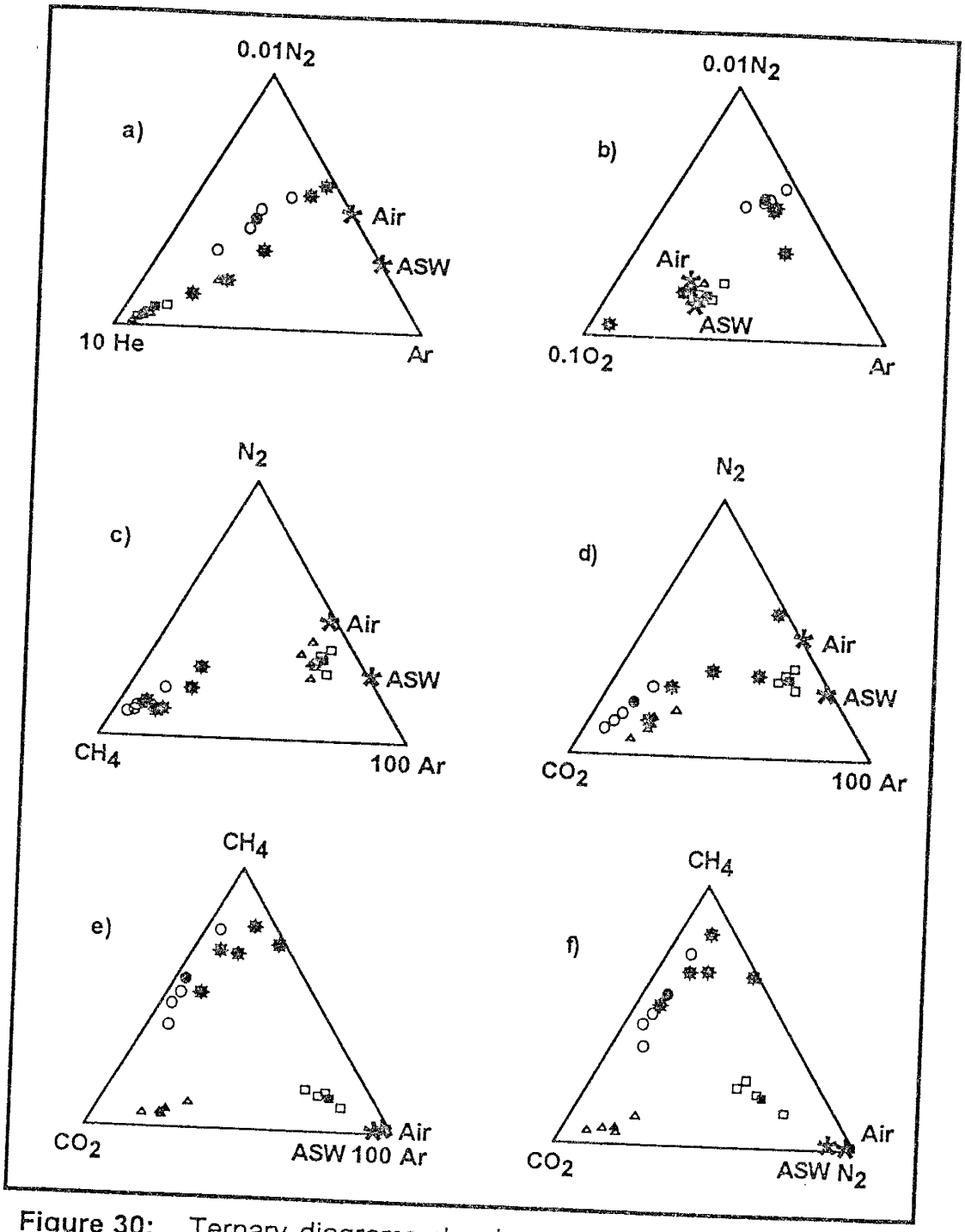

Figure 30: Ternary diagrams showing sample variation between analyses during multiple crushing (open symbols) and their individual means (closed symbols). The 8 pointed star symbol is pedogenic calcite (non-indurated), the circle is pedogenic calcite (indurated), the triangle is travertine and the square is hydrothermal vein calcite.

Figure 31 indicates that the concentrations of gases that have under gone repeated crushes were varying within one sigma range. Concentration of gases released during the initial crush in the case of pedogenic calcite (non-indurated) and calcretes were slightly higher than the following crushes.

We discussed the analyses of the samples based on the individual gases and their respective ratios. **Table B3** in appendix gives the gas to water ratios for the analysis of different carbonates. **Table 6** illustrates the variations in H_2O, their mean values and their range in H_2O to gas ratios. **Table 6** shows that less crystalline substances such as pedogenic calcite (non-indurated and indurated) varies widely in the amount of water.

Table 6: Variation of H_2O and H_2O/gas ratio in different carbonates during crushing:

Sample	Range in H_2O (in mole %)	Mean H_2O %	Range of H_2O/Gas ratio	Magnitude of Range
PC(NI)	20.7 to 83.6	53.9	0.3 to 5.1	>1 order
PC(I)	18.2 to 99.5	87.9	0.2 to 216.2	3 order
Act. Trav.	98.3 to 99.9	99.8	57.2 to 4974.3	2 order
Ant. Trav.	99.4 to 99.8	99.7	153.1 to 622.7	<1 order
H. V. C.	99.7 to 99.9	99.8	396.4 to 1142.3	<1 order
Calcrete	34.8 to 99.9	88.3	0.5 to 1093.4	>3 order

Abbreviations used in column "sample" are defined in **Table 3**, page 54.

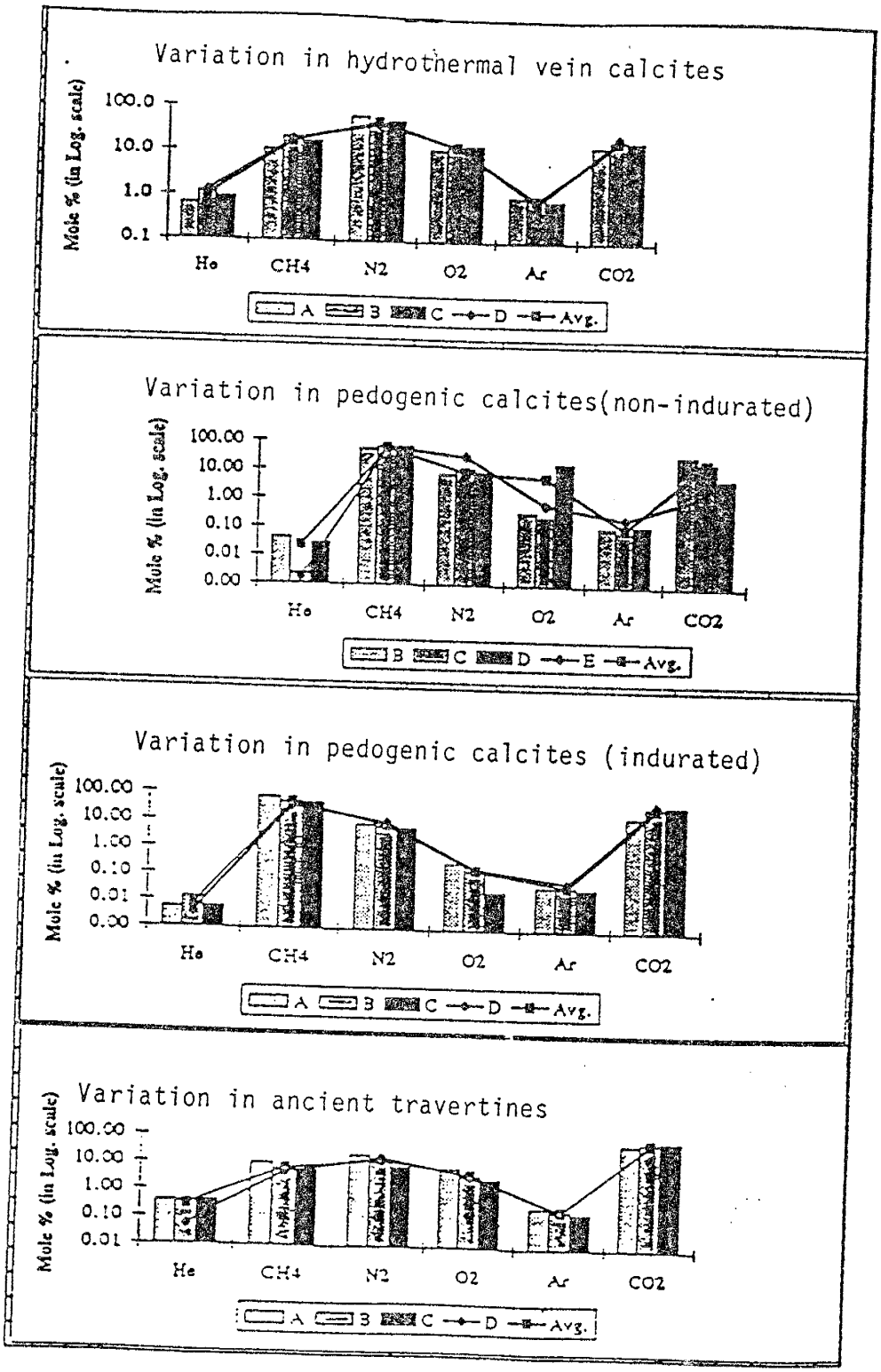

FIGURE 31: Variation of volatiles during multiple crushing on a X-Y diagram.

The low ratio of water to gas in the case of pedogenic calcites (non-indurated and indurated) may indicate that the fluid inclusions in the samples include a liquid phase as well as a vapor phase. Thus, at low temperatures and pressures, it is not possible for vapor dominant inclusions to dissolve in water. We speculate that the genesis of this vapor filled inclusion to occur at the vadose zone. Conversely, samples that show high water to gas ratios as in calcretes, hydrothermal vein calcites, ancient, and active travertines imply that water are a dominant phase within the inclusions. Hence, they occur with the deposition by deep ground waters.

For most of the samples, we applied descriptive statistics to check for the variance and standard deviation. **Table B4** in appendix gives the statistical description for all gaseous species analyzed individually for various carbonates and **Table B5** in appendix illustrates the statistical description in the case of water-free analyses. If the value of variance in a group of samples was low, then we infer that the low value of variance distributes samples within a narrow range. Conversely, high value of variance distributes samples within a wide range.

We made sigma error plots for all samples, individually as well as collectively, to check whether the concentration of gases released would fall within one sigma error or within two sigma errors. A sigma error implies that it's the range bordered by an upper limit and a lower limit, wherein, a maximum

number of samples will fall. We calculate the upper limit of the range by adding one standard deviation to the mean of the analyses, while we calculate the lower limit of the range by subtracting one standard deviation from the mean. The area increases two-fold when we consider twice the standard deviation in our calculation, to accommodate more number of samples. Once we know the number of samples falling within one or two sigma ranges, we then calculate their respective percentages. **Tables 8, 10, 12, 14, 16 and 18** show the percentage of samples falling within one sigma range. **Tables 7, 9, 11, 13, 15 and 17** show the variation of gases in different carbonates during crushing.

Pedogenic calcites (non-indurated)

When we crushed pedogenic calcites (non-indurated), the principle gas component evolved was CH4. The CH_4/H_2O ratios are less variable than the CH_4/CO_2 and H_2O/CO_2 ratios **(Table 7)**. Helium, O_2 and Ar showed low variance and lie within a narrow range, in contrast H_2O and CH_4 showed high variance while N_2 and CO_2 varied moderately (**Table B4**). Table 8 shows the percentage of samples falling within one sigma error and two sigma errors for pedogenic calcites (non-indurated). The number within parenthesis gives the sample size of the mineral collected from a given locality. Collectively, we see in most of the samples that their concentration of He and Ar lie within one sigma range.

Table 7: Variation of gases in pedogenic calcites (non-indurated) during crushing:

Principal gas and range (mole %)	Decreasing amounts of other gases	CH_4/CO_2 range (in mole %)	CH_4/H_2O range (in mole %)	H_2O/CO_2 range (in mole %)
CH_4, 9.8 to 51.9	N_2, CO_2, O_2, Ar and He	1.1 to 105.5	0.4 to 8.2	0.8 to 130.2

Table 8: Sigma variation in different pedogenic calcites (non-indurated) during crushing:

Gas	WB's (8)	NC's (6)	WR's (9)	Miss. (6)	Overall-1σ	Overall-2σ
He	88 %	83 %	89 %	83 %	97 %	100 %
CH_4	63 %	83 %	67 %	83 %	62 %	100 %
H_2O	63 %	50 %	67 %	50 %	69 %	100 %
N_2	75 %	83 %	78 %	83 %	79 %	90 %
O_2	88 %	83 %	89 %	50 %	86 %	97 %
Ar	88 %	67 %	56 %	67 %	90 %	93 %
CO_2	88 %	67 %	78 %	67 %	83 %	97 %

Pedogenic calcites (indurated)

In the analysis of pedogenic calcites (indurated), CO_2 was slightly more dominant gaseous phase (**Table B4).** We observed low variance in He and Ar suggesting that the concentrations of these gases lie within a narrow range. Samples showed high variability in the case of H_2O and CO_2, while N_2 and CH_4 varied moderately. We see from **Table 9** that CH_4/CO_2, H_2O/CO_2 and CH_4/H_2O ratios ranged within one, two and three orders of magnitude. It is observed that the pedogenic calcites (indurated) have relatively high concentrations of CO_2 and low concentrations of H_2O compared to the pedogenic calcite (non-indurated). **Table 10** shows the percentage of samples falling within one sigma error for pedogenic calcites (indurated).

Table 9: Variation of gases in pedogenic calcites (indurated) during crushing:

Principal gas and range (mole %)	Decreasing amounts of other gases	CH_4/CO_2 range (in mole %)	CH_4/H_2O range (in mole %)	H_2O/CO_2 range (in mole %)
CO_2, 0.1 to 13.9	N_2, CH_4 O_2, Ar and He	0.3 to 1.3	1.3 to 921.1	0.4 to 402.7

Table 10: Sigma variation in different pedogenic calcites (indurated):

Gas	PC's (7)	Overall-1σ (10)
He	86 %	80 %
CH_4	86 %	90 %
H_2O	86 %	90 %
N_2	71 %	80 %
O_2	86 %	90 %
Ar	71 %	80 %
CO_2	86 %	90 %

Travertines

When we compared volatiles in travertines with the analysis of parent spring waters we saw that trapping of the volatiles takes place during the precipitation of the travertines from active springs. The ratio of N_2/Ar in some spring waters appears to approach the ratio in air and this may be due to the turbulence of the spring waters. Generally, we observed that the ratios of N_2/Ar in travertines are similar to the present spring waters; however, some have N_2/Ar ratios nearer to the air saturated water. Sample-to-sample variations in the recent travertines from different springs, are due to the effervescence of the waters from the spring and their equilibration with the air. There is a systematic decrease of CO_2 in active travertines from La Cienaga when we collected samples away from the spring, but samples from Soda Dam did not show any variation (Norman et al., 1994).

We saw some differences in the volatile compositions within active and ancient travertines. **Table B4** in appendix shows that the ancient travertines have greater amounts of He, O2 and CO2 than travertines deposited by active springs. The concentrations of CH_4 and Ar are similar in paleo and recent travertines. Recent travertines have higher amounts of N_2 than paleo travertines. We assume that as travertines form, trapping of He, O_2 and CO_2 and degassing of N_2 continues within the system.

Active Travertines

Table B4 in appendix indicates that N_2 was the principle gas component evolved when we crushed active travertines. Helium, O_2, Ar and CO_2 show low variance and distribute within a narrow range. Water, N_2 and CH_4 show moderate variance. **Table 11** shows that the CH_4/CO_2 ratio was always less than one and ranged within an order of magnitude. We observed very high ratios of CH_4/H_2O and H_2O/CO_2 in active travertine samples that ranged within one and two orders of magnitude (**Table 11**). **Table 12** shows the percentage of samples falling within one sigma error for active travertines.

Table 11:
Variation of gases in active travertines during crushing:

Principal gas and range (in mole %)	Decreasing amounts of other gases	CH_4/CO_2 range (in mole %)	CH_4/H_2O range (in mole %)	H_2O/CO_2 range (in mole %)
N_2, 0.01 to 1.6	CO_2, CH_4, O_2, Ar and He	0.02 to 0.99	2059.9 to 69244.4	631.6 to 25005.2

Table 12: Sigma variation in different active travertines:

Gas	Overall -1σ (18)
He	94 %
CH_4	75 %
H_2O	88 %
N_2	88 %
O_2	88 %
Ar	88 %
CO_2	88 %

Ancient Travertines

When we crushed ancient travertines the principle gas component evolved was CO_2 (**Table B4** in appendix). The evolved gases exhibit low to moderate variance. The CH_4/CO_2 ratio was less than one, while CH_4/H_2O and H_2O/CO_2 ratios ranged within one order of magnitude **(Table 13)**. Table 14 shows the percentage of samples falling within one sigma error for all ancient travertines.

Table 13: Variation of gases in ancient travertines during crushing:

Principal gas and range (mole %)	Decreasing amounts of other gases	CH_4/CO_2 range (in mole %)	CH_4/H_2O range (in mole %)	H_2O/CO_2 range (in mole %)
CO_2, 0.1 to 0.4	N_2, CH_4, O_2, He and Ar	0.1 to 0.9	459.8 to 5179.7	235.0 to 1403.4

Table 14: Sigma variation in different ancient travertines:

Gas	NMT's (7)	AM's (5)	Overall -1σ (12)
He	57 %	60 %	75 %
CH_4	71 %	80 %	92 %
H_2O	86 %	60 %	83 %
N_2	71 %	80 %	83 %
O_2	86 %	100 %	92 %
Ar	86 %	80 %	83 %
CO_2	86 %	60 %	75 %

Hydrothermal vein calcites (H.V.C.'s)

Analyses of hydrothermal vein calcites plot in a similar fashion to those of travertines. When we crushed hydrothermal vein calcites the principle gas evolved was N_2 (**Table B4** in appendix) and the evolved gases exhibited low to moderate variance. The minor concentration of O_2 measured in the analysis of hydrothermal vein calcites was due to trapping of air after the precipitation of the hydrothermal vein calcites (Henley et al., 1984). The range of CH_4/CO_2 ratio was within one order of magnitude, while we observed that the range of CH_4/H_2O and H_2O/CO_2 ratios to be very high in all hydrothermal vein calcites **(Table 15)**. **Table 16** shows the percentage of samples falling within one sigma error for hydrothermal vein calcites.

Table 15: Variation of gases in H.V.C.'s during crushing:

Principal gas and range (mole %)	Decreasing amounts of other gases	CH_4/CO_2 range (in mole %)	CH_4/H_2O range (in mole %)	H_2O/CO_2 range (in mole %)
N_2, 0.03 to 0.1	CO_2, CH_4, O_2, He and Ar	0.2 to 1.4	1976.7 to 5082.2	723.3 to 4650.7

Table 16: Sigma variation in different hydrothermal vein calcites:

Gas	VC's-Luis Lopez (8)	VC's-Miss. (5)	Overall -1σ (13)
He	75 %	60 %	62 %
CH_4	75 %	80 %	77 %
H_2O	75 %	80 %	69 %
N_2	63 %	60 %	77 %
O_2	63 %	60 %	69 %
Ar	75 %	80 %	62 %
CO_2	75 %	60 %	85 %

Calcretes

When we crushed calcretes the principle gas component evolved was CH_4, N_2 and CO_2 (**Table B4** in appendix). The evolved gases exhibited low to high variance. We found that the mean concentration of CH_4, N_2 and CO_2, in water free system to be close to each other. The range of CH_4/CO_2 ratio was within one order of magnitude, while we observed that the range of CH_4/H_2O and H_2O/CO_2 ratios was 3 orders of magnitude in all calcretes **(Table 17)**. Table 18 gives the percentage of samples falling within one sigma error for calcretes.

Table 17: Variation of gases in calcretes during crushing:

Principal gas and range (mole %)	Decreasing amounts of other gases	CH_4/CO_2 range (in mole %)	CH_4/H_2O range (in mole %)	H_2O/CO_2 range (in mole %)
CH_4, N_2 and CO_2	O_2, Ar and He	0.4 to 7.6	1.0 to 2808.1	7.8 to 4273.4

Table 18: Sigma variation in different calcretes:

Gas	Calcretes (6)
He	83 %
CH_4	83 %
H_2O	83 %
N_2	83 %
O_2	83 %
Ar	83 %
CO_2	83 %

Statistical treatment of the analysis: Cluster Analysis

Cluster analysis separates a database into groups or clusters. Cluster analyses were performed on 126 analyses. The NCSS program (Hintze, 1992) separated the 126 analyses into two groups. Grouping was done using the major volatiles H_2O, CH_4, CO_2 and N_2. The percentage of variation for cluster 1 and cluster 2 are 100% and 58% respectively. **Table 19** shows the percentage means of the volatiles in each group and **Table 20** shows the lower and the upper limits of the different volatiles in these two groups.

Table 19 Cluster means report separating the analysis into two groups.

Gas	Group I (% means)	Group II (% means)
He	1.29E-01	6.83E-03
CH_4	1.43E-00	2.79E+01
H_2O	**9.75E+01**	**4.87E+01**
N_2	5.41E-01	1.41E+01
O_2	4.43E-01	8.64E-01
Ar	5.08E-01	1.67E-01
CO_2	5.03E-01	8.19E+00

Table 20 Lower and Upper limit of the volatiles in the two groups.

Gas	Group I (% limits); Lower to Upper.	Group II (% limits); Lower to Upper.
He	8.50E-07 to 5.71E-03	1.07E-03 to 4.02E-02
CH_4	1.44E-03 to 2.35E+01	3.22E+00 to 6.78E+01
H_2O	6.91E+01 to 1.00E+02	1.31E+01 to 7.79E+01
N_2	1.78E-03 to 7.83E+00	1.11E+00 to 5.84E+01
O_2	1.83E-05 to 1.22E+00	1.24E-03 to 8.23E+00
Ar	7.50E-05 to 9.88E-02	1.07E-02 to 6.94E-01
CO_2	1.51E-04 to 8.28E+00	4.11E-01 to 4.53E+01

Statistical treatment of the analysis: Factor Analysis

Factor analyses were also performed on all the 126 analyses. Factor analysis allows us to identify the contribution of individual factors to the total variance. It reduces the number of variables (i.e. the volatiles) in a database and finds a few weighted averages (factors) of the original variables that summarizes the overall information. Thus, using NCSS program (Hintze, 1992), we applied factor analyses on the two groups of the 126 analyses that were separated by the cluster analysis. Factor analysis on group I carbonates showed that N_2 correlated positively with CO_2, and O_2 correlated positively with Ar. The NCSS program observed a negative correlation between CH_4 and H_2O. Nitrogen correlated positively with CO_2 in Group II carbonates.

The eigenvalues are used to determine the number of factors to retain. **Table 21** shows the eigenvalues and their percentage of the total variation in the variables accounted for by the factor. The sum of the eigenvalues is equal to the number of the variables. Factors whose eigenvalues were greater than one were only considered while making the factor pattern plots. We consider only factor 1 and factor 2 in the factor pattern plots involving group I carbonates, while factor 1, factor 2 and factor 3 were considered in the factor pattern plots involving group II carbonates. Factor pattern plots determine the different volatiles that make up the factors. **Table 22** shows different volatiles within these factors,

while **Figures A26** and **A27** in appendix show the factor pattern plots for group I and group II carbonates.

Table 21 **Eigenvalues for Group I and Group II carbonate.**

Factor	Group I (high H_2O) Eigenvalue; %		Group II (low H_2O) Eigenvalue; %	
1	3.83;	54.75 %	2.58;	36.79 %
2	1.64;	23.48 %	1.61;	22.99 %
3	0.95;	13.51 %	1.39;	19.82 %
4	0.50;	7.16 %	0.80;	11.39 %
5	0.05;	0.62 %	0.48;	6.87 %
6	0.02;	0.34 %	0.13;	1.92 %
7	0.01;	0.14 %	0.01;	0.22 %

Table 22 **Volatiles in various factors for Group I and II carbonate.**

Factor	Volatiles in Group I: Factor 1 and Factor 2	Volatiles in Group II: Factor 1; Factor 2 and Factor 3
1	H_2O, CH_4 CO_2 and He	CO_2, N_2, H_2O and O_2
2	O_2 and Ar	CH_4, He and H_2O
3		Ar, O_2 and He

O_2 Contamination

The concentration of O_2 as measured in the hydrothermal vein calcites and ancient travertines appeared to be of secondary origin, because we obtained very small amounts of O_2 when the same samples were heated. We assumed that the source for excess O_2 in the analyses may be from air trapped in the micro-channels or adsorbed air trapped by post formation of the carbonate coatings. Because the concentration of trapped O_2 was relatively small, we made no corrections to the measured N_2 and Ar concentrations.

Discrimination diagrams

Since analyses of each type of carbonate mineral exhibited gross similarities on selected ternary diagrams, each analysis occupies different portions of the figure. We constructed ternary diagrams and we altered the proportions of the analyzed gases to spread the analyses on the diagram. Each Figures illustrates six ternary diagrams with different axes and we named them from 'a' to 'f'. **Figures 32 to 37** show the distribution of different samples such as ancient travertines, travertines deposited by active springs, pedogenic calcites (non-indurated), pedogenic calcites (indurated), hydrothermal vein calcites and calcretes on these six ternary diagrams.

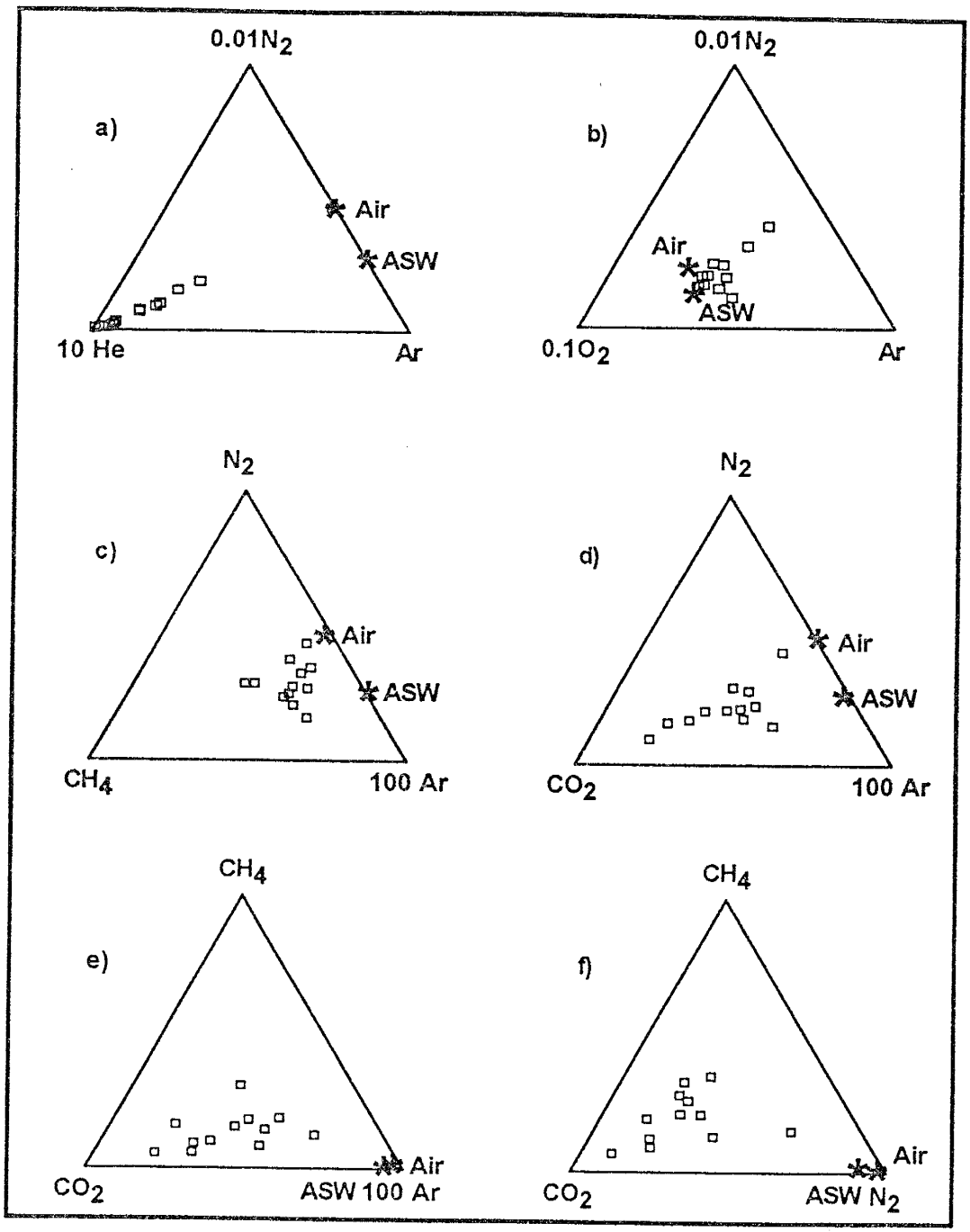

FIGURE 32: Ternary diagrams showing variation of analyses in 12 ancient travertines (open square symbols). The samples were collected from Aparejo Mesa and from New Mexico Travertine Company, near Belen.

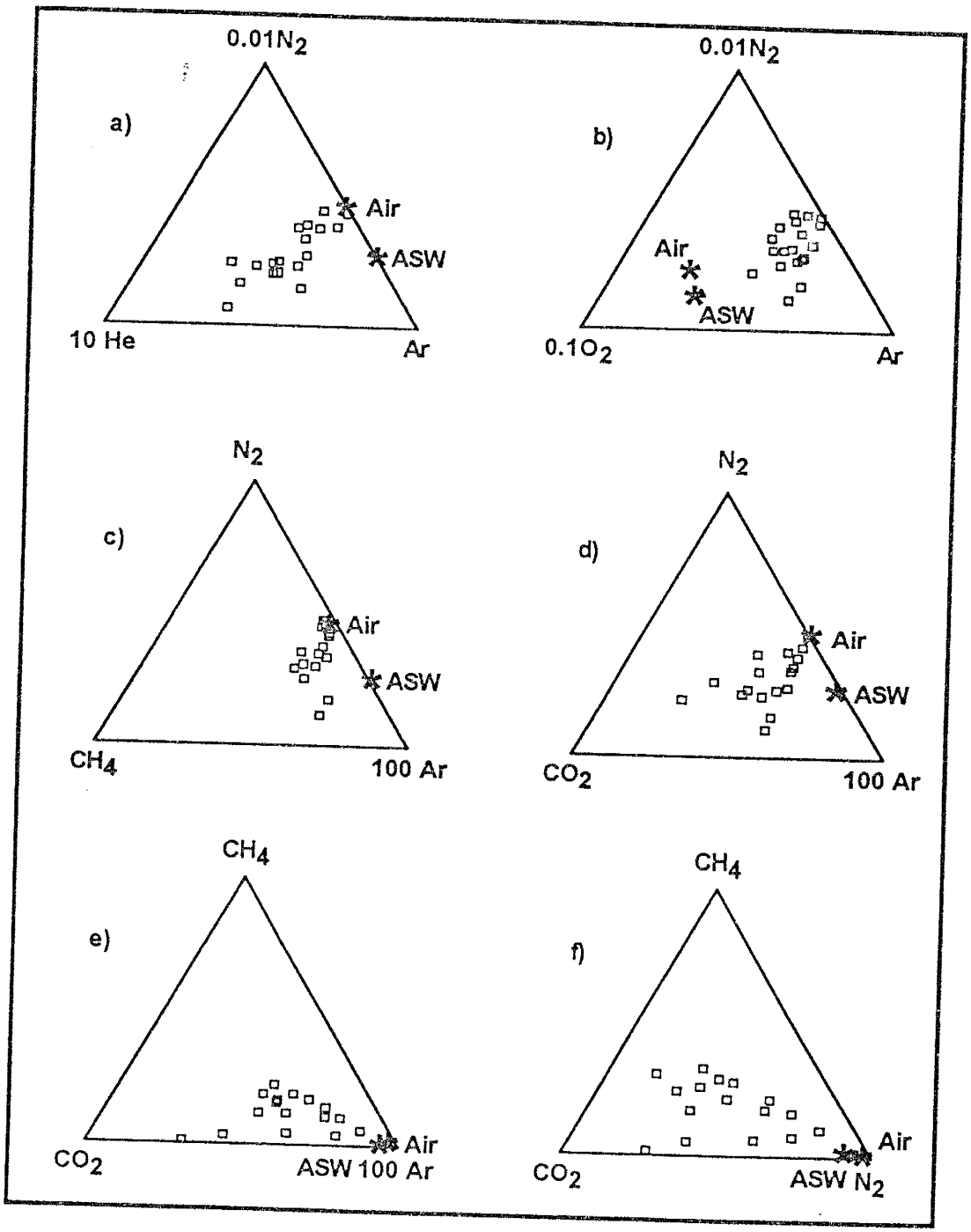

FIGURE 33: Ternary diagrams showing variation of analyses in 18 active travertines which were deposited at various springs (open squares symbols). The samples were collected from Soda Dam, Arroyo Salado, La Cienaga, Las Huertas and Mimbres Hot Springs in New Mexico.

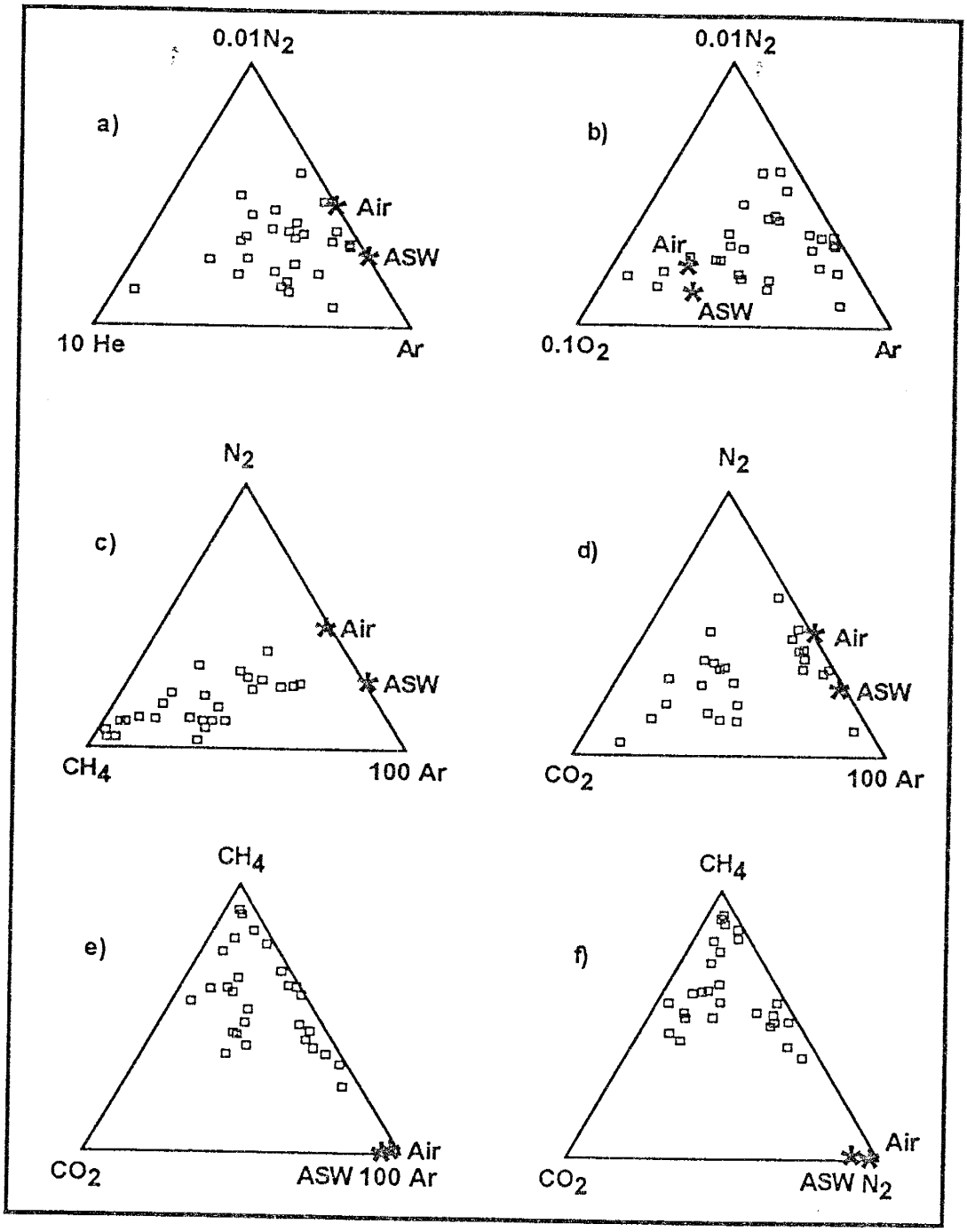

FIGURE 34: Ternary diagrams showing variation of analyses in 29 pedogenic calcites (non-indurated) that are shown as open square symbols. The samples were collected from White Rock, from West of I-25 near Belen, from San Antonio and from East of Socorro, New Mexico.

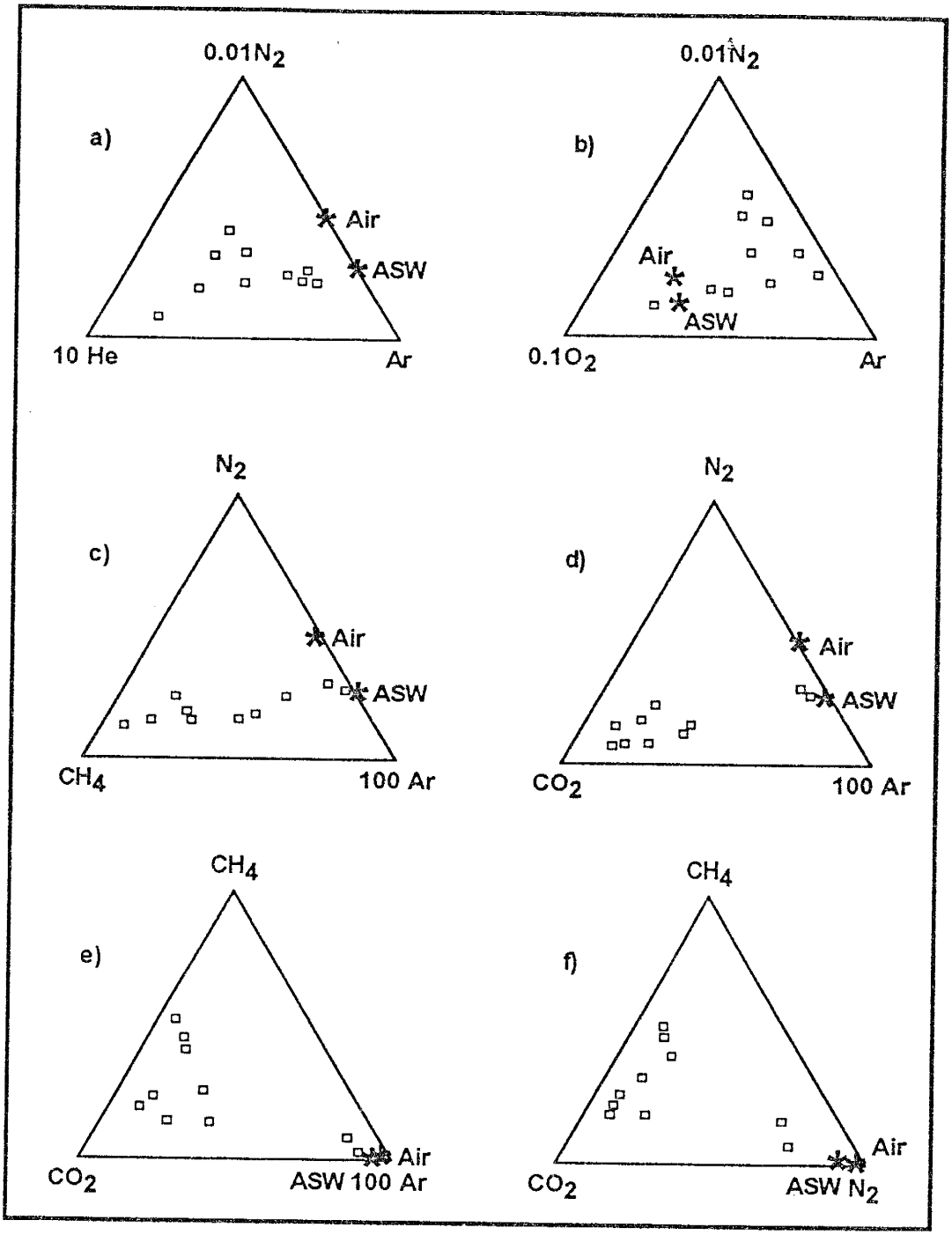

FIGURE 35: Ternary diagrams showing variation of analyses in 10 pedogenic calcites (indurated) shown here as open square symbols. The samples were collected at East of Socorro (in Loma De Las Canas Quadrangle), New Mexico.

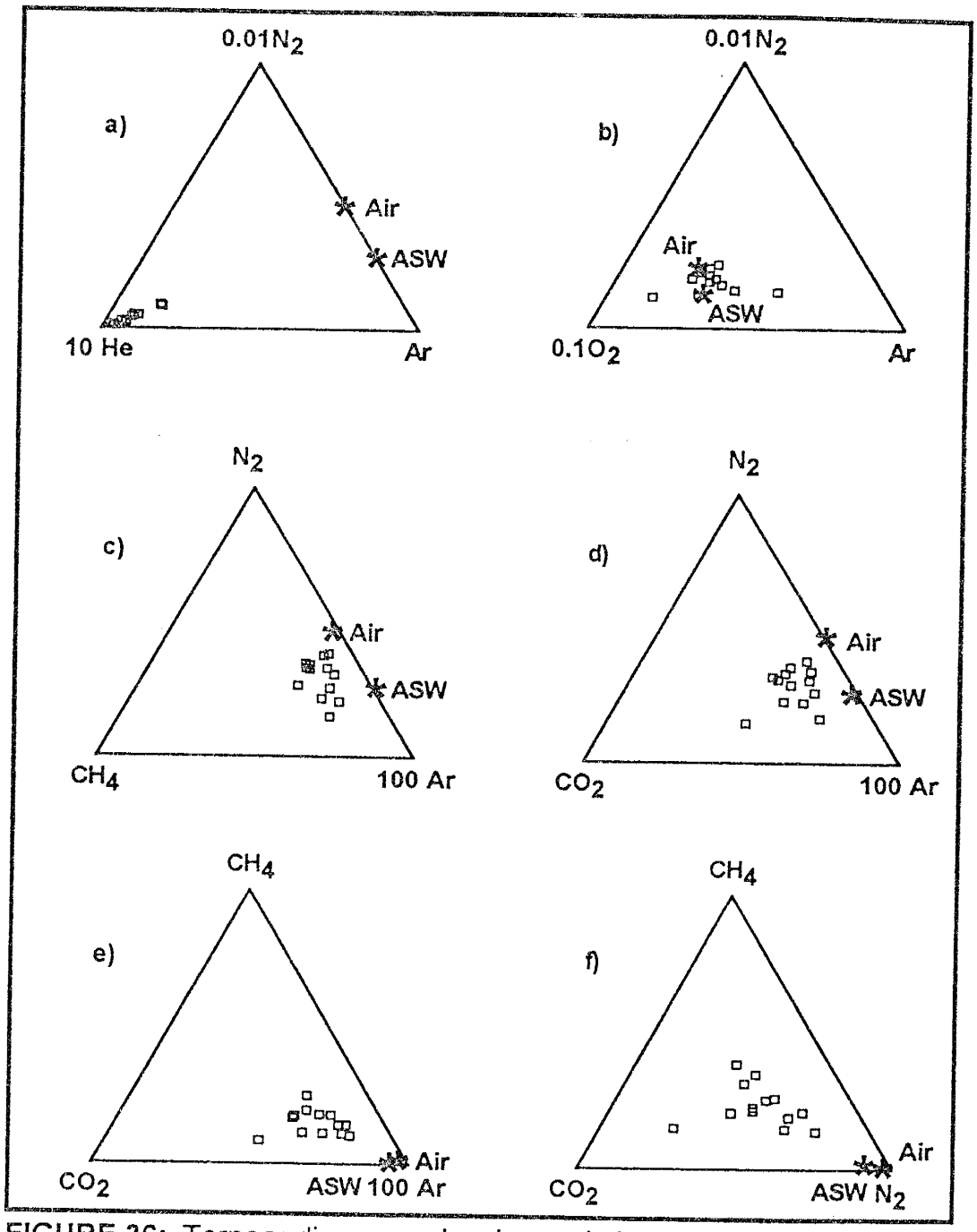

FIGURE 36: Ternary diagrams showing variation of analyses in 13 hydrothermal vein calcites (open square symbols). Eight hydrothermal vein calcites were collected from San Luis manganese district near Socorro, New Mexico. The rest were collected from Jauntia mine, Fairview mine, Mannie Baird mine, San Pedro mine, and a core sample from Valles Caldera, New Mexico.

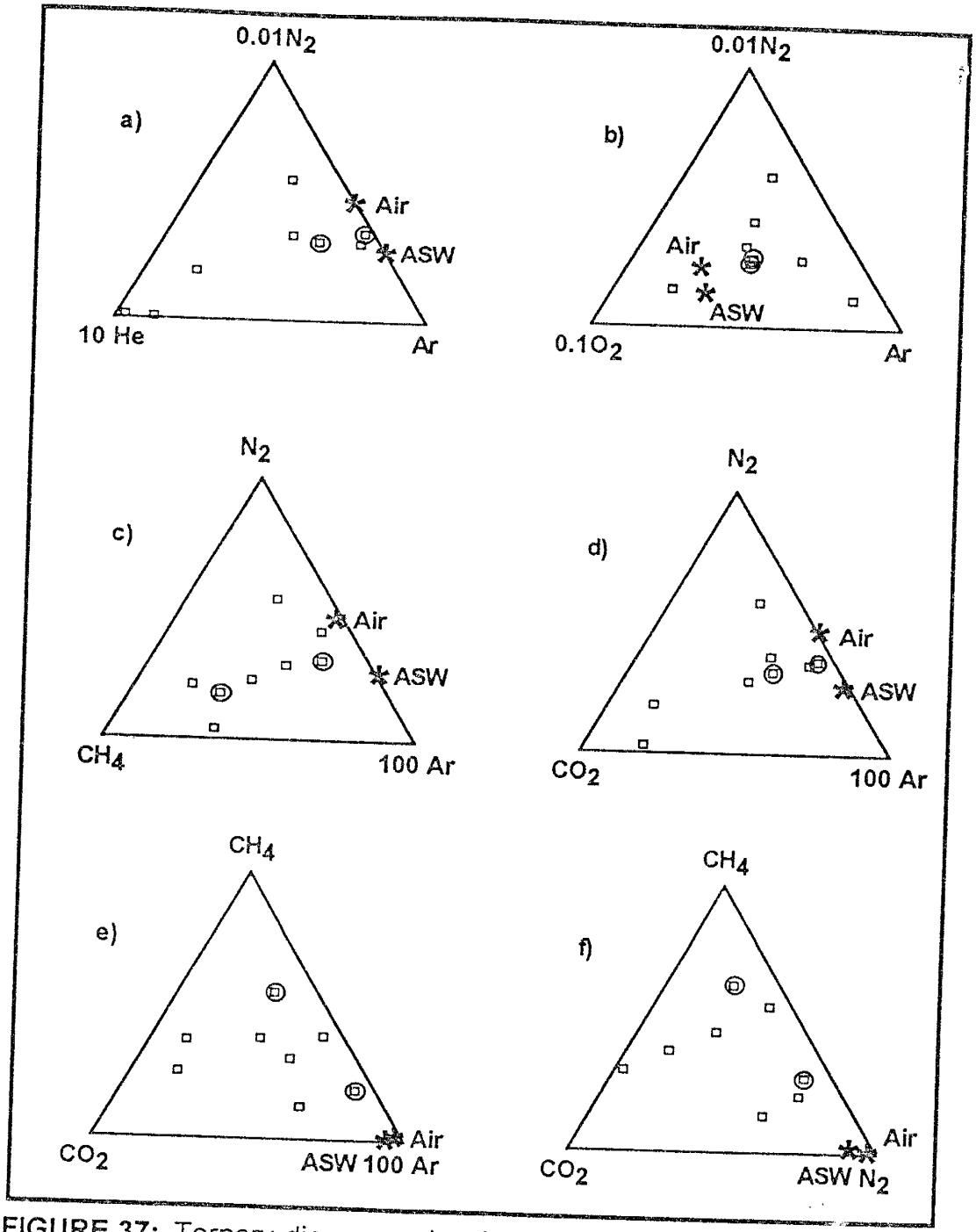

FIGURE 37: Ternary diagrams showing variation of analyses in 6 calcretes and 2 calcite concretions in sand. Six calcretes were collected near San Antonio and near Socorro (open square symbols) in New Mexico. Two calcite concretions in sand (open square symbols that are circled) were collected near Bosque, New Mexico.

From **Figure 32a** we observed that the analyses of ancient travertines do plot linearly near the He axis. We see depleted concentrations of O_2 in travertines deposited by active springs (**Figure 33b**). Pedogenic calcites (non-indurated) produced high amounts of CH_4 (**Figure 34e and f**), while pedogenic calcites (indurated) were rich in CO_2. Hydrothermal vein calcites always plot together within a narrow region (**Figure 36a to e**) while calcretes showed maximum spread in the analyses (**Figure 37**). The concentration of CH_4 was lower in the pedogenic calcites (indurated) than in the pedogenic calcites (non-indurated). Also, the gas to water ratio was high in pedogenic calcites (non-indurated and indurated), hence, pedogenic calcites (indurated) separates themselves from the calcretes, travertines and hydrothermal vein calcites.

We combined ternary diagram "e" from figures 32 to 37 and we show the resultant plot on **Figure 38a**. Since the amount of H_2O in various carbonates was varying, we constructed different ternary diagrams with H_2O in one of its axis (**Figure 38b to d**). The ternary diagrams were differentiated into two regions based on the grouping of the carbonates from the cluster analysis. The line that separated the two groups of carbonates had the amount of H_2O equal to 73.5 %. In **Figure 38b,** we see that the analyses of ancient travertines, travertines

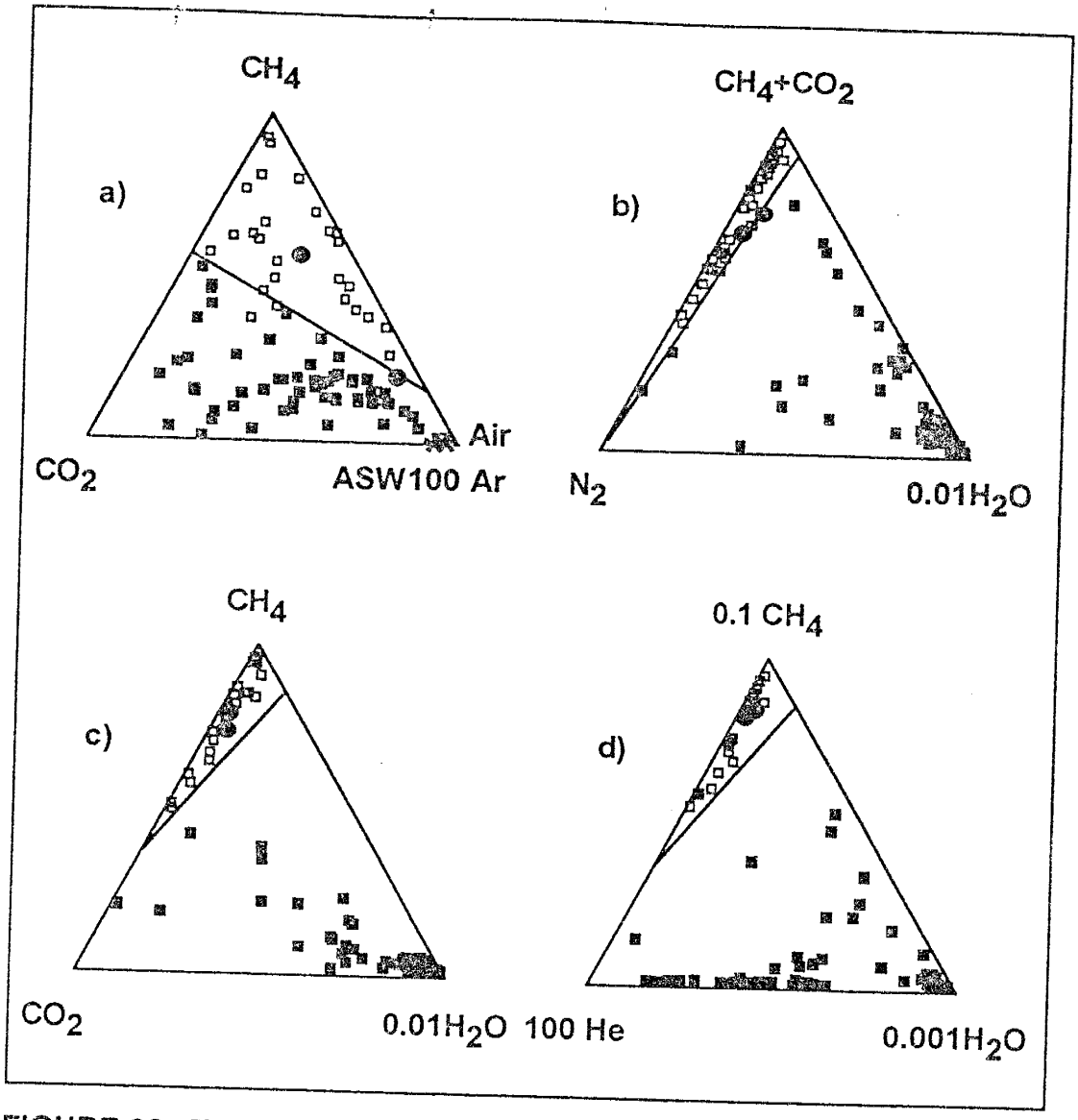

FIGURE 38: Ternary diagrams showing variation of analyses in 92 different types of carbonates. Fluid inclusion analyses of all pedogenic calcites (non-indurated) is indicated by open square symbols. Analyses of all hydrothermal vein calcites, pedogenic calcites (indurated), calcretes, active and ancient travertines are indicated by filled square symbols. The 2 calcite concretions in sand given by Peter Mozley, were collected near Bosque and indicated as filled circles.

deposited by active springs, hydrothermal vein calcites and calcretes were clearly distinct from the analyses of pedogenic calcites (non-indurated). Also, pedogenic calcites (indurated) extend from the field occupied by pedogenic calcites (non-indurated) to the field occupied by the ancient travertines, travertines deposited by active springs, hydrothermal vein calcites and calcretes. In **Figures 38c** and **38d,** where He replaces CO_2 in one of the axis, and the ternary diagram includes CH_4 and H_2O, it shows that the analyses of pedogenic calcites (non-indurated) and the calcite concretions occur within a narrow range. Vein calcites from trenches and fracture-fillings within LANL were similar to the analyses of pedogenic calcites (non-indurated). **Figure 39** illustrates graphically all the analyses of LANL samples on the diagrams that discriminates pedogenic calcites (non-indurated) from other carbonates.

Pedogenic calcites (indurated) samples taken from top to bottom in an outcrop indicate a systematic change in the analyses. Analyses of samples taken from the top of an outcrop have concentration of gases similar to the analyses of pedogenic calcites (non-indurated), while samples collected from the bottom have more water. We also observed that as the depth of the sample collection increases, the ratio of CO_2 to CH_4 increases **(Figure 40)**.

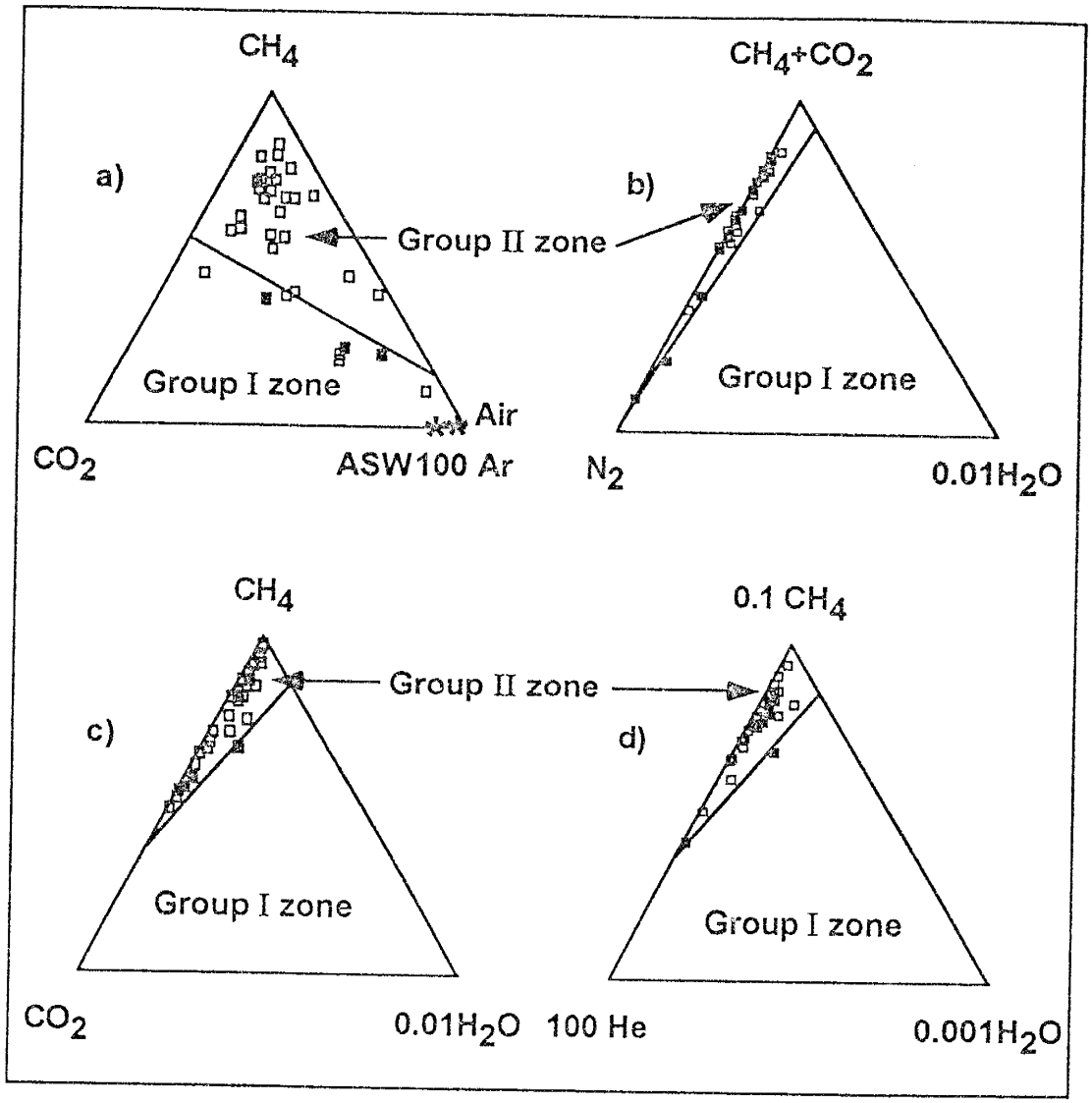

FIGURE 39: Ternary diagrams showing variation of analyses in 32 LANL vein calcites on diagrams similar to FIGURE 38. The area on which fluid inclusion analyses of pedogenic calcite (non-indurated) were plotted was indicated as "Group II zone". The area where fluid inclusion analyses of all hydrothermal vein calcites, calcretes, pedogenic calcites (indurated), active and ancient travertines were plotted was indicated as "Group I zone". Open square symbols are analyses of vein calcites from LANL and filled square symbols are analyses of travertines coated with vein calcites from Nevada Test Site (NTS).

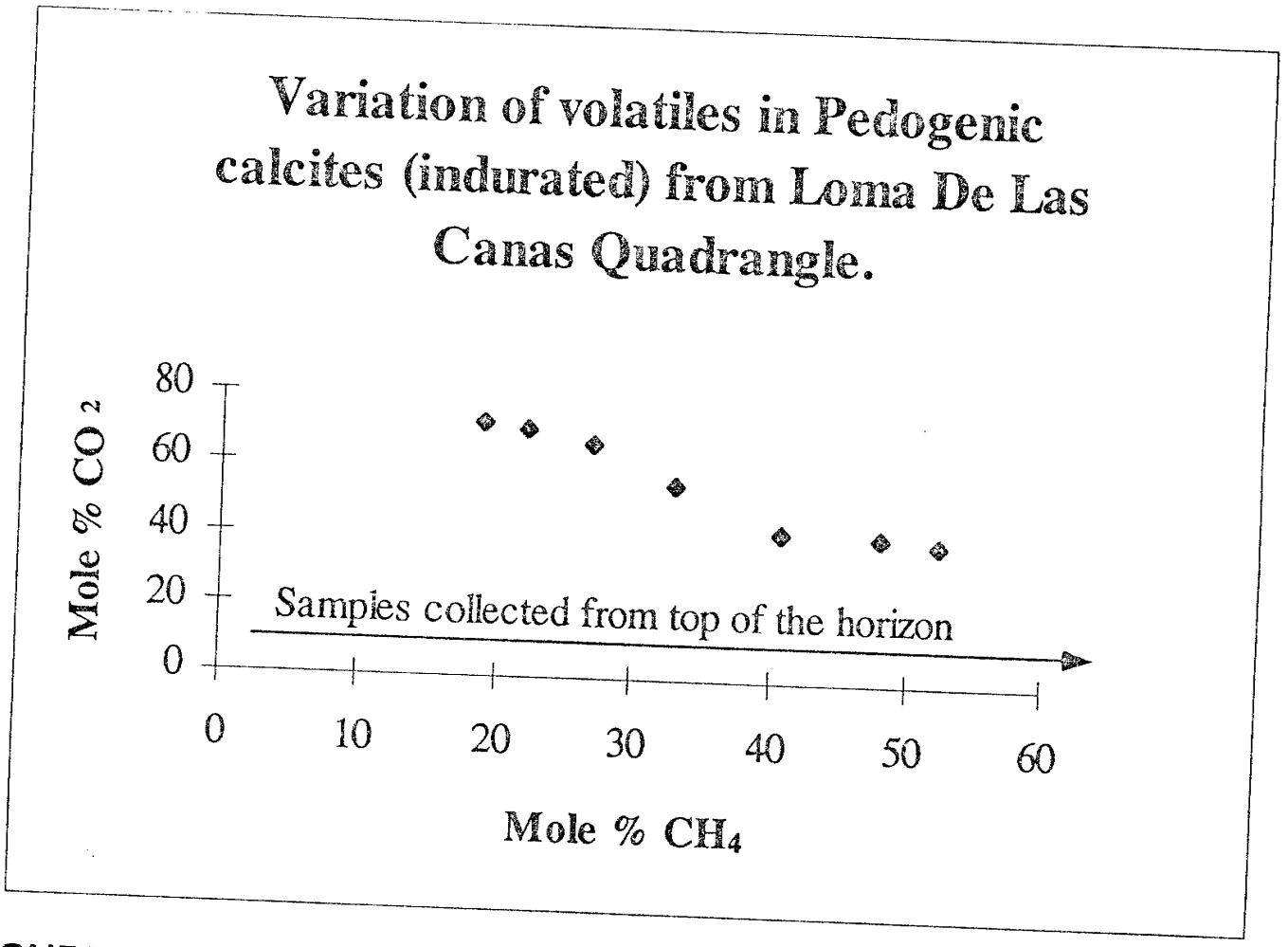

FIGURE 40: Variation of CO_2 and CH_4 in pedogenic calcite (indurated).

DISCUSSION

Analyses of various carbonates indicate that H_2O was the dominant species in fluid inclusions of group I carbonates. Gaseous species dominate in fluid inclusions of group II carbonates. Group I inclusions have the mean concentration of H_2O equal to 97.5 %, whereas inclusions in pedogenic calcites (non-indurated) have about 18 to 70 % H_2O. In the analyses of pedogenic calcites (non-indurated and indurated), CH_4 and CO_2 dominate. In travertines deposited by active springs and in ancient travertines, N_2 and CO_2 dominates. In the analyses of hydrothermal vein calcites, N_2 dominates while, N_2, CH_4 & CO_2 dominates in the analyses of calcretes. The CH_4/CO_2 ratio is greater than one in analyses of pedogenic calcite (non-indurated) and vein calcites from LANL. The N_2/Ar ratio in pedogenic calcite (non-indurated) is greater than the ratio in air.

Pedogenic calcites (non-indurated and indurated) have lower water to gas ratios than travertines, hydrothermal vein calcites and calcretes. This indicates that fluid inclusions trapped both liquid and vapor. At low temperatures and pressures, it is not possible to dissolve large amounts of gaseous species in water, hence, trapping of these gaseous species occur in the vapor-filled inclusions. This suggests formation in the vadose zone. Analyses for the other types of carbonate minerals are compatible with formation in the phreatic zone

because the ratios of inclusion water to gaseous species are similar to ground water (Norman et al., 1994).

Differences in analysis of pedogenic calcites (non-indurated & indurated):

It is not clear whether pedogenic calcite (indurated and non-indurated) share a common genesis. Since their formation, some of which may be nearly a million years old (Hawley et al., 1987), pedogenic calcites (indurated) may have experienced numerous changes. Changes in climatic conditions and fluctuations of the water table may have altered the carbonate surface. Alteration of the pedogenic calcite (non-indurated) surface by solution and precipitation of the carbonates indurated the pedogenic calcite surface. Our data indicate that volatiles in the pedogenic calcites (indurated) varied from the composition similar to the pedogenic calcites (non-indurated) to composition similar to the calcretes **(Figure 38b)**. We postulate that through the action of ground water, some processes have altered or added to the volatiles within paleo pedogenic calcite (non-indurated) and in course of time have created pedogenic calcites (indurated).

Helium in Pedogenic calcites (non-indurated)

Logically we expected that the analyses of pedogenic calcites (non-indurated) would be similar to the analysis of typical soil gas and air saturated water where the concentrations of He were near detectable limits. In the analysis of pedogenic calcites (non-indurated), however, we detected He. We observed that the mean concentration of He from the analyses of pedogenic calcites (non-indurated and indurated) and calcretes were one order of magnitude higher than the concentration of He in air (Rose et al., 1979) (**Table 23**).

Table 23 Variation of He in air, in pedogenic calcites (non-indurated and indurated) and in calcrete:

Helium in air (mole %); (Rose et al., 1979).	Mean amount of He in PC(NI) (mole %)	Mean amount of He in PC(I) (mole %)	Mean amount of He in Calcrete (mole %)
5.24E-04	5.95E-03	2.73E-03	1.31E-03

Radioactive decay of U and Th contained within the pedogenic calcites (non-indurated) may have resulted in showing excess amount of He in the analyses. We did not measure the concentrations of U and Th in the pedogenic calcite (non-indurated) samples, hence, the do not know age of the pedogenic calcites (non-indurated) analyzed and we could not check the above

hypothesis. It is conceivable that above average crustal concentrations of U may occur in pedogenic calcites (non-indurated). In some calcretes, ore-grade U do occur (Mann and Deutscher, 1978), and we considered that ground water deposited this U. It is also possible that He was fluxing from the crust of the Earth and being trapped preferentially within pedogenic calcite (non-indurated). However, the mechanism for preferential trapping of He within pedogenic calcites (non-indurated) is not clear. We can explain, similarly, excess He in older pedogenic calcites (indurated) and calcretes by the above processes.

Methane in Pedogenic calcites (non-indurated)

Analyses of pedogenic calcite (non-indurated) indicate that CH_4 was a dominant gas among other gaseous species released when we crushed fluid inclusions within the sample. We inferred from the high ratio of CH_4/CO_2 in the analyses of pedogenic calcites (non-indurated) that pedogenic calcites (non-indurated) formed under an environment depleted in O_2. We obtained similar analyses with pedogenic calcites (non-indurated) from different locations where CH_4 was the principal gas. The similar nature of included gaseous species in pedogenic calcite (non-indurated) and vein calcite from Los Alamos city indicates that the gaseous species represent some aspect of the soil environment that hosts the carbonate. We postulated that either during the precipitation of pedogenic calcite (non-indurated), or incorporation into

secondary inclusions or bacterial action of calcite-encapsulated organic material, CH_4 may occur in the environment. There is no field evidence to prove that CH_4 could have occurred in an anaerobic environment either during the precipitation of pedogenic calcite (non-indurated), or been incorporated into secondary inclusions. However, **Figure 41** shows that pedogenic calcites (non-indurated) were plotting in an O_2-depleted micro-environment, when we plotted all the individual crushes of pedogenic calcites (non-indurated) on an X-Y plot.

When we optically examined pedogenic calcite (non-indurated), we could not detect fluid inclusions in the laboratory. However, when we heated it, the volatiles started to evolve at 250 °C. We postulated that the grain sizes in the pedogenic calcites (non-indurated) were not larger than the size of the bacteria. From this we concluded that the formation of CH_4 in pedogenic calcite (non-indurated) due to the bacterial action of calcite-encapsulated organic material remains impractical. We concluded that micro-organisms produced CH_4 in pedogenic calcites (non-indurated) in a micro-anaerobic (O_2-depleted) environments during or after the deposition of calcium carbonate. Literature survey showed evidence that involved micro-organisms in the precipitation of pedogenic calcite (non-indurated) (Folk, 1993; Monger et al., 1991). It is not clear whether the precipitation of pedogenic calcite (non-indurated) occurred in an anaerobic or an aerobic environment. Analysis showing sample to sample

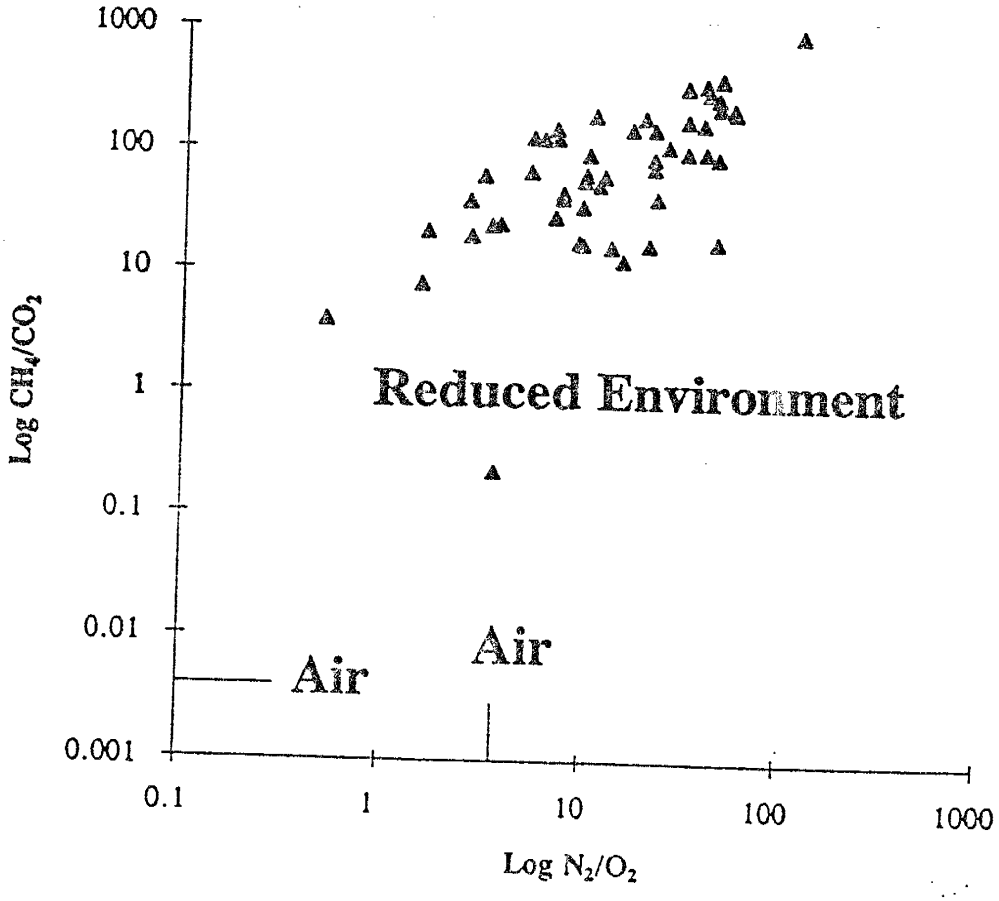

FIGURE 41: X-Y plot showing individual crushes of a pedogenic calcites (non-indurated) plotting within the field of reduced environment.

variation in N_2/Ar ratios indicates enrichment or depletion of N_2 from air. In a local environment, N_2 enrichment and depletion may occur due to biological processes such as N_2 fixation by micro-organisms. Where we find pedogenic calcite (non-indurated), we observe depletion of N_2 in the local environment if bacterial processes use N_2 or enrichment of N_2, if N_2 or NH_3 is the product of respiration. It is possible that deposition of pedogenic calcite (non-indurated) occurs in association with anaerobic micro-organisms. The analytical data suggests that this is the case (**Figure 41**).

The occurrence of organic material in pedogenic calcite (non-indurated) cannot explain the high ratios of CH_4 over CO_2 as measured in the analyses. Most of the pedogenic calcite (non-indurated) and pedogenic calcites (indurated) studied were almost pure white. Very little organic material like grass and roots are present in pedogenic calcite (non-indurated) and pedogenic calcites (indurated). We observed thick growths of algae in travertines deposited by active springs. We also saw leaves, twigs and layers of organic matter of algal origin trapped within these active travertines. We also know that coloration in ancient travertines is due to the trapped organic material within them.

Genesis and location of volatiles

All evidence is consistent with the occurrence of the majority of the volatiles measured in fluid inclusions trapped during mineral growth. Similar analyses obtained on specific types of carbonate sampled at different locations suggests that trapping of volatiles takes place during the precipitation of a mineral. Strongly supporting this contention is the agreement of the water content of fluid inclusion volatiles with the mode of formation and the general agreement between travertine analyses and those of the parent spring water (Norman et al. 1994).

Included Gas as an Indicator of Ground water Flow

We determined the genesis of carbonate minerals by analyzing the trapped volatiles and we indicated this by the analytical data presented here. Ground water deposits calcium carbonate as cements and as fracture fillings, hence, we can identify ground water flow by the occurrence of carbonate mineralization. Without mineralogic evidence, the occurrence of paleo ground water is difficult to determine. We can also produce calcite through pedogenic processes, and data shows that vein calcites also forms in similar manner in the fracture fillings at LANL.

We can identify overprinting of group I carbonate from group II carbonate and vice versa by the analysis of the volatiles. We demonstrated this by analyzing five carbonates, three from Riley (location shown in **Figure 9**) and two from Veguita Quadrangle (location shown in **Figure 18**). When we analyzed samples comprising of group I and group II carbonates, the resultant analyses will give an admixture of volatiles from the two carbonate groups. In ternary diagrams such as CH_4-CO_2-H_2O, we can identify mixing between two generations of carbonates by a linear trend given by multiple analyses of samples that infers that overgrowth of a second generation of carbonate is not uniform. The analyses of five carbonates presented here indicated that more than one generation of carbonates being mixed showed much scatter in the data, but we cannot see mixing relationship due to the limited number of samples (**Figure 42**). Analyses of carbonates from Nevada Test site (samples provided by Schon S. Levy) indicate scatter of data, hence also implies a complicated genesis (**Figure 42**).

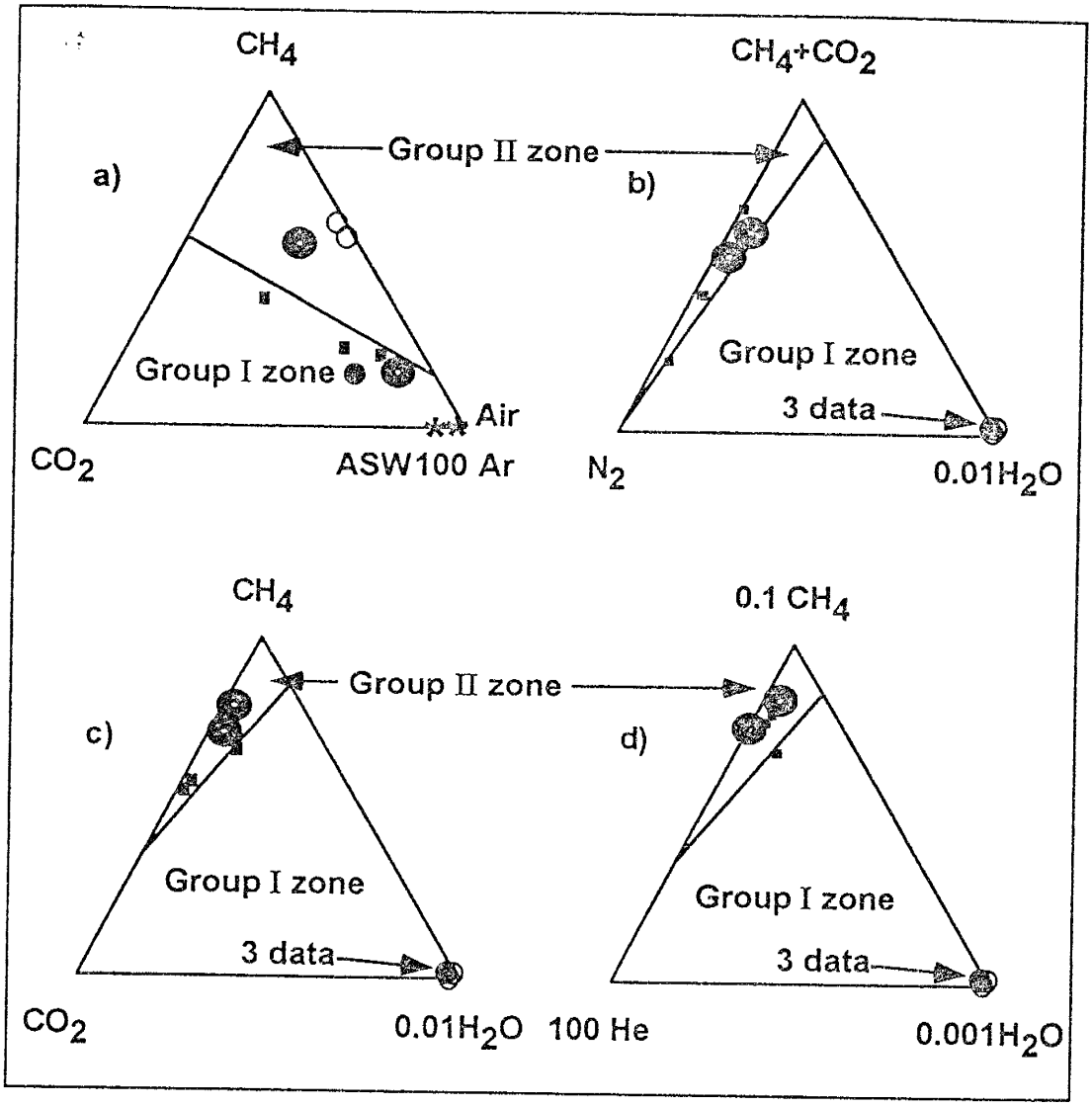

FIGURE 42: Ternary diagrams showing travertines from Nevada Test Site (NTS) and carbonates from Riley and from Veguita quadrangle on diagrams similar to FIGURE 38 exhibiting complex genesis. Travertine from Riley display two forms of carbonate, one of which appears to be pedogenic calcite (non-indurated) in white color veining the travertine (open circle). Filled circle is an analysis of mostly gray travertine from Riley. Analyses of travertines from NTS is shown in filled square symbols. Calcite concretions in sand from Veguita Quadrangle is displayed as concentric circles. Note that the data plot in an opposite fashion on the "a" and "b to d" diagrams.

SUMMARY

- Analytical data presented here indicates that we can determine the genesis of the carbonate minerals by the analysis of trapped volatiles within the carbonate minerals.
- Ground water commonly deposits calcite as cements and fracture fillings, hence, the occurrence of carbonate mineralization suggests ground water flow.
- Pedogenic processes can also produce carbonate minerals, and our data indicates that in the vadose zone, fracture carbonate mineralization occurs in the similar manner.
- Any quantitative analytical method such as analysis by quadrupole mass spectrometry may help in knowing the concentration of the volatiles.
- High sensitivity of the quadrupole mass spectrometer is preferred over other mass spectrometers. Also, we required small amount (0.5 to 1.0 grams) of the sample for the analysis.
- We obtained best results when we crushed samples under vacuum and when we analyzed the released volatiles using a quadrupole mass spectrometer.

CONCLUSIONS

- We can distinguish pedogenic calcites (non-indurated) from hydrothermal vein calcites, pedogenic calcites (indurated), calcretes, ancient and active travertines by the analysis of fluid inclusion volatiles.
- Crushing samples under vacuum and analyzing the released volatiles using a quadrupole mass spectrometer gave the best results.
- Cluster analysis distinguishes group I carbonates (calcretes, hydrothermal vein calcites, pedogenic calcites (indurated), ancient and active travertines) from group II carbonates (pedogenic calcites (non-indurated)).
- Concentration of H_2O distinguishes group I carbonates (mean concentration is equal to 9.75E+01) from group II carbonates (mean concentration is equal to 4.87E+01).
- The CH_4/CO_2 ratio was greater than one in group II carbonates, while the ratio was less than one in group I carbonates.
- Volatile species that helped in discriminating various carbonates were H_2O, CH_4, CO_2, and He.
- Ternary plots such as $0.01H_2O$-CH_4+CO_2-N_2, $0.01H_2O$-CH_4-CO_2 and $0.001H_2O$-CH_4-100He show clear separation of group II carbonates from group I carbonates.
- LANL vein calcites have volatiles identical to pedogenic calcite (non-indurated) and hence their genesis is analogous.

REFERENCES

Austin, G. S. and Barker, J. M. (1990); Commercial travertine in New Mexico; New Mexico Geology, Science and Service, V. 12, No. 3, p. 50-58.

Balderer, W. and Lehmann B. E., (1989); $^{3}He/^{4}He$-ratios as indicators of the origin of helium in ground water; examples from the deep Nagra boreholes in northern Switzerland. Proceedings of 6th international symposium on Water-rock interaction, Malvern, 6. p. 45-47.

Barker, J. M. (1983); Preliminary investigations of the origin of the Riley travertine, Socorro County, New Mexico; New Mexico Geological Society Guidebook, 34th field conference, Socorro Region II; p. 269-276.

Bates, R. L. and Jackson, J. A. (1984); Dictionary of Geological Terms; Third edition, Anchor Press/Doubleday, Garden City, New York; p. 1-571.

Butler, S. S. (1985); Neglected aspects of engineering hydrology; Hydrological Science and Technology, Short Papers; 1. (1). p. 1-5.

Eggleston, T. L., Norman, D. I. and Chapin, C. E. (1983); New Mexico Geol. Soc. 34th Annual field conference, Socorro Region II at Socorro; p. 241-246.

Elliot T., (1990); Geochemical indicators of ground water ageing; Doctoral thesis, p. 474.

Fischer, J. N. (1986); Hydrogeologic factors in the selection of shallow land burial sites for the disposal of low-level radioactive waste; U.S. Geological Survey; CIRC-973.

Folk, R. L. (1993); SEM imaging of bacteria and nannobacteria in carbonate sediments and rocks; Journal of Sedimentary Petrology. 63. (5). p. 990-999.

Hawley, J. W., McLemore, V. T. and Bowie, C. E. (1987); Guide book to the Socorro Area, (New Mexico Bureau of Mines and Geology, Socorro); p. 25-32.

Heaton, T. H. E., (1984); Rates and sources of (4)He accumulation in ground water; Hydrological Sciences, 29. (1). p. 29-47.

Henley, R. W., Truesdell. A. H., Barton, P. B. Jr., and Whitney J. A. (1984); Fluid-mineral equilibria in hydrothermal systems; Reviews in Economic Geology, 1. p. 267.

Hintze, J. L. (1992); Number Cruncher Statistical System, version 5.03; Installation and Reference Manual; p. 1-442.

Machette, M. N., (1985); Calcic soils of the southwestern United States; Geological Society of America, Special paper 203, p. 1-21.

Mann, A. W. and Deutscher, R. L. (1978); Genesis principles for the precipitation of carnotite in calcrete drainages in Western Australia; Econ. Geol. 73. (8). p. 1724-1737.

Marrin, D. L., (1987); Soil gas sampling strategies; deep vs. shallow aquifers; Proceedings of the First national outdoor action conference on aquifer restoration, ground water monitoring and geophysical methods; Natl. Water Well Assoc., Dublin, OH; p. 437-454.

Mazor, E. (1975); The atmospheric noble gases as potential multitracers in geothermal prospection and steam production studies; Second United Nations symposium on the development and use of geothermal resources, San Francisco, Calif., May 20-29, 1975, p 793-802.

Mazor E., Bosch A., (1987); Noble gases in formation fluids from deep sedimentary basins; a review; Applied-Geochemistry. 2. (5-6). p. 621-627.

Mazor, E., Dubois, J. D., Fluck, J. and Jaffe, F. C. (1988); Nobel gases as tracers identifying geothermal components in regions devoid of surface geothermal manifestations: a case study in the Baden springs area, Switzerland; Chemical Geology, Isotope Geoscience Sec., 72, p. 47-61.

McGrath, D. B. and Hawley, J. W. (1987); Guide book to the Socorro Area, (New Mexico Bureau of Mines and Geology, Socorro); p. 55-67.

Monger, H. C., Daugherty, L. A., Lindemann, W. C. and Liddell, C. M. (1991); Microbial precipitation of pedogenic calcite; Geology (Boulder), 19. (10). p. 997-1000.

Musgrave, J. A. (1992); Chemical evolution and mineralization of the sulphur springs CSDP site, Valles Caldera, New Mexico; Doctoral thesis, New Mexico Tech., p. 1-174.

Musgrave, J. A. and Norman, D. I. (1995); Geochimica et Cosmochimica Acta. (in press).

Norman, D. I. and Sawkins, F. J., (1987); Analysis of volatiles in fluid inclusions by mass spectrometry; Chemical-Geology. 61. (1-4). p. 1-10.

Norman, D. I., Benton, L. D. and Albinson, T. F., (1991); Source, Transportation and Deposition of Metals (Balkema, Rotterdam,); p. 209-212.

Norman, D. I., and Musgrave, J. A. (1994); N_2-Ar-He compositions in fluid inclusions; implicators of fluid source; Geochimica-et-Cosmochimica-Acta. 58. (3). p. 1119-1131.

Norman, D. I., Gundimeda, M., Wilkowske, C. and Levy, S. S. (1994); N_2-Ar-He in minerals: A simple, sensitive method for assessing long term ground water flow at waste remediation sites; Technical Completion Report, WERC Project Number: 01-4-23197; p. 1-38.

Roedder, E. (1984); Reviews in Minerology; 12 (Mineralogical Society of America, Blacksburg).

Rose A. W., Hawkes H. E., and Webb J. S. (1979); Geochemistry in Mineral Exploration, Second Edition, Academic Press, Ch. 18, p. 494.

Rose S. E., (1987); Dissolved oxygen systematics in the Tucson Basin aquifer, Arizona; Doctoral thesis, 185 p.

Ruff R. K. (1993); Gas Analysis of Fluid Inclusions: Application Towards Precious Metal Exploration, Steeple Rock Mining District, Grant County, New Mexico (MS Thesis, New Mexico Tech).

Stute, M. Sonntag, C. Deak, J. and Schlosser P., (1992); Helium in deep circulating ground water in the Great Hungarian Plain; flow dynamics and crustal and mantle helium fluxes; Geochimica-et-Cosmochimica-Acta. 56. (5). p. 2051-2067.

Szymanski, J. (1989); Internal DOE report on the Yucca Mountain High Level Disposal Site (Nevada Operations Office DOE (1987). 3.); U. S. Geol. Survey Report YMP-USGS-SP-8-31521 (1989).

Warner, D. L., Davis, S. N. and Syed, T., (1986); Evaluation of confining layers for containment of injected wastewater; Proceedings of the International symposium on subsurface injection of liquid wastes. U. S., National Water Well Association, Dublin, OH, United-States. p. 417-446.

Winograd, I. J. and Doty, G. (1980); Paleohydrology of the southern Great Basin; Geological Survey Professional Paper (USGS-OFR-80-569, 98p) (Washington,-D.C.), (1175). p. 280-281.

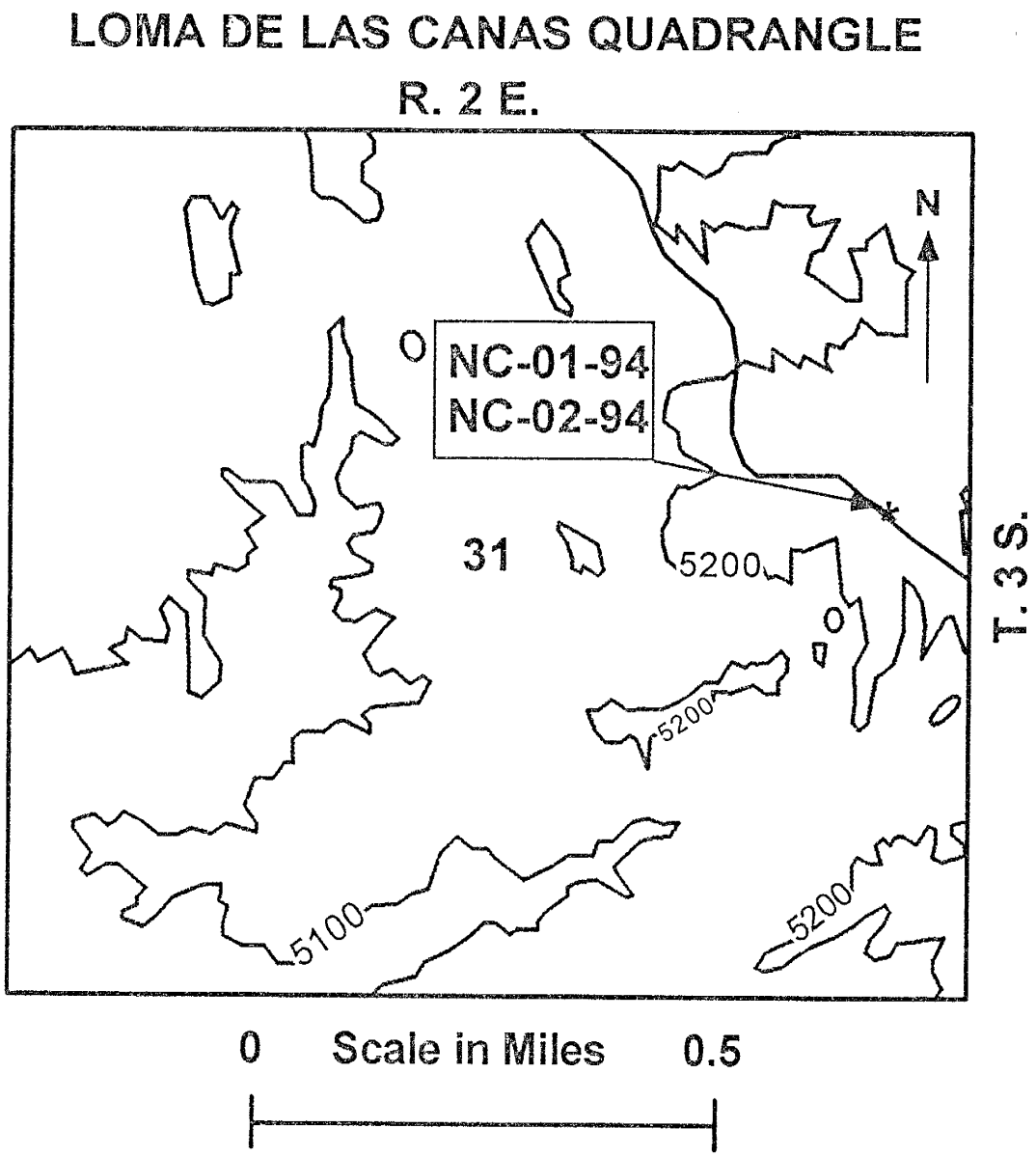

FIGURE A1: Pedogenic calcite (non-indurated) samples NC-01-94 and NC-02-94 were collected from the Loma De Las Canas Quadrangle, East of Socorro, New Mexico.

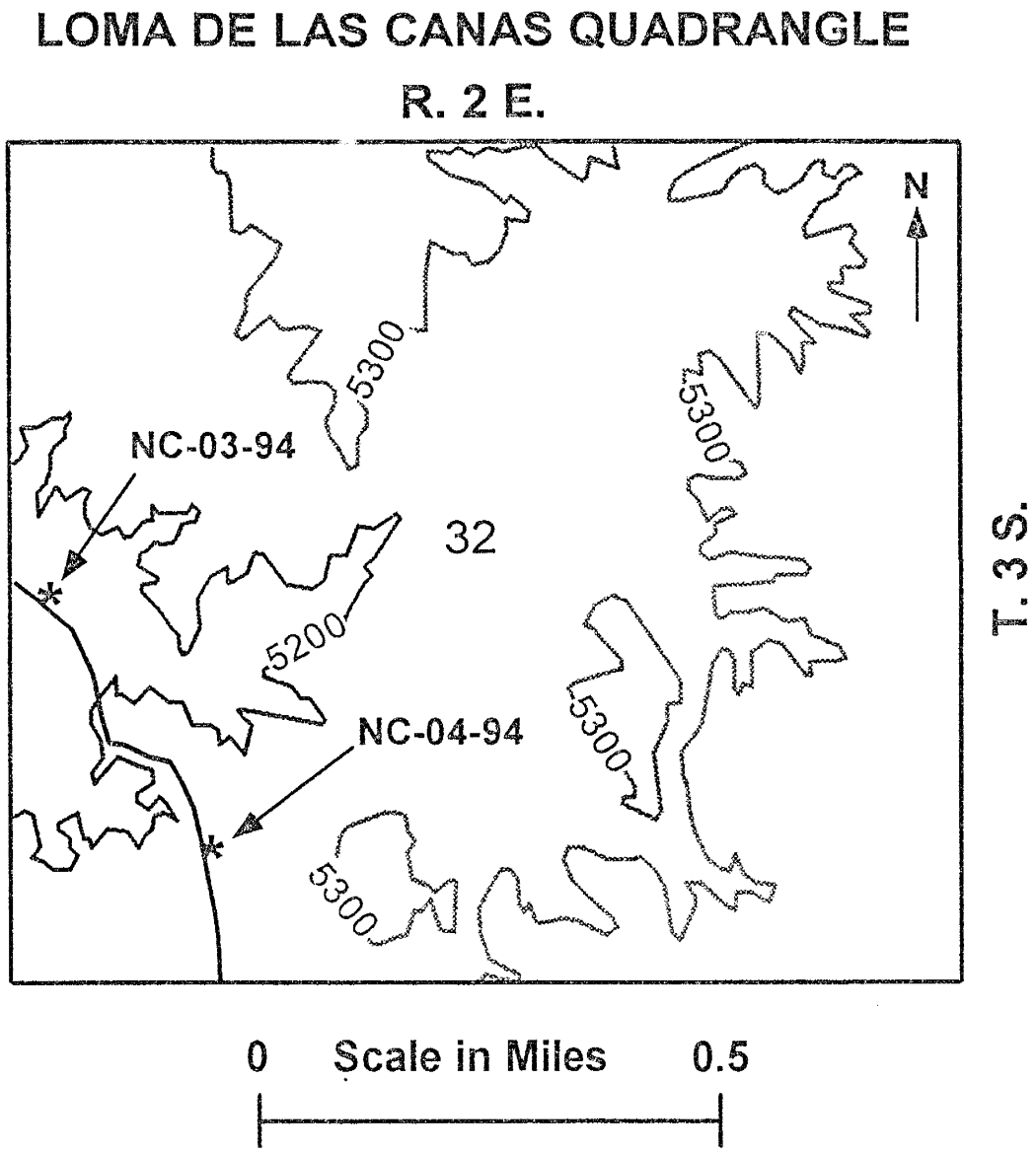

FIGURE A2: Pedogenic calcite (non-indurated) samples NC-03-94 and NC-04-94 were collected from the Loma De Las Canas Quadrangle, East of Socorro, New Mexico.

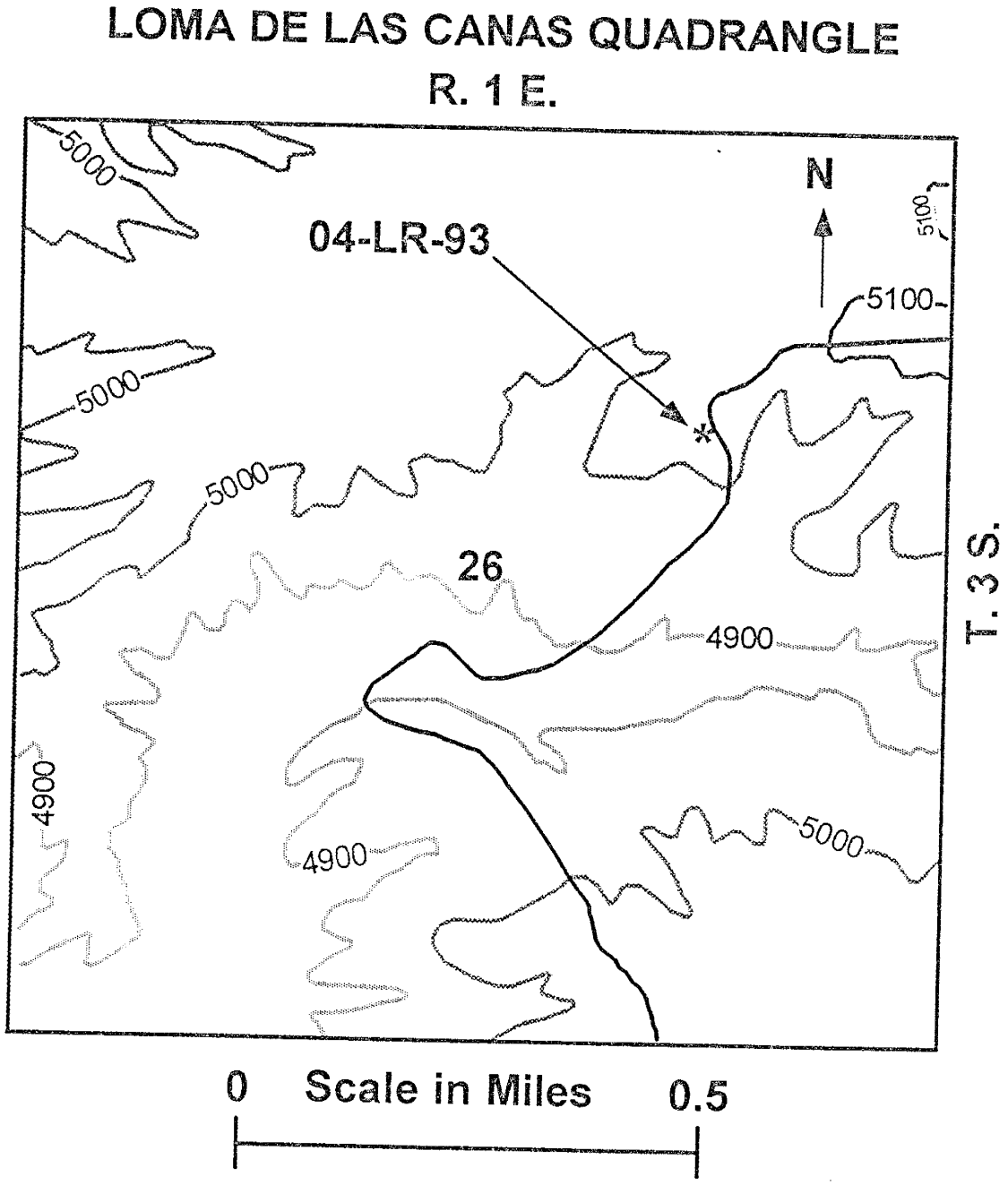

FIGURE A3: Pedogenic calcite (non-indurated) sample 04-LR-93 was collected from the Loma De Las Canas Quadrangle, East of Socorro, New Mexico.

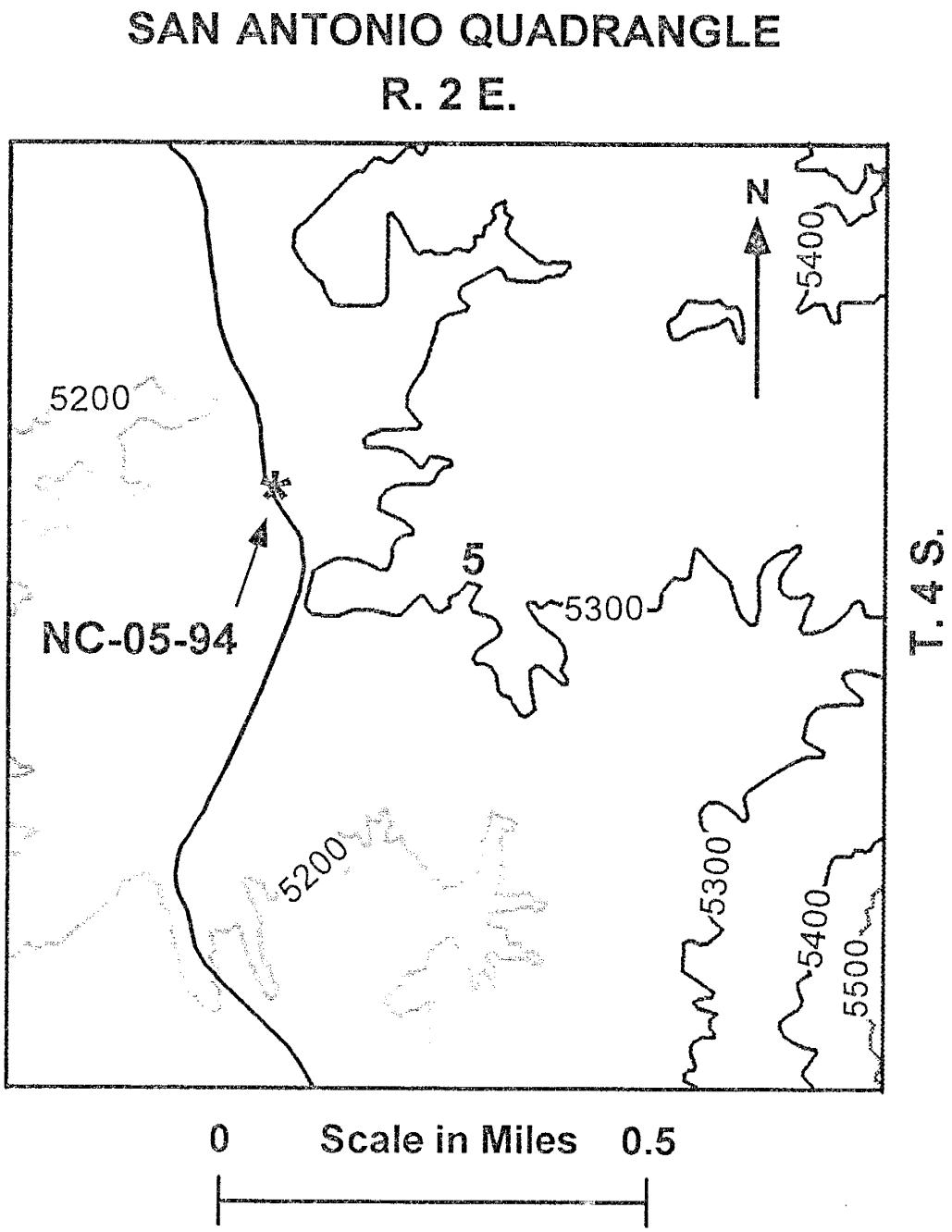

FIGURE A4: Pedogenic calcite (non-indurated) sample NC-05-94 was collected from the San Antonio Quadrangle, South-East of Socorro, New Mexico.

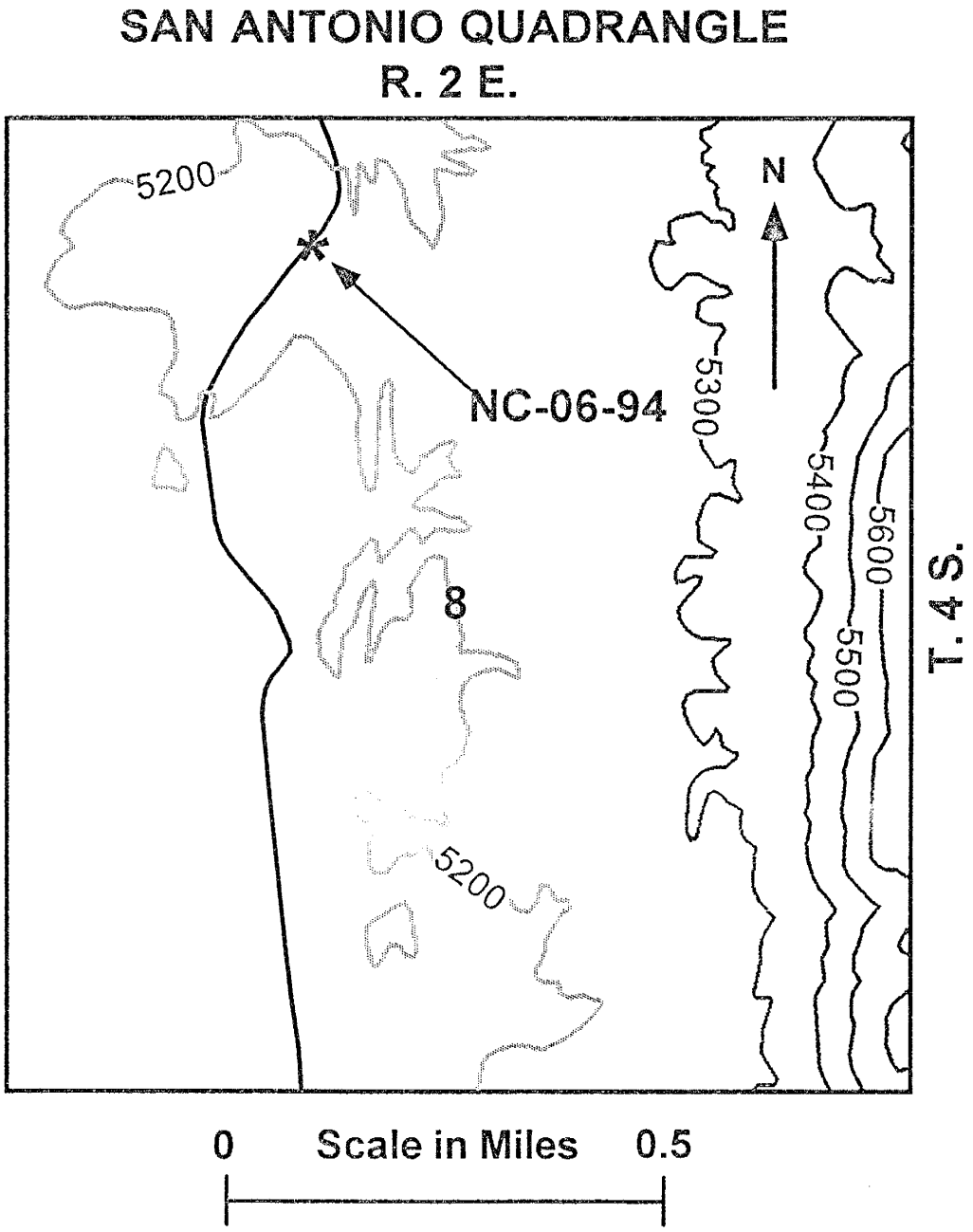

FIGURE A5: Pedogenic calcite (non-indurated) sample NC-06-94 was collected from the San Antonio Quadrangle, South-East of Socorro, New Mexico.

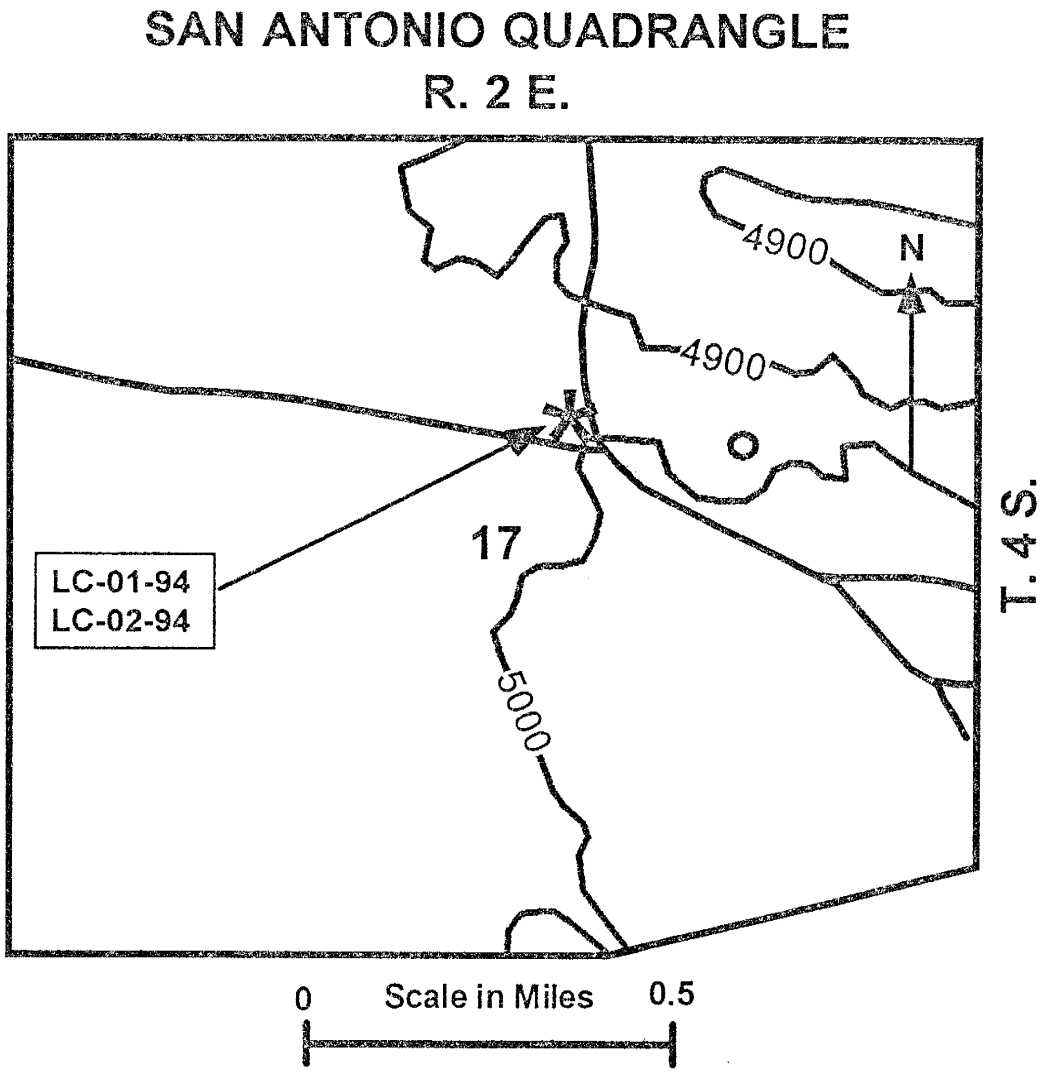

FIGURE A6: Pedogenic calcite (non-indurated) samples LC-01-94 and LC-02-94 were collected from the San Antonio Quadrangle, South-East of Socorro, New Mexico.

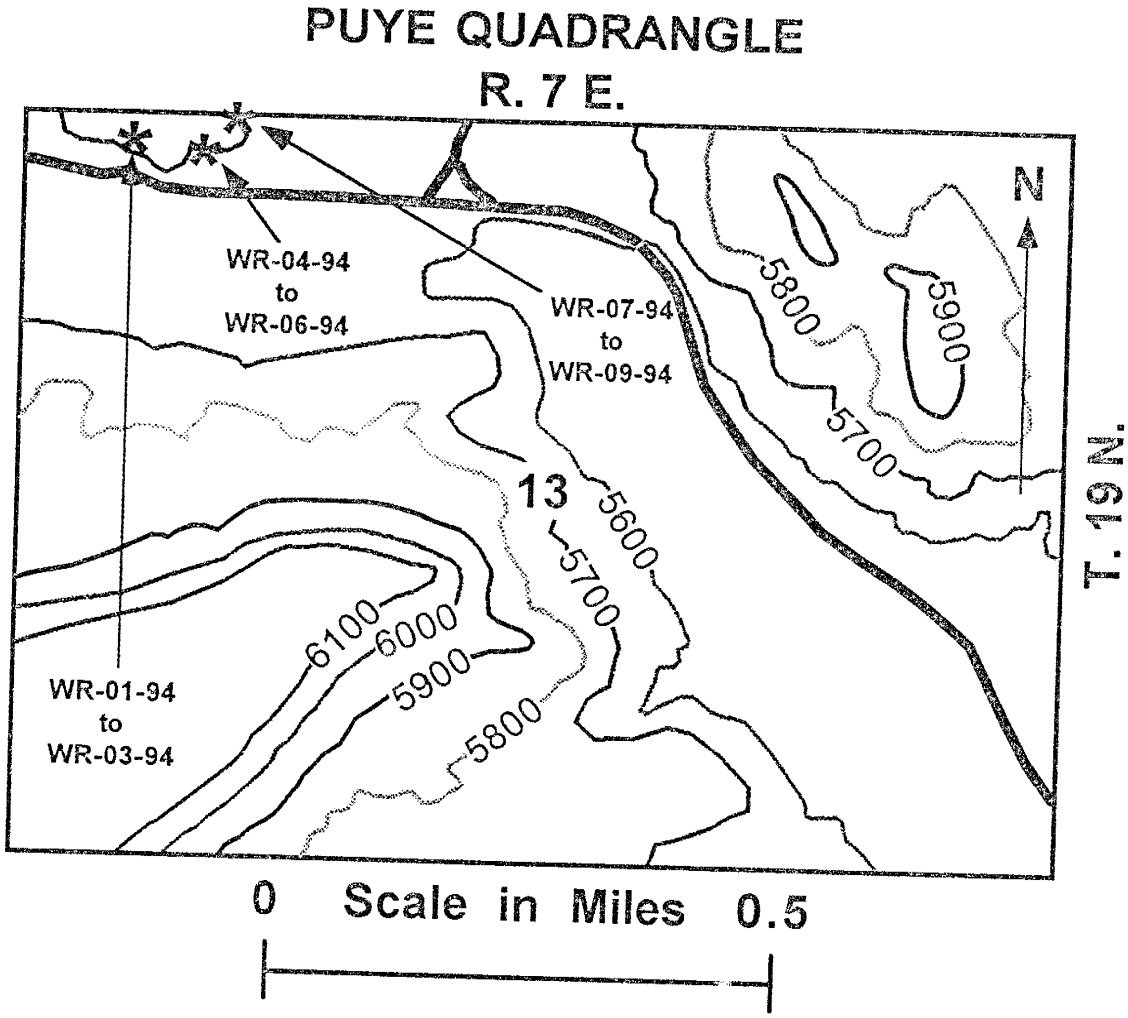

FIGURE A7: Pedogenic calcite (non-indurated) samples WR-01-94 to WR-09-94 were collected from the Puye Quadrangle, near White Rock, New Mexico.

BELEN QUADRANGLE

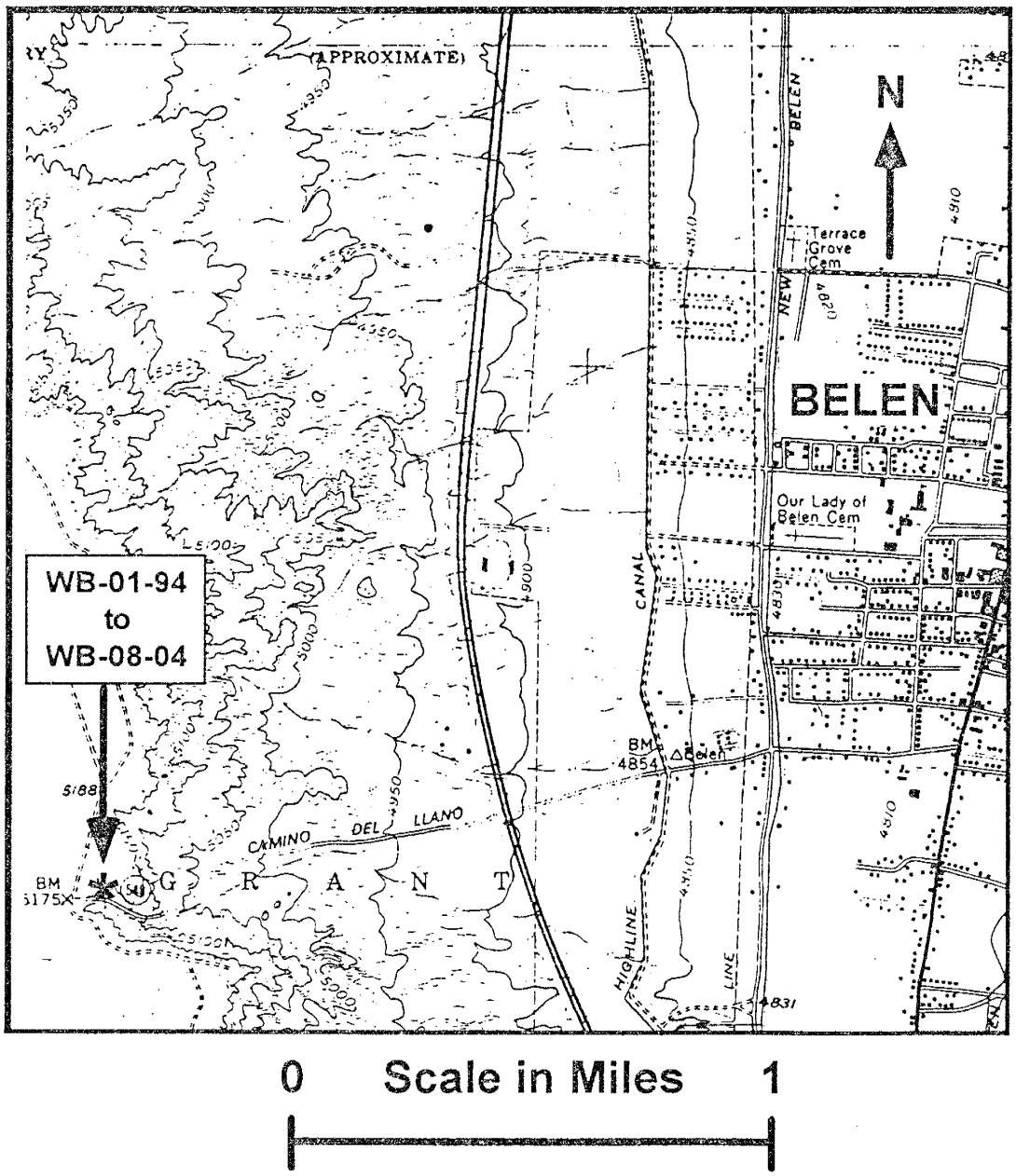

FIGURE A8: Pedogenic calcite (non-indurated) samples WB-01-94 to WB-08-94 were collected from the Belen Quadrangle, West of I-25 near Belen, New Mexico.

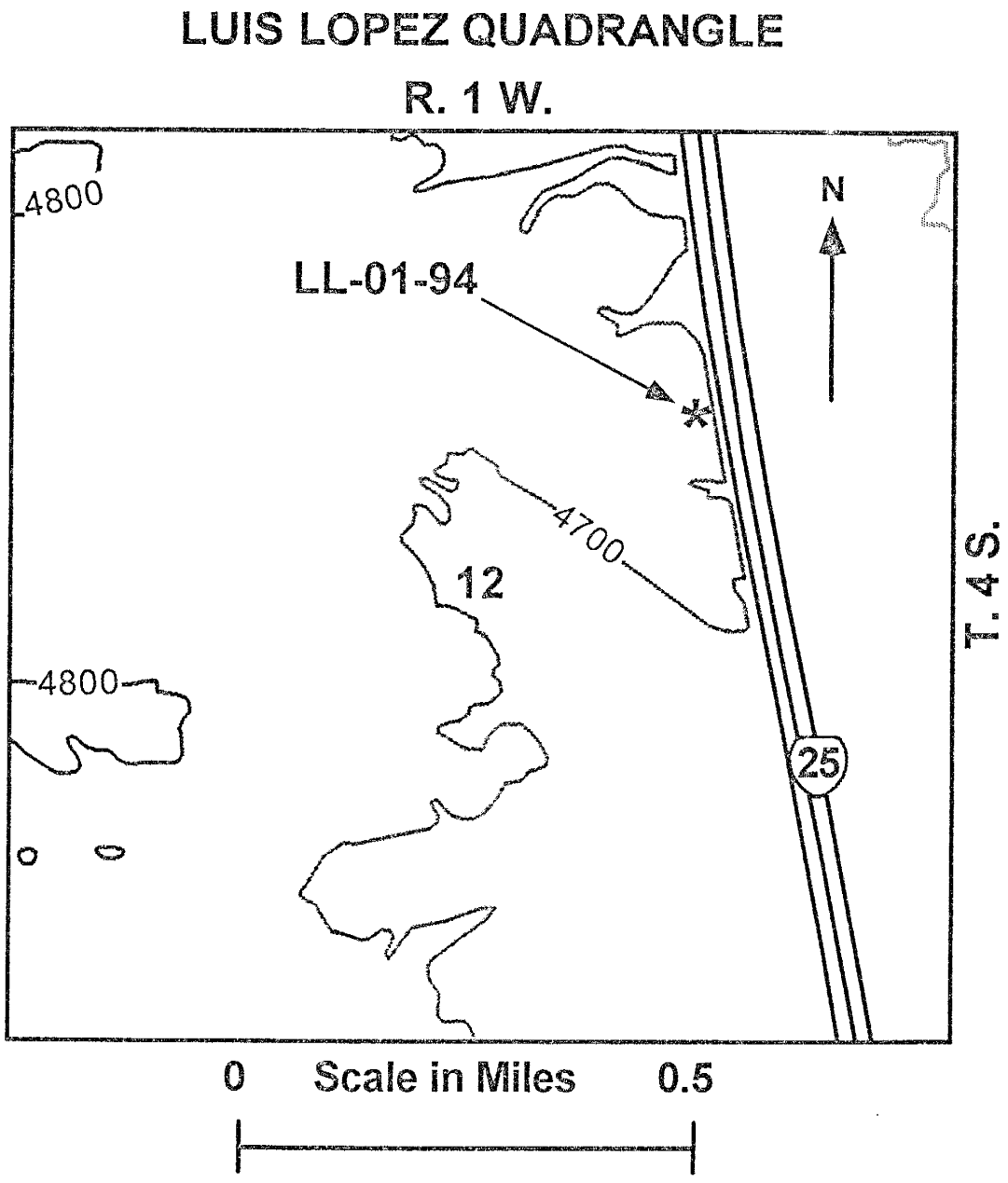

FIGURE A9: Pedogenic calcite (non-indurated) sample LL-01-94 was collected from the Luis Lopez Quadrangle, South-East of Socorro, New Mexico.

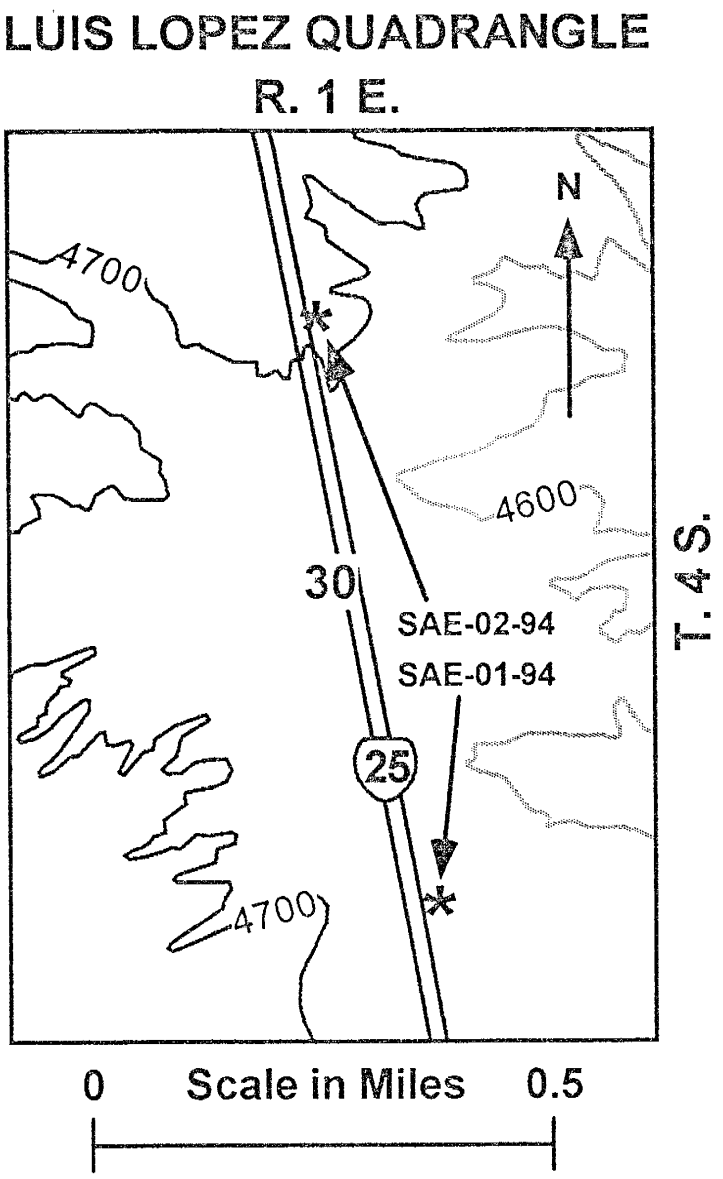

FIGURE A10: Pedogenic calcite (non-indurated) samples SAE-01-94 and SAE-02-94 were collected from the Luis Lopez Quadrangle, North of I-25, near San Antonio exit, New Mexico.

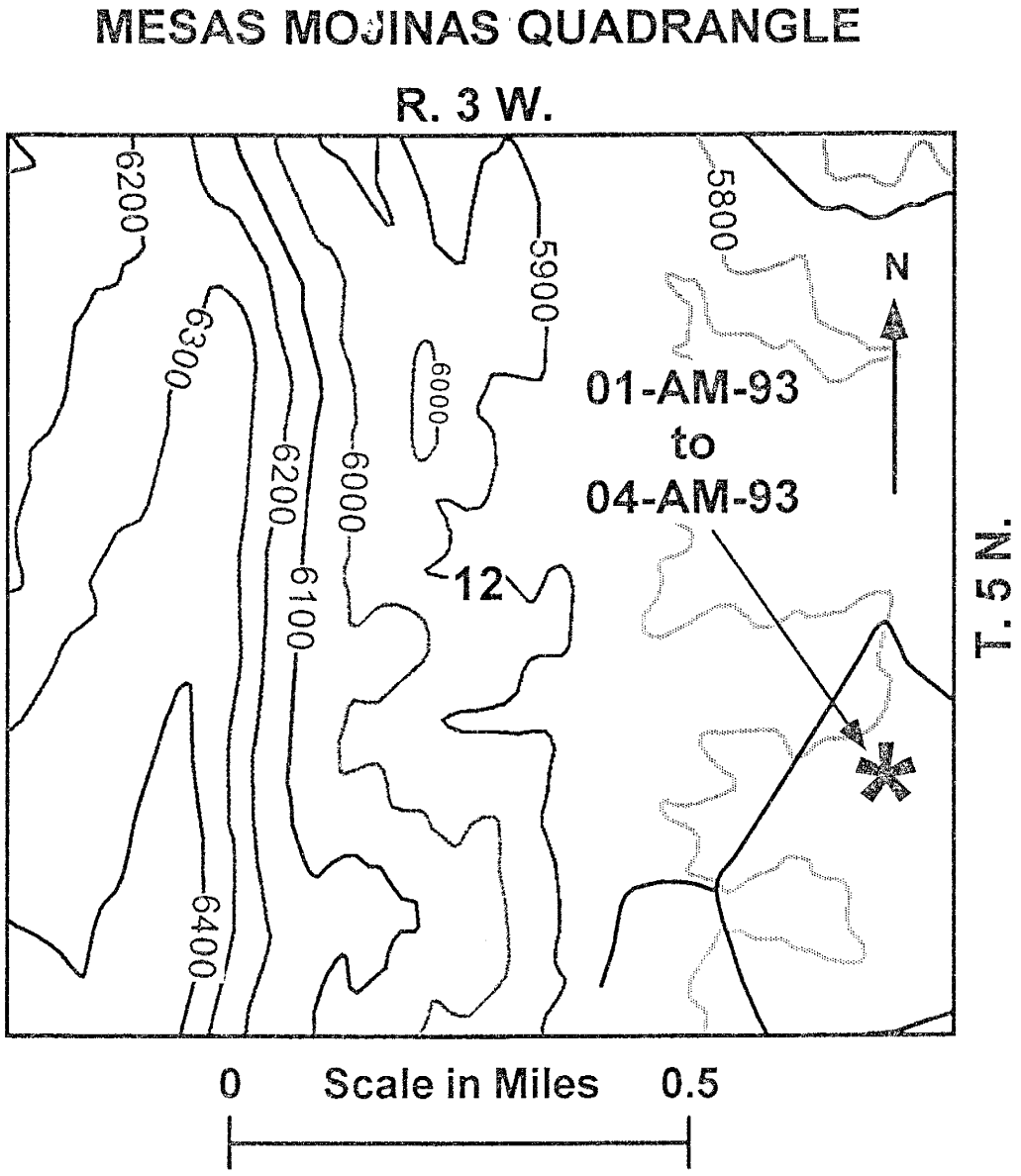

FIGURE A11: Ancient travertine samples 01-AM-93 to 04-AM-93 were collected from the Mesas Mojinas Quadrangle, West of Belen, New Mexico.

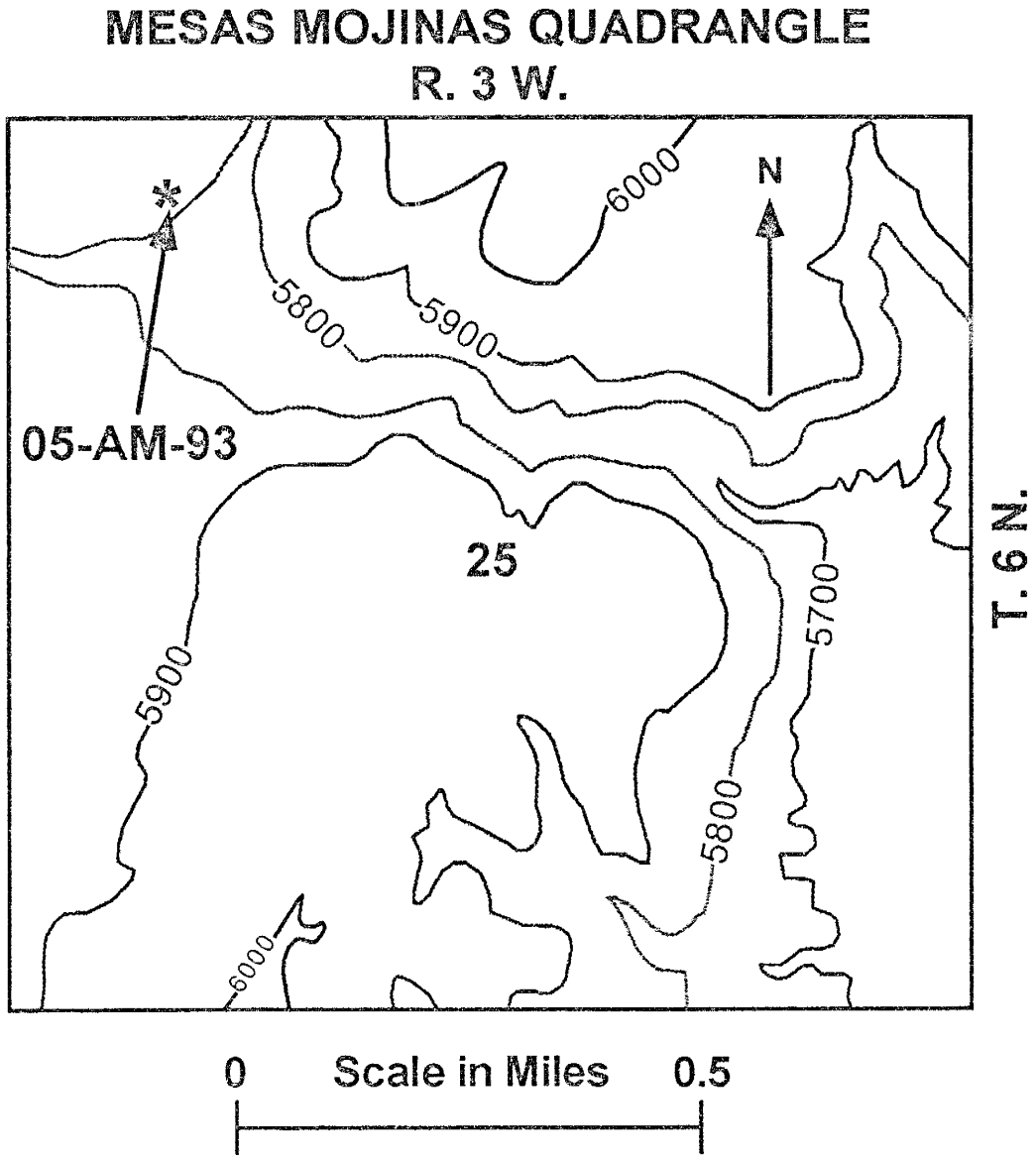

FIGURE A12: Ancient travertine sample 05-AM-93 was collected from the Mesas Mojinas Quadrangle, West of Belen, New Mexico.

BELEN QUADRANGLE

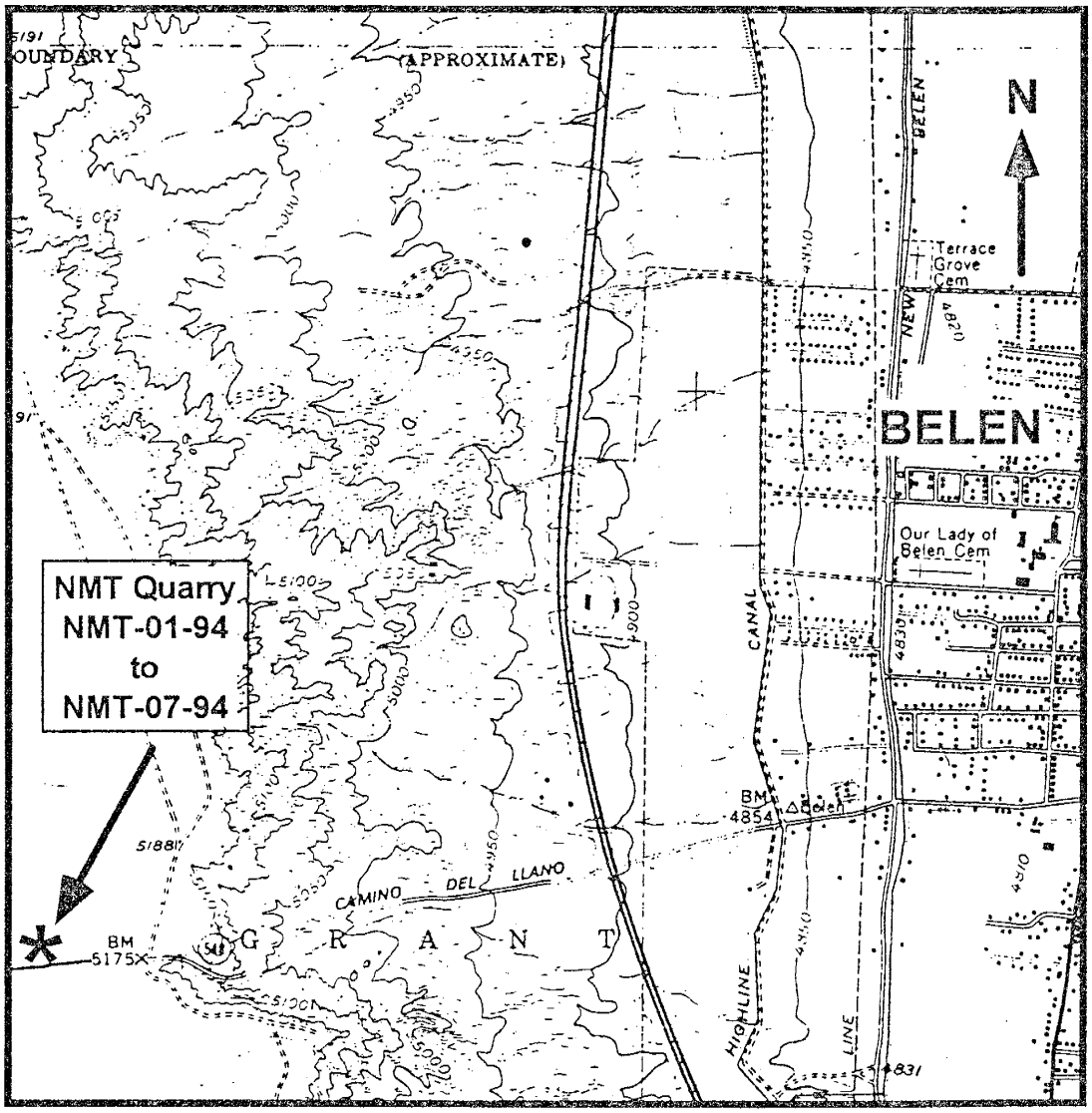

FIGURE A13: Ancient travertine samples NMT-01-94 to NMT-07-94 were collected from the Belen Quadrangle, West of Belen, New Mexico.

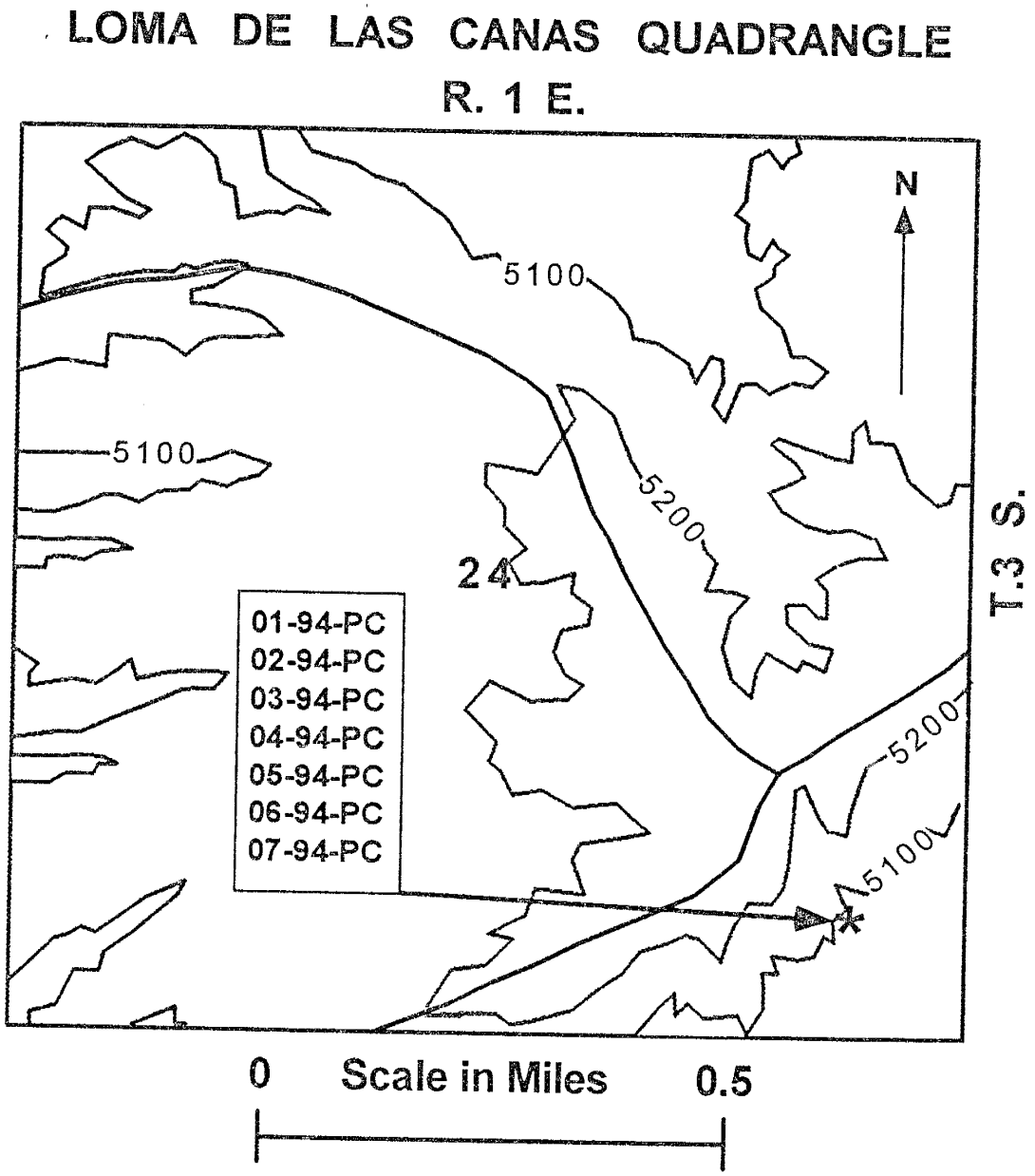

FIGURE A14: Pedogenic calcite (indurated) samples, 01-94-PC to 07-94-PC, were collected from the Loma De Las Canas Quadrangle, East of Socorro, New Mexico.

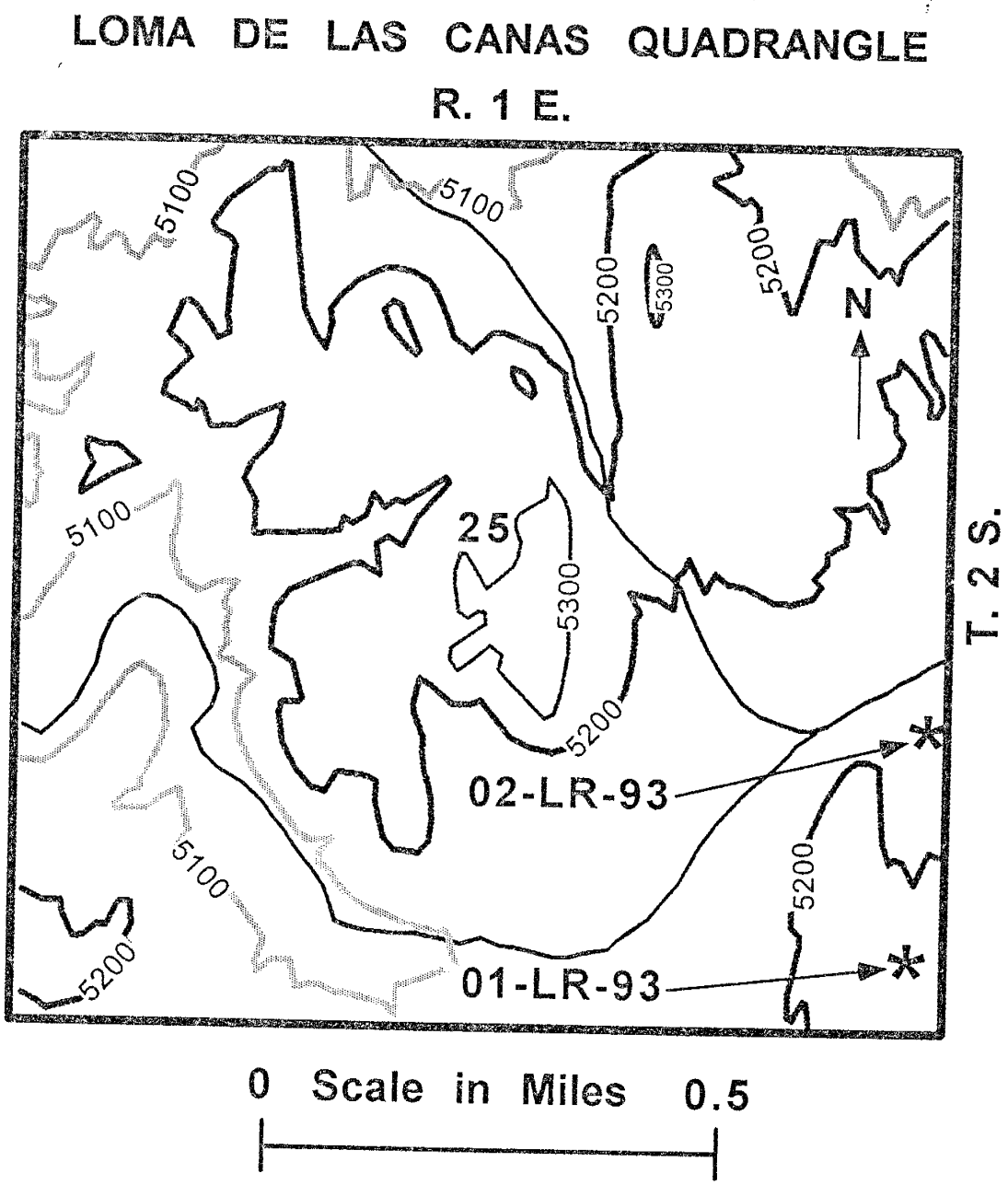

FIGURE A15: Pedogenic calcite (indurated) samples, 01-LR-93 and 02-LR-93, were collected from the Loma De Las Canas Quadrangle, East of Socorro, New Mexico.

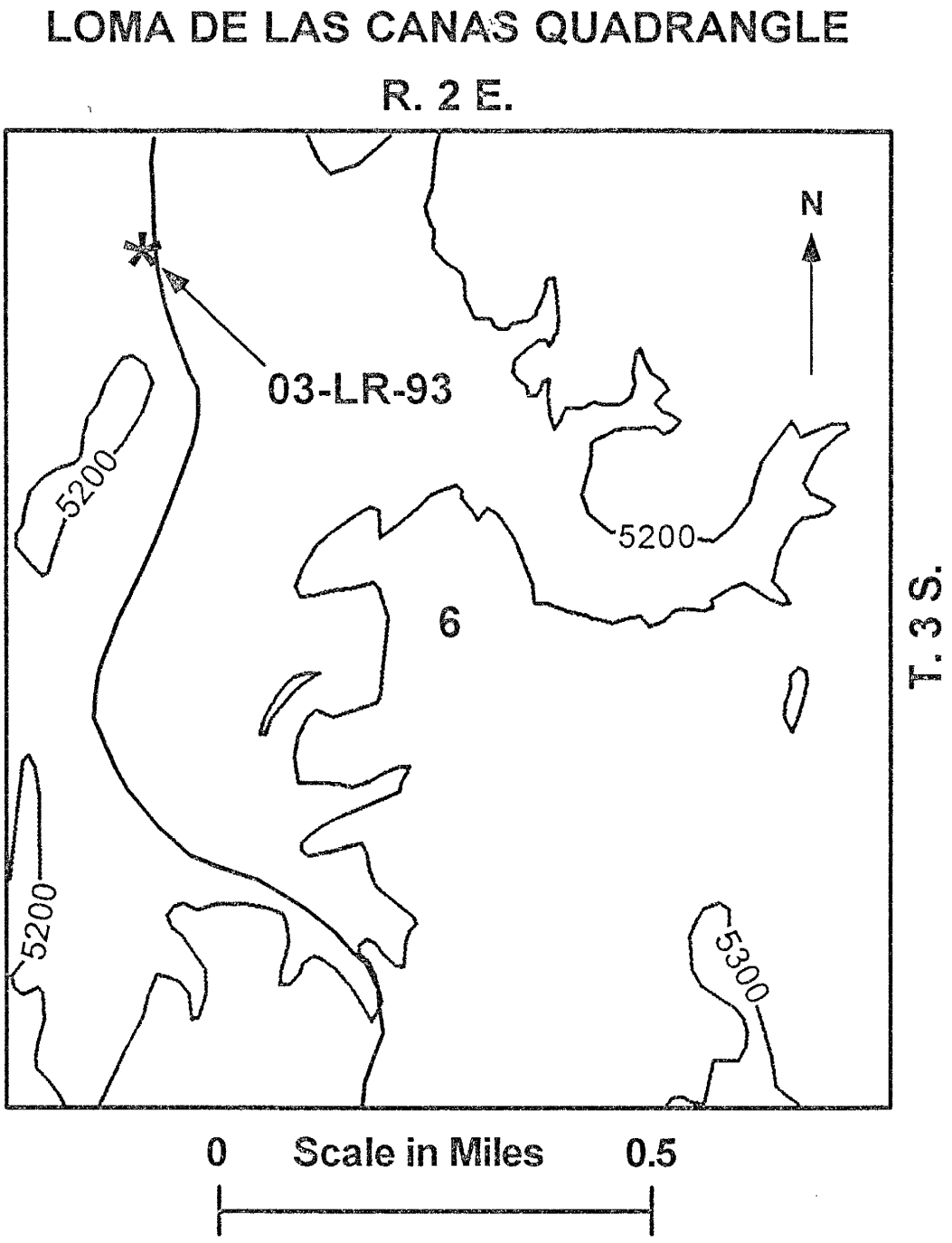

FIGURE A16: Pedogenic calcite (indurated) sample, 03-LR-93, was collected from the Loma De Las Canas Quadrangle, East of Socorro, New Mexico.

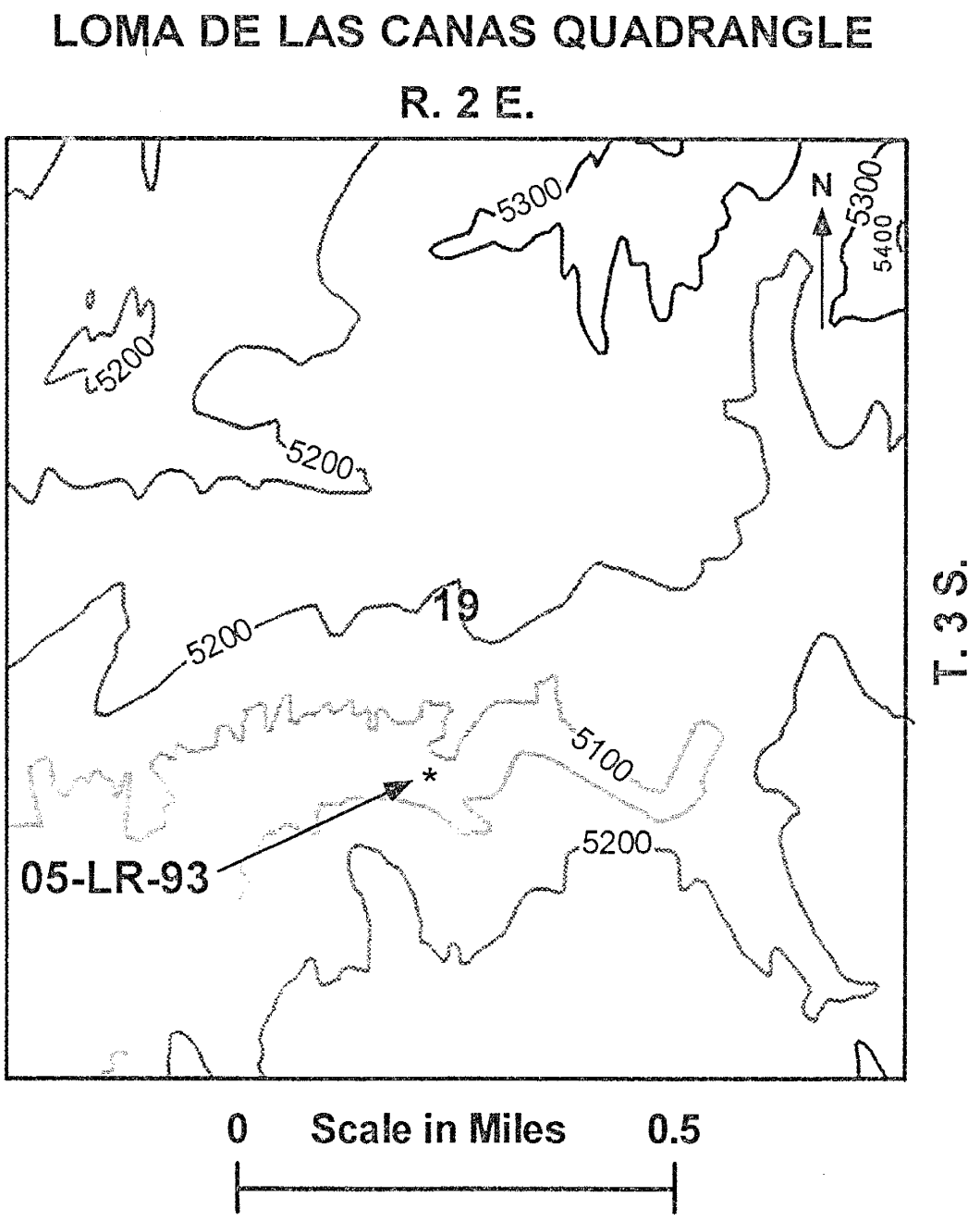

FIGURE A17: Pedogenic calcite (indurated) sample, 05-LR-93, was collected from the Loma De Las Canas Quadrangle, East of Socorro, New Mexico.

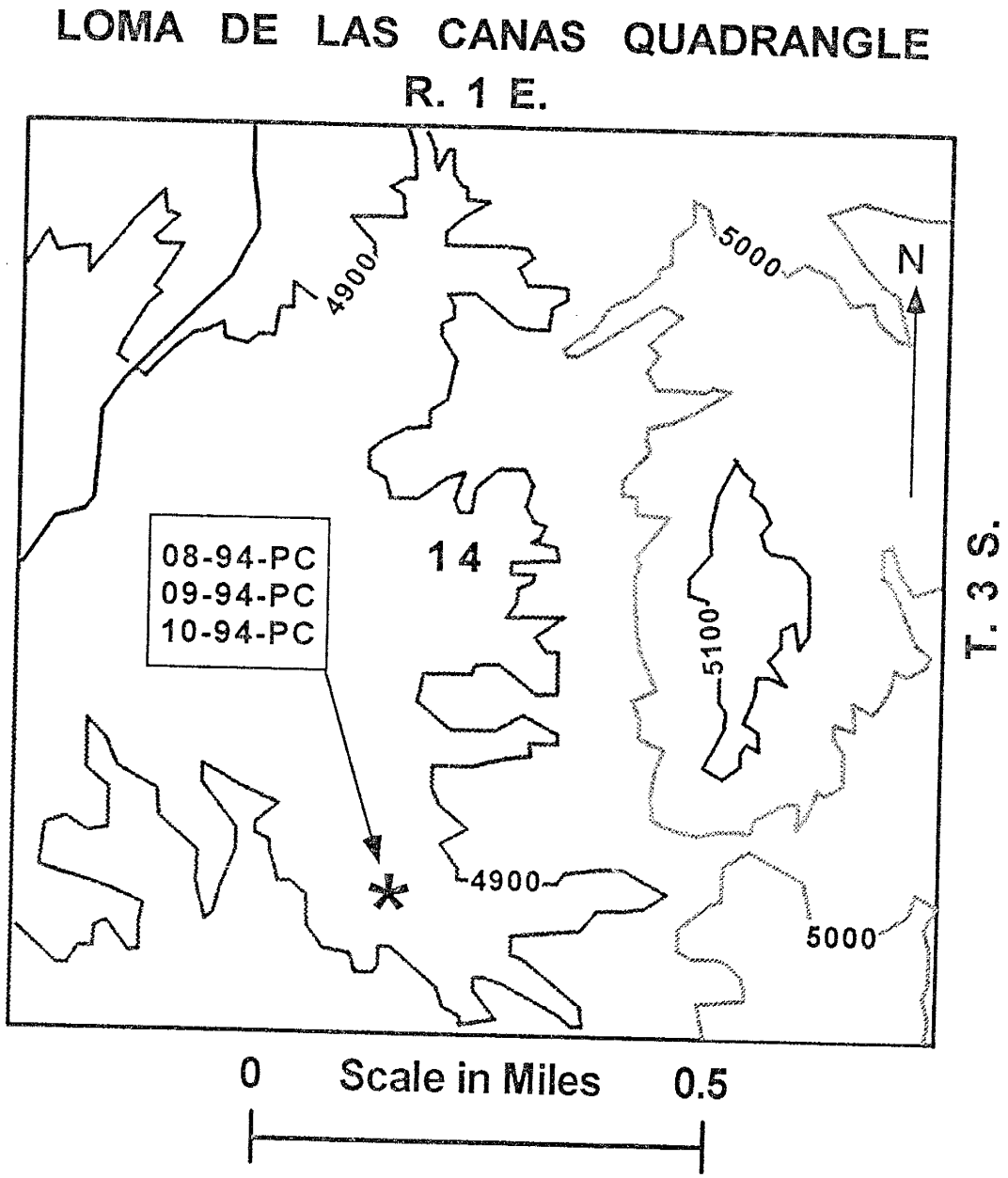

FIGURE A18: Calcrete samples 08-94-PC to 10-94-PC were collected from the Arroyo Del Tajo interpretive site in the Loma De Las Canas Quadrangle, East of Socorro, New Mexico.

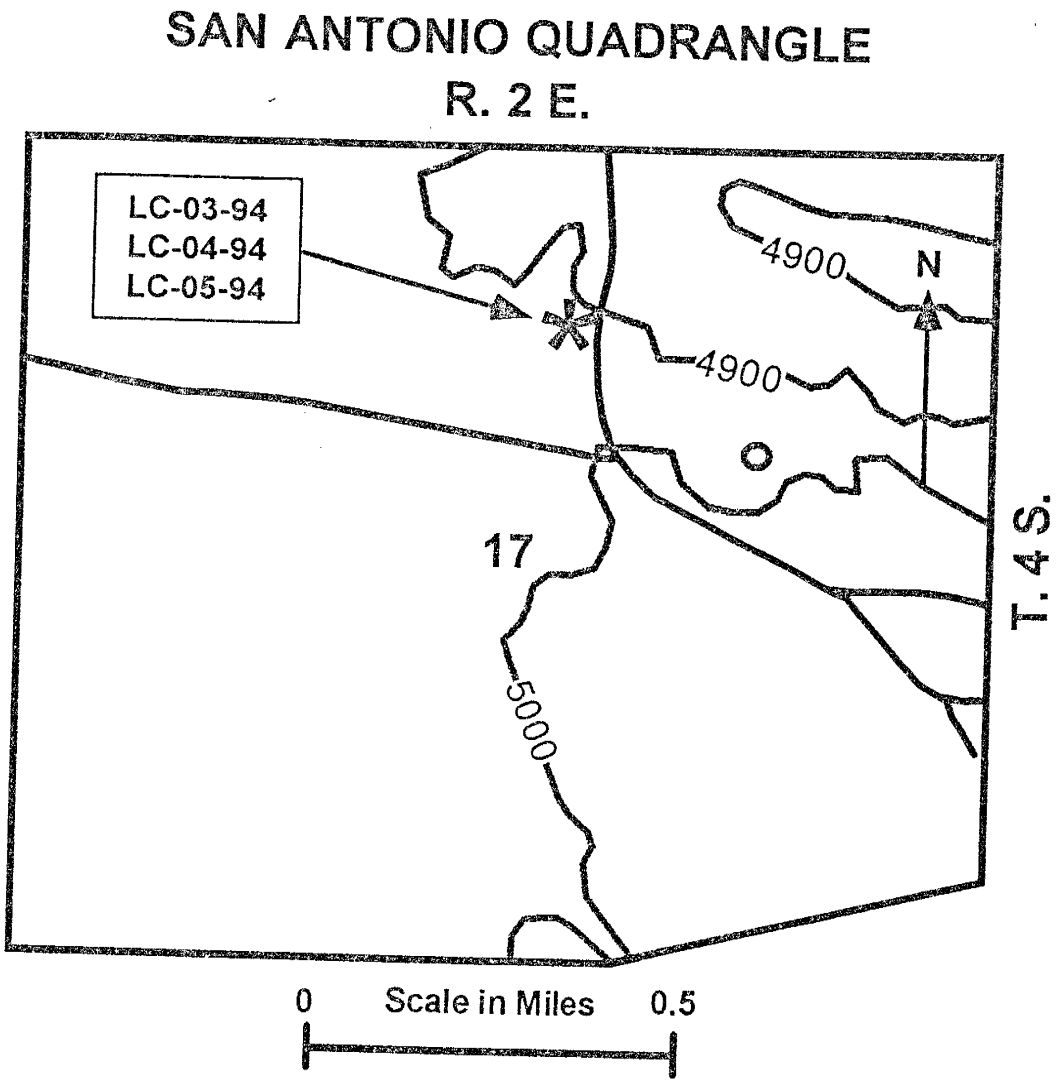

FIGURE A19: Calcrete samples LC-03-94 to LC-05-94 were collected from the San Antonio Quadrangle, South-East of Socorro, New Mexico.

VEGUITA QUADRANGLE

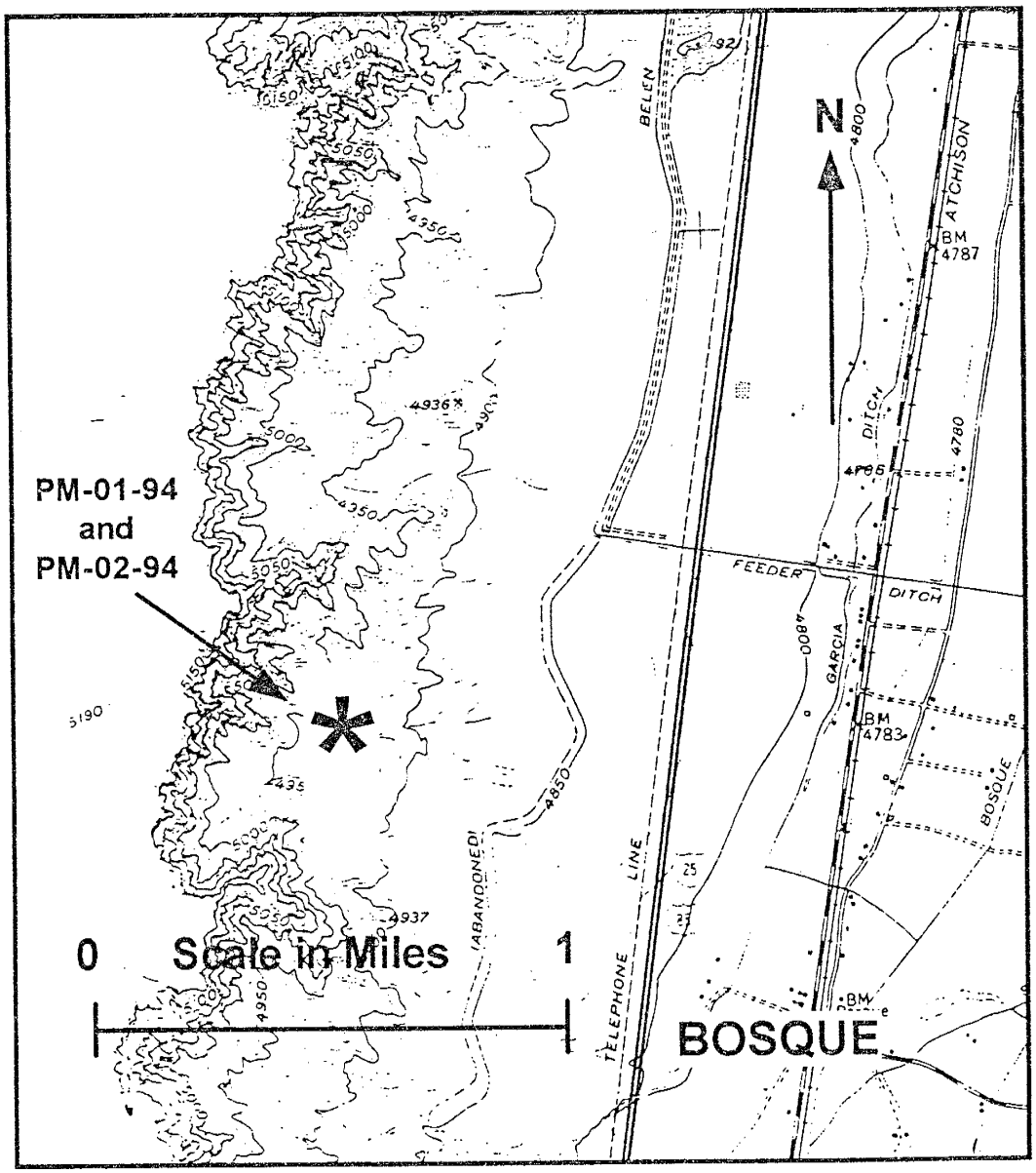

FIGURE A20: Calcrete samples PM-01-94 and PM-02-94 are calcite concretions in sand and were given for analysis by Peter Mozley, faculty member at New Mexico Tech, and collected from the Veguita Quadrangle, North of Socorro, New Mexico.

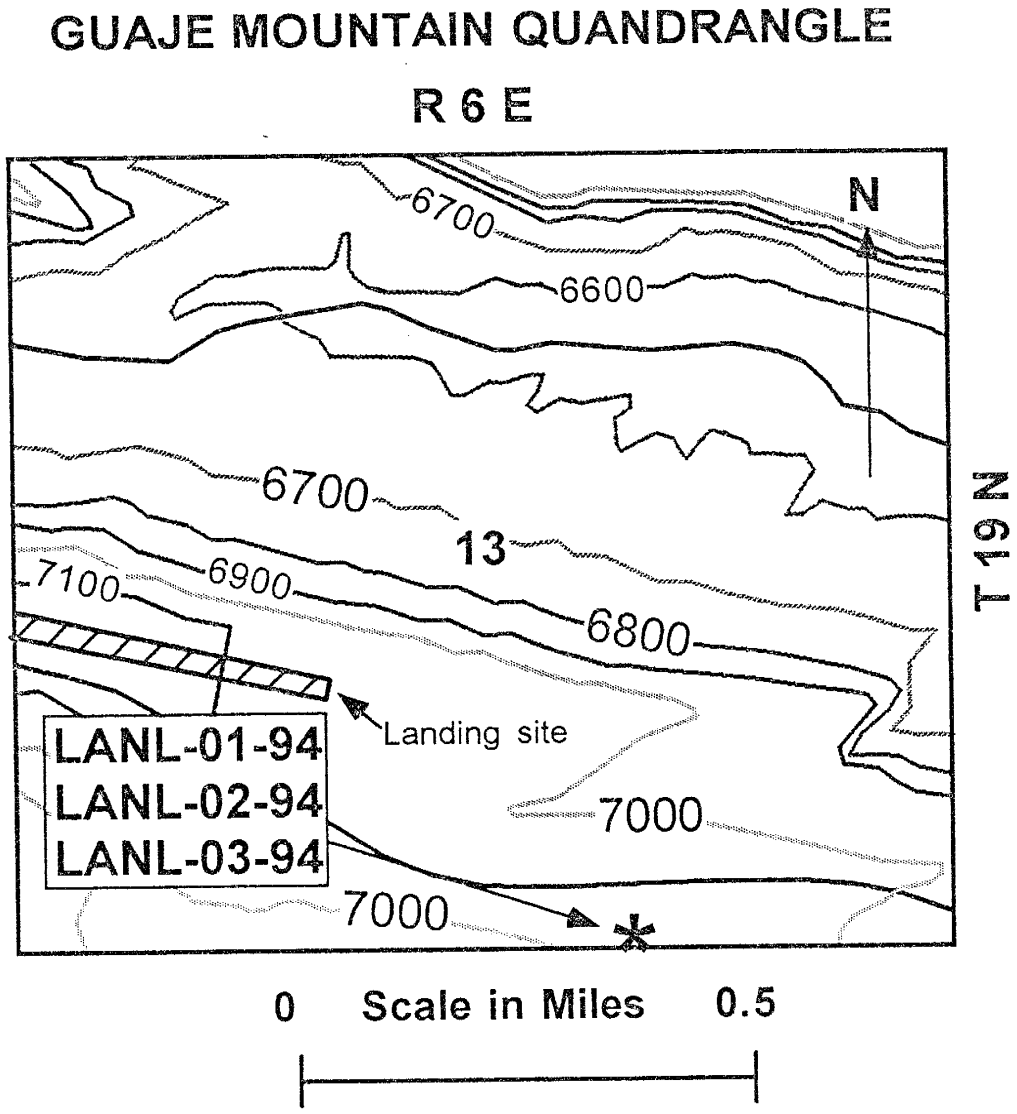

FIGURE A21: LANL vein calcite samples, LANL-01-94 to LANL-03-94, were collected from the Guaje Mountain Quadrangle, South of Los Alamos, New Mexico.

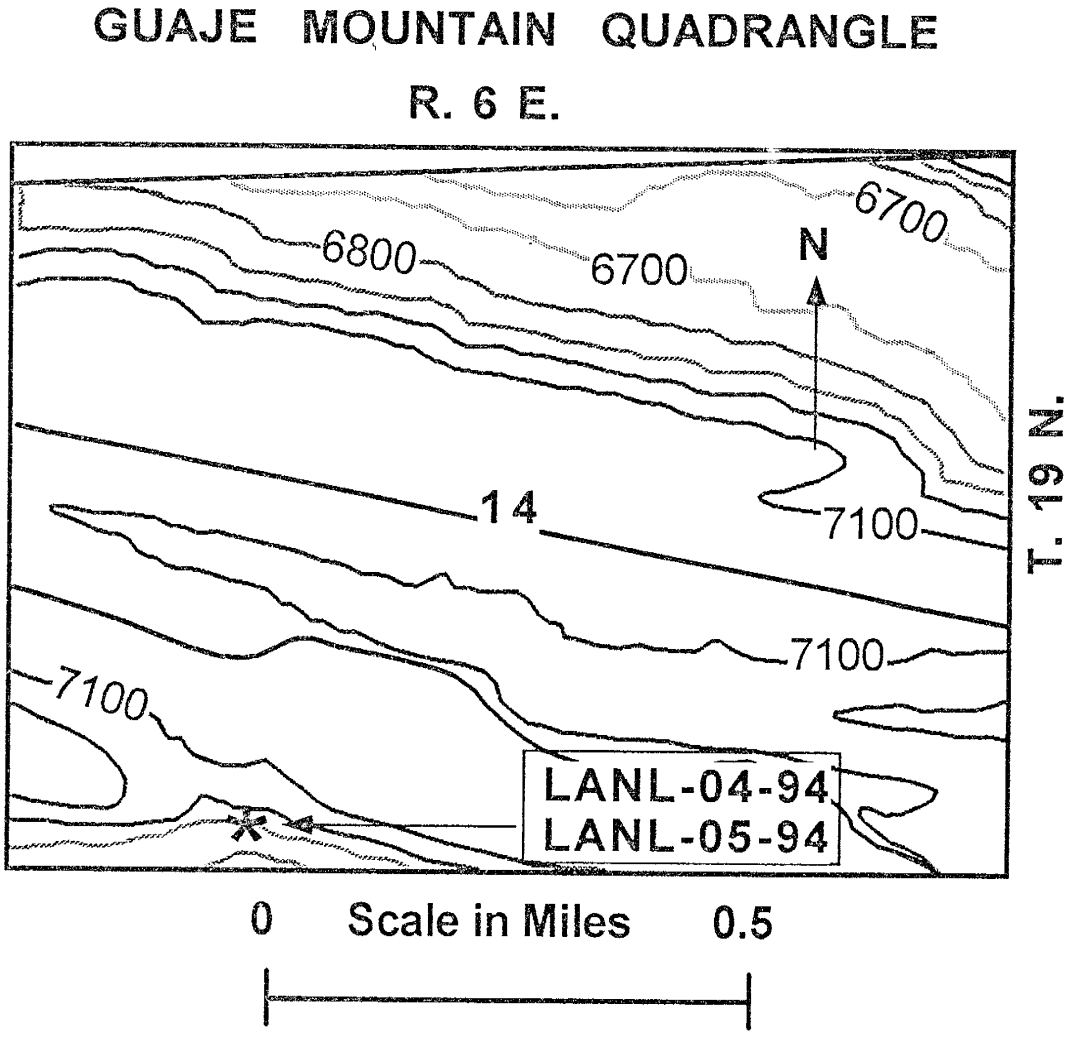

FIGURE A22: LANL vein calcite samples, LANL-04-94 and LANL-05-94, were collected from the Guaje Mountain Quadrangle, within Los Alamos, New Mexico.

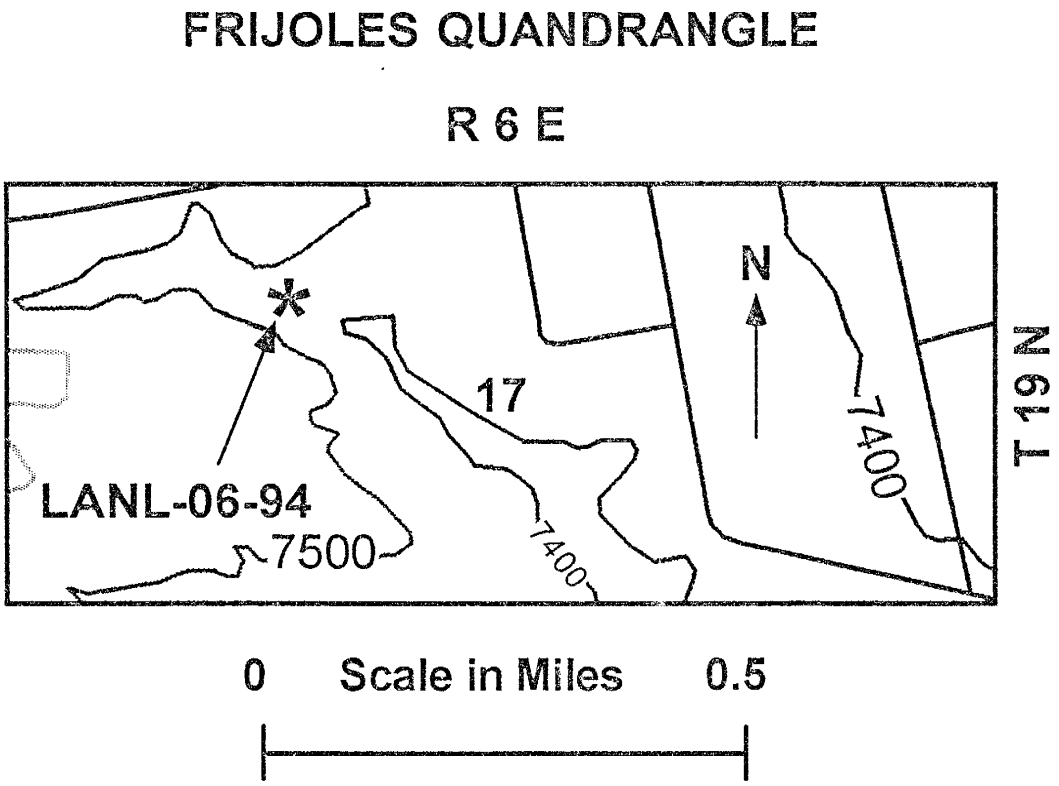

FIGURE A23: LANL vein calcite sample LANL-06-94 was collected from the Frijoles Quadrangle within Los Alamos, New Mexico.

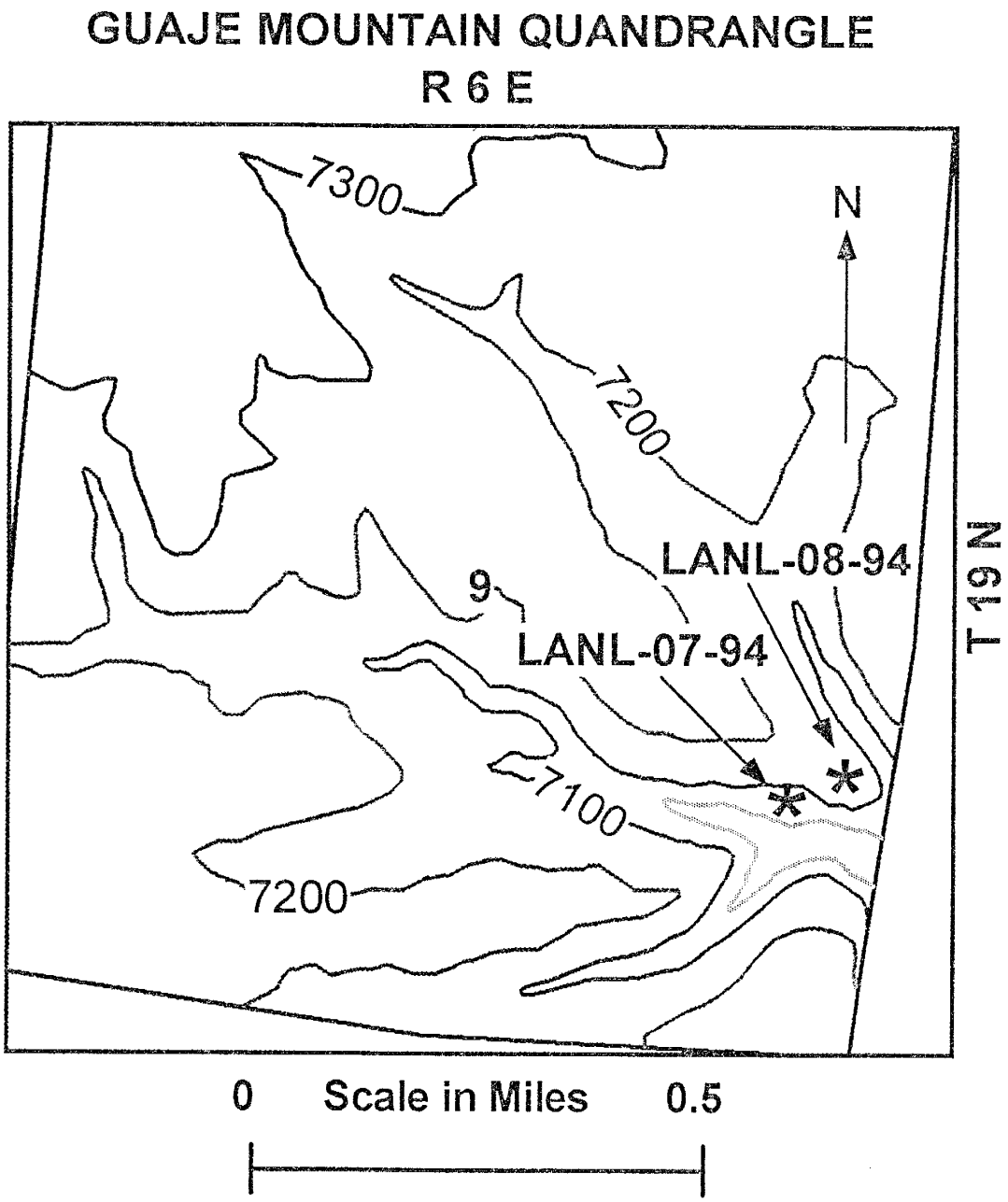

FIGURE A24: LANL vein calcite samples, LANL-07-94 and LANL-08-94, were collected from the Guaje Mountain Quadrangle, within Los Alamos, New Mexico.

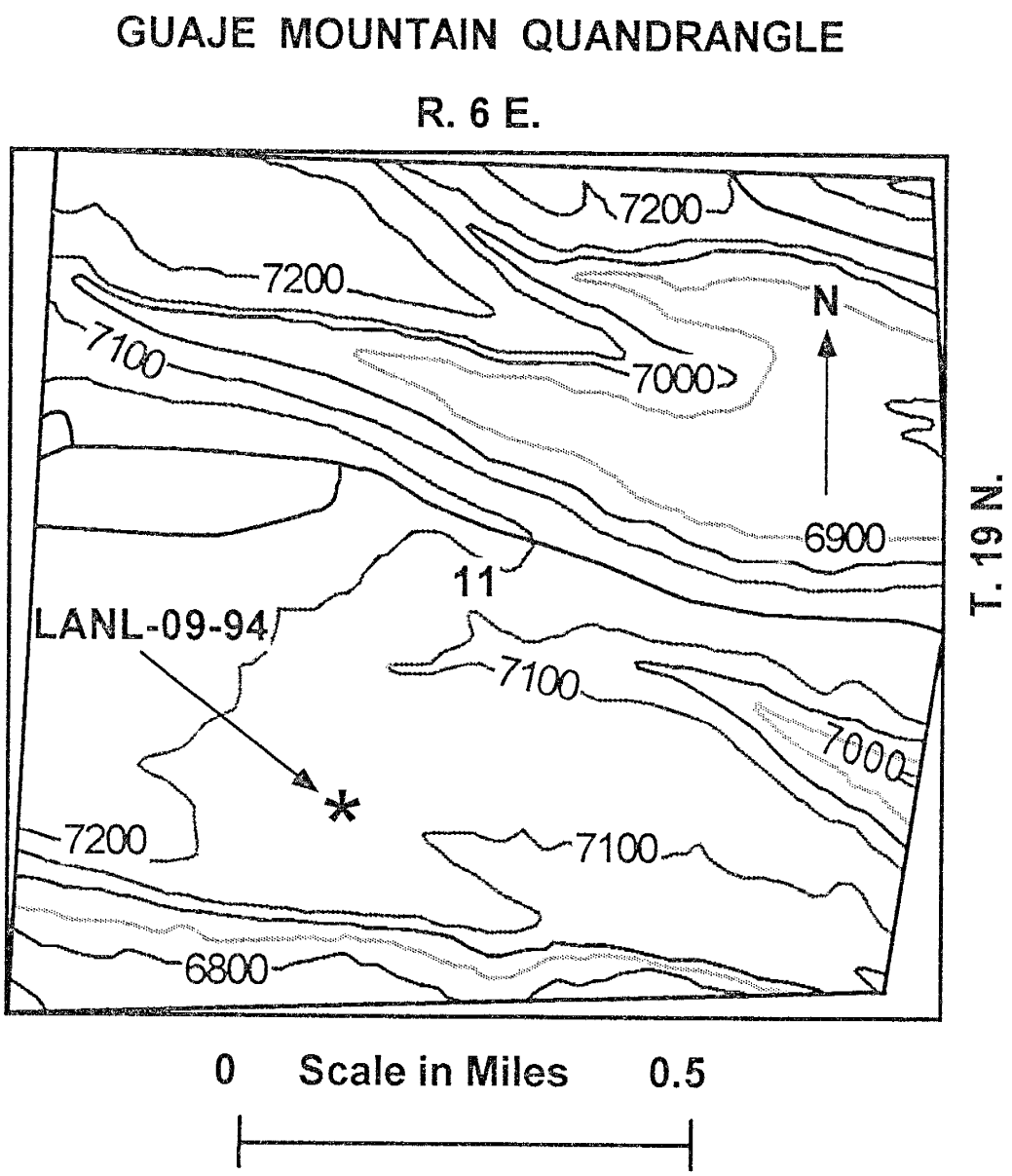

FIGURE A25: LANL vein calcite sample, LANL-09-94, was collected from the Guaje Mountain Quadrangle, within Los Alamos, New Mexico.

FIGURE A26: Factor pattern plots for group I carbonates:

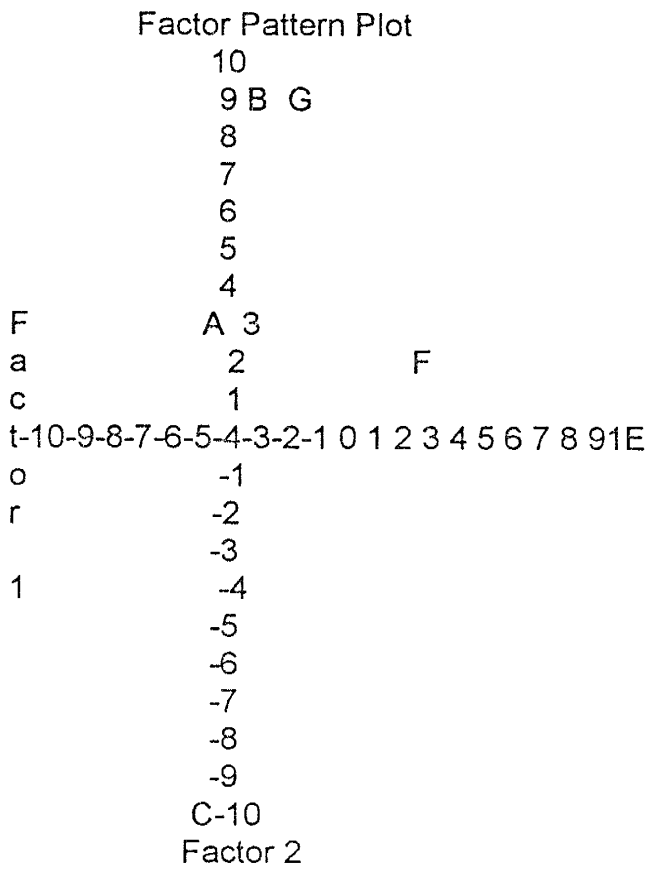

A: C1 = He
B: C2 = CH_4
C: C3 = H_2O
D: C4 = N_2
E: C5 = O_2
F: C6 = Ar
G: C7 = CO_2

FIGURE A27: Factor pattern plots for group II carbonates:

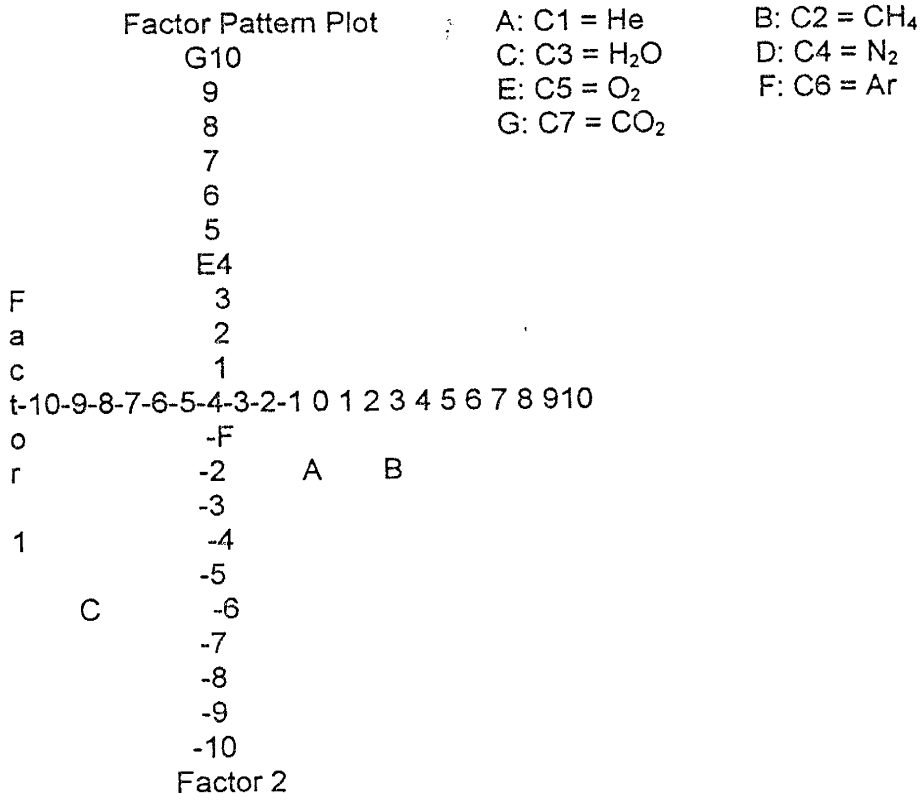

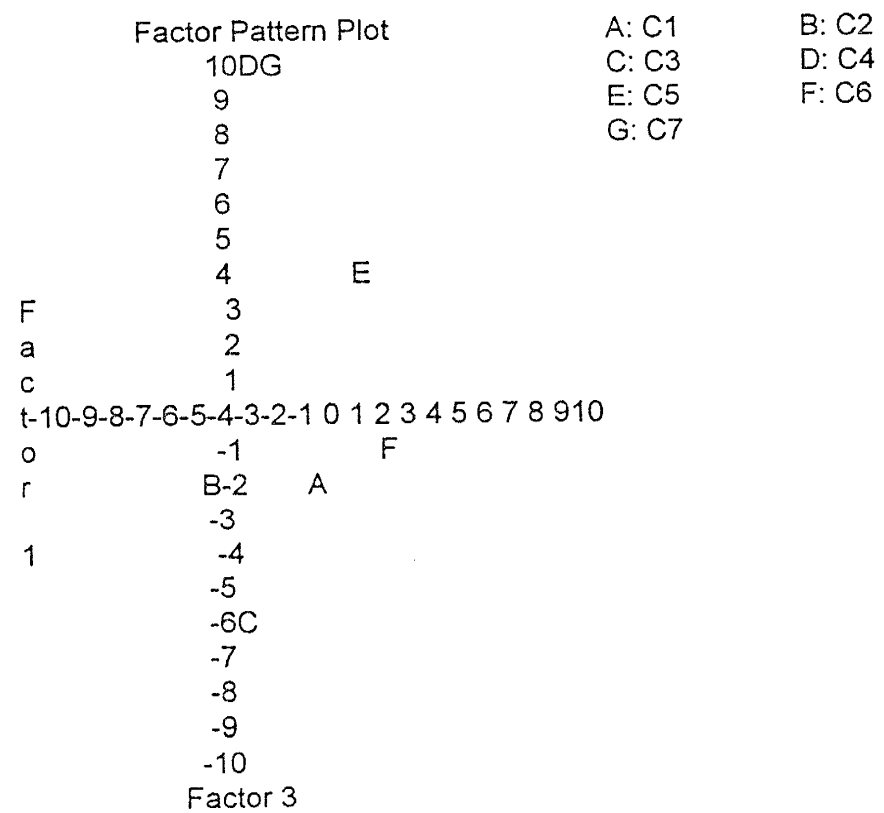

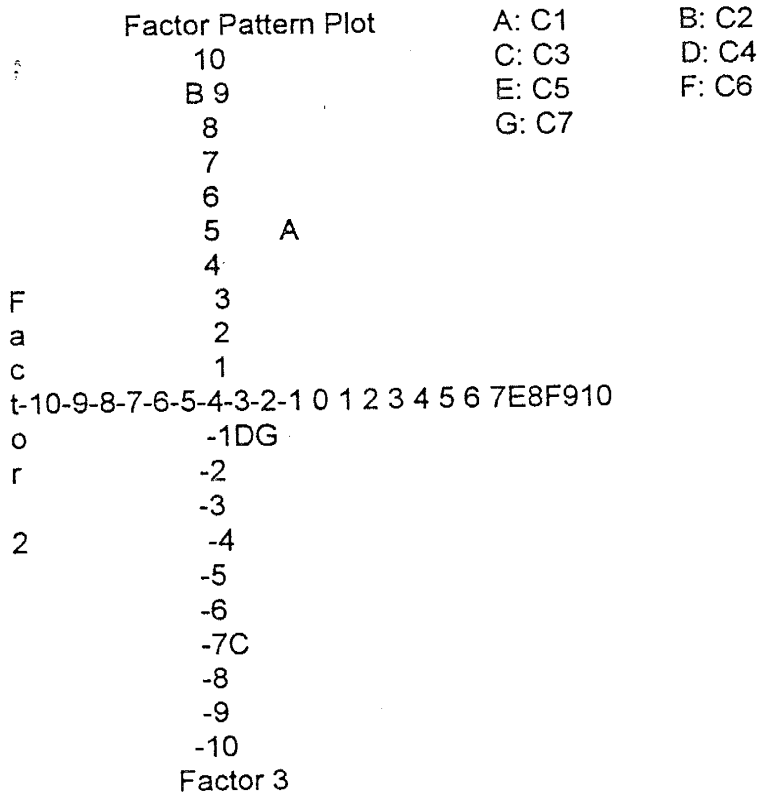
Factor Pattern Plot
A: C1
B: C2
C: C3
D: C4
E: C5
F: C6
G: C7
10
B 9
8
7
6
5 A
4
F 3
a 2
c 1
t-10-9-8-7-6-5-4-3-2-1 0 1 2 3 4 5 6 7E8F910
o -1DG
r -2
-3
2 -4
-5
-6
-7C
-8
-9
-10
Factor 3

APPENDIX B

TABLE B1: Cracking outline for measured gas species.

This is the sensitivity matrix.

Mass #	He	CH_4	H_2O	N_2	O_2	Ar	CO_2
4	0.9842						
15		0.8949					
18			0.6786				
28				0.8899			0.1492
32					0.8602		
40						0.6959	
44							1.2608

This is the inverted matrix used in the calculation.

Mass #	He	CH_4	H_2O	N_2	O_2	Ar	CO_2
4	1.0161						
15		1.1174					
18			1.4736				
28				1.1237			-0.1330
32					1.1625		
40						1.4368	
44							0.7932

TABLE B2:
Concentration of gases evolved during crushing of different carbonates

Caliches Sample #	Run #	He %	CH4 %	H2O %	N2 %	O2 %	Ar %	CO2 %
WB-01-94	4507	6.51E-03	2.04E+01	5.39E+01	6.29E+00	2.10E-01	1.34E-01	1.90E+01
WB-02-94	4425	6.57E-03	2.30E+01	6.36E+01	5.53E+00	1.69E+00	5.12E-02	6.10E+00
WB-03-94	4426	7.22E-03	5.05E+01	2.07E+01	1.05E+01	3.56E-01	1.06E-01	1.79E+01
WB-04-94	4428	4.05E-03	4.53E+01	4.22E+01	5.76E+00	2.76E-01	3.77E-02	6.39E+00
WB-05-94	4427	3.91E-03	3.48E+01	2.65E+01	6.57E+00	7.54E-01	7.75E-02	3.13E+01
WB-06-94	4429	4.02E-02	5.16E+01	3.03E+01	6.25E+00	1.11E-01	3.24E-02	1.16E+01
WB-07-94	4430	2.86E-03	1.87E+01	7.00E+01	2.75E+00	2.58E-01	2.53E-02	8.28E+00
WB-08-94	4508	5.39E-03	3.18E+01	4.24E+01	5.59E+00	2.66E-01	1.70E-01	1.97E+01
NC-01-94	4657	4.31E-03	2.34E+01	4.40E+01	2.78E+01	8.79E-02	6.05E-01	4.12E+00
NC-02-94	4658	2.54E-03	2.16E+01	5.82E+01	1.89E+01	8.49E-02	3.94E-01	8.48E-01
NC-03-94	4659	3.40E-03	2.00E+01	6.36E+01	1.23E+01	1.49E-01	2.20E-01	3.78E+00
NC-04-94	4660	3.00E-03	4.30E+01	2.68E+01	2.81E+01	2.22E-01	1.67E-01	1.69E+00
NC-05-94	4661	4.47E-03	3.65E+01	2.63E+01	2.99E+01	5.74E-01	4.74E-01	6.29E+00
NC-06-94	4662	4.45E-03	2.84E+01	5.21E+01	9.31E+00	1.02E-01	7.30E-02	1.00E+01
WR-01-94	4666	3.59E-03	9.83E+00	8.05E+01	7.26E+00	1.22E+00	9.88E-02	1.09E+00
WR-02-94	4704	9.33E-03	4.34E+01	5.36E+01	2.49E+00	5.14E-02	5.32E-02	4.11E-01
WR-03-94	4705	8.29E-03	3.68E+01	5.75E+01	4.66E+00	1.09E-01	3.42E-02	9.23E-01
WR-04-94	4667	4.70E-03	3.06E+01	6.64E+01	1.56E+00	2.12E-01	1.60E-01	1.04E+00
WR-05-94	4668	1.53E-03	3.58E+01	5.88E+01	2.57E+00	1.05E+00	1.07E-02	1.75E+00
WR-06-94	4669	1.48E-03	1.47E+01	8.36E+01	7.18E-01	1.41E-01	6.81E-03	7.51E-01
WR-07-94	4654	2.84E-03	3.03E+01	6.16E+01	4.82E+00	2.24E+00	6.58E-02	9.36E-01
WR-08-94	4655	1.78E-03	1.30E+01	6.50E+01	1.94E+01	8.15E-01	1.95E-01	1.58E+00
WR-09-94	4656	5.70E-03	1.64E+01	6.77E+01	1.30E+01	4.59E-01	1.44E-01	2.28E+00
LL-01-94	4607	7.71E-03	1.34E+01	7.45E+01	5.05E+00	5.44E-01	6.93E-02	6.43E+00
LC-01-94	4608	6.95E-03	1.49E+01	7.21E+01	3.06E+00	8.50E-02	1.09E-01	9.81E+00
LC-02-94	4609	6.86E-03	2.27E+01	6.35E+01	4.30E+00	8.53E-01	9.87E-02	8.55E+00
SAE-01-94	4671	4.64E-03	3.01E+01	4.25E+01	1.52E+01	8.07E-01	1.55E-01	1.13E+01
SAE-02-94	4672	5.62E-03	5.19E+01	3.97E+01	5.19E+00	2.21E-01	4.26E-02	2.98E+00
04-LR-93	4421	2.64E-03	2.60E+01	5.66E+01	1.11E+00	1.24E-03	2.11E-02	1.63E+01

Active Travertine Sample #	Run #	He %	CH4 %	H2O %	N2 %	O2 %	Ar %	CO2 %
as-01-94	4515	6.92E-04	3.87E-02	9.83E+01	1.59E+00	1.37E-02	1.83E-02	5.22E-02
as-02-94	4516	1.71E-04	3.48E-02	9.99E+01	1.93E-02	4.46E-03	1.08E-03	6.20E-02
as-03-94	4517	4.19E-05	4.84E-02	9.97E+01	2.17E-01	5.39E-03	3.13E-03	5.19E-02
sd-01-94	4522	1.72E-05	4.70E-02	9.92E+01	5.57E-01	3.11E-02	7.06E-03	1.57E-01
sd-02-94	4524	5.43E-05	2.02E-02	9.99E+01	3.26E-02	1.58E-03	7.03E-04	2.19E-02
lc-01-94	4519	6.01E-05	3.43E-02	9.98E+01	7.31E-02	1.75E-03	1.34E-03	1.03E-01
lc-02-94	4520	2.07E-05	1.66E-02	9.99E+01	3.59E-02	1.20E-04	4.95E-04	2.74E-02
lc-04-94	4521	2.00E-05	6.49E-03	9.99E+01	5.70E-02	1.83E-05	7.39E-04	7.34E-03
sd2-01-94	4589	2.94E-05	6.49E-03	1.00E+02	2.31E-02	1.35E-03	3.92E-04	9.47E-03
sd2-02-94	4590	2.79E-05	1.21E-02	9.99E+01	1.34E-02	1.54E-03	5.10E-04	2.58E-02
sd2-03-94	4591	1.93E-05	3.94E-03	1.00E+02	1.12E-02	7.86E-04	1.77E-04	4.00E-03
sd2-04-94	4586	1.72E-05	7.60E-03	9.99E+01	8.80E-02	1.54E-03	9.22E-04	4.85E-02
sd2-05-94	4587	1.36E-05	3.07E-03	9.99E+01	2.67E-02	1.03E-03	3.01E-04	3.84E-02
sd2-06-94	4588	4.90E-05	1.44E-03	9.99E+01	2.52E-02	5.15E-04	2.91E-04	6.47E-02
mhs-01-94	4526	1.44E-05	8.74E-03	1.00E+02	8.21E-03	7.23E-04	1.78E-04	1.00E-02
mhs-02-94	4525	3.76E-05	9.73E-03	1.00E+02	1.28E-02	1.95E-03	2.73E-04	1.12E-02
lh-01-94	4527	1.67E-05	8.66E-03	1.00E+02	1.17E-02	5.74E-04	2.02E-04	1.43E-02
lh-02-94	4523	4.65E-05	2.58E-02	9.99E+01	3.91E-02	2.20E-03	8.58E-04	6.01E-02

TABLE B2, Continue:

Ancient Travertine

Sample #	Run #	He %	CH4 %	H2O %	N2 %	O2 %	Ar %	CO2 %
01-AM-93	4503	1.05E-03	1.93E-02	9.98E+01	3.72E-02	9.43E-03	5.89E-04	9.43E-02
02-AM-93	4504	6.66E-04	2.07E-02	9.97E+01	5.78E-02	1.00E-02	8.94E-04	1.84E-01
03-AM-93	4505	2.45E-04	9.28E-02	9.95E+01	8.03E-02	1.46E-02	1.11E-03	3.36E-01
04-AM-93	4496	1.87E-03	3.15E-02	9.95E+01	5.18E-02	1.79E-02	1.08E-03	4.23E-01
05-AM-93	4497	7.56E-04	2.16E-01	9.94E+01	1.78E-01	1.71E-02	2.29E-03	2.35E-01
NMT-01-94	4566	5.71E-03	5.43E-02	9.98E+01	3.55E-02	1.44E-02	1.46E-03	8.11E-02
NMT-02-94	4567	3.24E-03	3.60E-02	9.98E+01	3.76E-02	1.16E-02	7.88E-04	7.11E-02
NMT-03-94	4568	3.99E-03	4.15E-02	9.98E+01	5.21E-02	1.56E-02	1.01E-03	1.12E-01
NMT-04-94	4579	1.46E-03	6.48E-02	9.94E+01	2.09E-01	3.73E-02	3.22E-03	2.51E-01
NMT-05-94	4580	2.57E-03	3.34E-02	9.98E+01	5.17E-02	1.17E-02	1.08E-03	7.71E-02
NMT-06-94	4581	5.32E-03	5.08E-02	9.98E+01	4.09E-02	1.34E-02	1.13E-03	9.60E-02
NMT-07-94	4612	7.91E-04	5.45E-02	9.95E+01	9.90E-02	2.36E-02	1.62E-03	3.34E-01

Pedogenic Calcrete

Sample #	Run #	He %	CH4 %	H2O %	N2 %	O2 %	Ar %	CO2 %
01-94-PC	4440	1.35E-04	2.39E-01	9.94E+01	9.69E-02	3.69E-03	7.34E-04	2.47E-01
02-94-PC	4441	2.38E-04	1.09E+00	9.77E+01	2.35E-01	5.70E-03	2.34E-03	9.42E-01
03-94-PC	4611	5.95E-05	1.24E-01	9.95E+01	3.14E-02	6.80E-04	5.89E-04	3.04E-01
04-94-PC	4509	1.52E-04	5.76E-01	9.83E+01	1.97E-01	4.38E-03	5.67E-03	9.67E-01
05-94-PC	4442	1.61E-04	1.24E+00	9.76E+01	1.89E-01	4.24E-03	1.10E-03	9.43E-01
06-94-PC	4423	1.33E-03	1.47E+00	9.33E+01	4.57E-01	3.08E-02	6.47E-03	4.72E+00
07-94-PC	4596	7.45E-04	1.55E-01	9.92E+01	7.11E-02	7.65E-03	2.01E-03	5.97E-01
01-LR-93	4401	1.44E-02	3.22E+00	7.71E+01	1.29E+01	3.06E+00	2.86E-01	3.43E+00
02-LR-93	4402	9.15E-03	1.39E+01	1.82E+01	1.40E+01	8.23E+00	3.05E-01	4.53E+01
05-LR-93	4422	9.76E-04	1.07E-01	9.84E+01	9.98E-01	2.18E-01	2.63E-02	2.72E-01

Phreatic Calcrete (Calcite cemented gravels).

Sample #	Run #	He %	CH4 %	H2O %	N2 %	O2 %	Ar %	CO2 %
08-94-PC	4597	5.50E-04	1.76E-01	9.86E+01	7.44E-01	8.05E-02	8.51E-03	3.73E-01
09-94-PC	4598	2.94E-04	3.54E-01	9.83E+01	1.08E+00	2.21E-02	5.28E-03	2.30E-01
10-PC-94	4673	4.71E-03	3.41E+01	3.48E+01	2.46E+01	1.54E+00	4.90E-01	4.48E+00
LC-03-94	4603	6.31E-04	1.64E-01	9.95E+01	1.31E-02	9.19E-04	8.92E-04	3.64E-01
LC-04-94	4604	4.62E-04	4.15E-01	9.90E+01	1.49E-01	9.49E-03	1.20E-03	5.44E-01
LC-05-94	4605	1.22E-03	3.56E-02	9.99E+01	2.06E-02	1.03E-02	3.05E-04	2.34E-02

Phreatic Calcrete (Vein Calcites).

Sample #	Run #	He %	CH4 %	H2O %	N2 %	O2 %	Ar %	CO2 %
UNK-01-93	4486	1.57E-03	2.38E-02	9.98E+01	9.72E-02	1.91E-02	1.30E-03	4.10E-02
UNK-02-93	4487	5.79E-04	1.97E-02	9.99E+01	4.30E-02	2.87E-02	6.05E-04	3.05E-02
MCA-01-94	4532	1.35E-03	2.30E-02	9.99E+01	7.24E-02	1.97E-02	1.33E-03	2.67E-02
MCA-02-94	4533	1.70E-03	2.22E-02	9.99E+01	2.77E-02	1.36E-02	7.20E-04	2.15E-02
MCA-03-94	4535	2.62E-03	4.08E-02	9.98E+01	1.23E-01	3.32E-02	1.99E-03	3.28E-02
MCA-04-94	4536	3.41E-03	4.14E-02	9.99E+01	4.83E-02	1.43E-02	8.65E-04	2.98E-02
Tower-01-94	4534	8.21E-04	2.25E-02	9.98E+01	1.10E-01	2.52E-02	1.50E-03	2.48E-02
Tower-02-94	4537	1.78E-03	3.44E-02	9.98E+01	7.17E-02	1.93E-02	1.01E-03	4.91E-02
NMBMG-02	4539	4.83E-03	5.05E-02	9.99E+01	4.32E-02	9.98E-03	1.75E-03	3.88E-02
NMBMG-04	4548	2.58E-03	3.41E-02	9.99E+01	6.57E-02	2.11E-02	9.34E-04	3.48E-02
NMBMG-05	4549	5.57E-03	4.91E-02	9.98E+01	9.67E-02	2.98E-02	2.23E-03	4.42E-02
NMBMG-06	4560	4.85E-03	4.47E-02	9.97E+01	8.67E-02	2.67E-02	1.99E-03	8.67E-02
TC-01-94	4547	3.11E-03	3.15E-02	9.98E+01	5.29E-02	1.74E-02	1.57E-03	1.38E-01

Phreatic Calcrete (Calcite concretions in sand).

Sample #	Run #	He %	CH4 %	H2O %	N2 %	O2 %	Ar %	CO2 %
PM-01-94	4664	4.86E-03	2.51E+01	5.91E+01	8.64E+00	1.09E+00	1.31E-01	5.98E+00
PM-02-94	4665	1.52E-03	1.09E+01	5.75E+01	2.44E+01	3.61E+00	4.08E-01	3.24E+00

TABLE B2, Continue:

Carbonates from Los Alamos National Laboratory

Sample #	Run #	He %	CH4 %	H2O %	N2 %	O2 %	Ar %	CO2 %
1-AL-93	4446	7.03E-03	3.05E+01	3.78E+01	1.90E+01	1.26E-01	1.32E-01	1.23E+01
2-AL-93	4483	1.91E-02	4.27E+01	4.52E+01	6.07E+00	2.67E-01	7.56E-02	5.74E+00
3-AL-93	4448	1.92E-02	2.26E+01	7.00E+01	2.32E+00	5.45E-01	2.52E-02	4.48E+00
4-AL-93	4447	2.61E-03	1.88E+01	6.45E+01	1.11E+01	1.54E-01	8.22E-02	5.35E+00
5-AL-93	4449	3.88E-03	3.01E+01	5.96E+01	8.93E+00	1.80E-02	2.84E-02	1.31E+00
6-LA-93	4450	1.07E-03	3.13E+01	2.74E+01	3.96E+01	6.19E-01	4.74E-01	5.08E-01
7-LA-93	4451	5.35E-03	6.78E+01	1.31E+01	9.70E+00	7.06E-02	8.82E-02	9.20E+00
8-LA-93	4484	4.10E-03	1.83E+01	6.53E+01	1.24E+01	7.64E-02	5.37E-02	3.87E+00
9-LA-93	4485	1.32E-03	7.03E+00	3.07E+01	5.84E+01	1.83E+00	6.94E-01	1.29E+00
TA63(1-1)	4489	8.68E-03	3.22E+01	3.68E+01	2.43E+01	9.46E-01	5.91E-02	5.89E+00
TA63(1-2)	4490	7.17E-04	8.41E+00	8.62E+01	3.27E+00	8.32E-02	1.56E-02	1.97E+00
TA63(1-3)	4491	1.62E-03	1.03E+01	7.83E+01	7.83E+00	4.99E-02	3.63E-02	3.48E+00
TA63(1-4)	4492	3.36E-03	2.25E+01	6.04E+01	1.57E+01	7.97E-02	4.36E-02	1.21E+00
LANL-01-94	4715	4.72E-03	4.76E+01	3.33E+01	1.23E+01	1.21E+00	1.39E-01	5.31E+00
LANL-02-94	4716	1.18E-02	3.59E+01	4.16E+01	1.72E+01	1.21E-01	9.49E-02	5.09E+00
LANL-03-94	4707	7.59E-03	2.90E+01	2.31E+01	3.04E+01	9.35E-01	2.72E-01	1.63E+01
LANL-04-94	4717	2.77E-02	2.25E+01	4.28E+01	1.91E+01	9.79E-01	2.07E-01	1.44E+01
LANL-05-94	4708	6.15E-03	1.75E+01	2.08E+01	4.17E+01	3.55E+00	5.01E-01	1.59E+01
LANL-06-94	4709	6.99E-03	1.51E+01	1.79E+01	4.76E+01	1.93E+00	5.06E-01	1.69E+01
LANL-07-94	4718	9.27E-03	3.93E+01	4.23E+01	1.57E+01	1.50E+00	1.46E-01	1.01E+00
LANL-08-94	4719	6.83E-03	3.45E+01	5.57E+01	7.17E+00	1.89E-01	4.00E-02	2.43E+00
LANL-09-94	4720	4.99E-03	4.59E+01	2.87E+01	1.50E+01	2.05E-01	6.43E-02	1.01E+01
LAH-4-A	4699	1.19E-02	3.99E+01	3.63E+01	7.66E+00	2.39E-01	5.94E-02	1.58E+01
LAH-4-B	4700	5.11E-03	2.00E+01	6.51E+01	4.71E+00	1.01E-01	3.16E-02	1.00E+01
LAH-4-C	4701	7.27E-03	2.69E+01	5.55E+01	5.17E+00	2.45E-01	5.13E-02	1.21E+01
LAL-8898A	4675	2.53E-03	2.35E+01	6.91E+01	4.32E+00	1.80E-01	1.48E-02	2.92E+00
LAL-8898B	4676	3.20E-03	2.87E+01	6.02E+01	5.91E+00	1.17E-01	3.82E-02	5.09E+00
LAL-8898C	4677	6.94E-03	1.93E+01	5.65E+01	5.61E+00	6.49E-02	3.99E-02	1.85E+01
LAL8898-30	4706	7.01E-03	1.29E+01	7.79E+01	6.96E+00	5.96E-01	1.41E-01	1.47E+00

Samples from Brent Newman

Sample #	Run #	He %	CH4 %	H2O %	N2 %	O2 %	Ar %	CO2 %
LAH-4-A	4699	1.19E-02	3.99E+01	3.63E+01	7.66E+00	2.39E-01	5.94E-02	1.58E+01
LAH-4-B	4700	5.11E-03	2.00E+01	6.51E+01	4.71E+00	1.01E-01	3.16E-02	1.00E+01
LAH-4-C	4701	7.27E-03	2.69E+01	5.55E+01	5.17E+00	2.45E-01	5.13E-02	1.21E+01
LAL-8898A	4675	2.53E-03	2.35E+01	6.91E+01	4.32E+00	1.80E-01	1.48E-02	2.92E+00
LAL-8898B	4676	3.20E-03	2.87E+01	6.02E+01	5.91E+00	1.17E-01	3.82E-02	5.09E+00
LAL-8898C	4677	6.94E-03	1.93E+01	5.65E+01	5.61E+00	6.49E-02	3.99E-02	1.85E+01
LAL8898-30	4706	7.01E-03	1.29E+01	7.79E+01	6.96E+00	5.96E-01	1.41E-01	1.47E+00

Samples from Nevada Test Site

Sample #	Run #	He %	CH4 %	H2O %	N2 %	O2 %	Ar %	CO2 %
LANL-357	4493	2.80E-03	1.26E+01	4.95E+01	2.63E+01	2.12E+00	3.28E-01	9.15E+00
GTE-1	4494	1.30E-03	4.80E+00	7.14E+01	1.99E+01	1.94E+00	1.64E-01	1.77E+00
WS-5-SSL	4495	3.01E-03	1.66E+01	5.71E+01	1.13E+01	1.21E+00	1.33E-01	1.36E+01

Carbonates from Reylieh, N.M.

Sample #	Run #	He %	CH4 %	H2O %	N2 %	O2 %	Ar %	CO2 %
ry-01-94	4649	8.50E-07	6.20E-03	1.00E+02	2.81E-02	1.37E-03	3.09E-04	9.51E-03
ry-02-94	4650	4.45E-06	1.33E-02	1.00E+02	1.78E-03	4.17E-04	7.50E-05	1.51E-04
ry-03-94	4651	4.45E-06	1.22E-02	1.00E+02	2.36E-03	3.94E-04	7.56E-05	1.68E-04

TABLE B3:
Gas to water ratios for different samples

Caliches

Sample #	H2O/Gas
WB-01-94	1.2
WB-02-94	1.7
WB-03-94	0.3
WB-04-94	0.7
WB-05-94	0.4
WB-06-94	0.4
WB-07-94	2.3
WB-08-94	0.7
NC-01-94	0.8
NC-02-94	1.4
NC-03-94	1.7
NC-04-94	0.4
NC-05-94	0.4
NC-06-94	1.1
WR-01-94	4.1
WR-02-94	1.2
WR-03-94	1.4
WR-04-94	2.0
WR-05-94	1.4
WR-06-94	5.1
WR-07-94	1.6
WR-08-94	1.9
WR-09-94	2.1
LL-01-94	2.9
LC-01-94	2.6
LC-02-94	1.7
SAE-01-94	0.7
SAE-02-94	0.7
04-LR-93	1.3

Active Travertine

Sample #	H2O/Gas
as-01-94	57.2
as-02-94	820.0
as-03-94	305.5
sd-01-94	124.2
sd-02-94	1296.7
lc-01-94	466.6
lc-02-94	1241.8
lc-04-94	1395.0
sd2-01-94	2449.2
sd2-02-94	1869.4
sd2-03-94	4974.3
sd2-04-94	681.2
sd2-05-94	1436.9
sd2-06-94	1083.0
mhs-01-94	3583.1
mhs-02-94	2780.8
lh-01-94	2821.2
lh-02-94	779.6

Ancient Travertine

Sample #	H2O/Gas
01-AM-93	616.8
02-AM-93	364.3
03-AM-93	189.6
04-AM-93	188.6
05-AM-93	153.1
NMT-01-94	518.2
NMT-02-94	622.7
NMT-03-94	442.0
NMT-04-94	175.4
NMT-05-94	562.3
NMT-06-94	480.7
NMT-07-94	193.8

Phreatic Calcrete (VC.).

Sample #	H2O/Gas
UNK-01-93	542.7
UNK-02-93	812.0
MCA-01-94	691.2
MCA-02-94	1142.3
MCA-03-94	426.2
MCA-04-94	723.8
Tower-01-94	540.0
Tower-02-94	563.0
NMBMG-02	669.5
NMBMG-04	703.0
NMBMG-05	438.5
NMBMG-06	396.4
TC-01-94	408.2

Phreatic Calcrete (Calcite concr

Sample #	H2O/Gas
PM-01-94	1.4
PM-02-94	1.4

Samples from NTS.

Sample #	H2O/Gas
LANL-357	1.0
GTE-1	2.5
WS-5-SSL	1.3

Carbonates from Riley

Sample #	H2O/Gas
ry-01-94	2198.7
ry-02-94	6365.8
ry-03-94	6568.9

Phreatic Calcrete (CCG).

Sample #	H2O/Gas
08-94-PC	71.3
09-94-PC	58.2
10-PC-94	0.5
LC-03-94	183.0
LC-04-94	99.7
LC-05-94	1093.4

Carbonates from LANL.

Sample #	H2O/Gas
1-AL-93	0.6
2-AL-93	0.8
3-AL-93	2.3
4-AL-93	1.8
5-AL-93	1.5
6-LA-93	0.4
7-LA-93	0.2
8-LA-93	1.9
9-LA-93	0.4
TA63(1-1)	0.6
TA63(1-2)	6.3
TA63(1-3)	3.6
TA63(1-4)	1.5
LANL-01-94	0.5
LANL-02-94	0.7
LANL-03-94	0.3
LANL-04-94	0.7
LANL-05-94	0.3
LANL-06-94	0.2
LANL-07-94	0.7
LANL-08-94	1.3
LANL-09-94	0.4
LAH-4-A	0.6
LAH-4-B	1.9
LAH-4-C	1.2
LAL-8898A	2.2
LAL-8898B	1.5
LAL-8898C	1.3
LAL8898-300	3.5

Pedogenic Calcrete

Sample #	H2O/Gas
01-94-PC	169.2
02-94-PC	42.9
03-94-PC	216.2
04-94-PC	56.1
05-94-PC	41.0
06-94-PC	13.9
07-94-PC	118.8
01-LR-93	3.4
02-LR-93	0.2
05-LR-93	59.8

TABLE B4:
Statistical description of different carbonates:

Caliches	He	CH4	H2O	N2	O2	Ar	CO2
Mean	5.95E-03	28.930	53.9	9.168	4.81E-01	1.32E-01	7.351
Std. Error	1.28E-03	2.285	3.2	1.537	9.83E-02	2.60E-02	1.389
Median	4.47E-03	28.391	57.5	5.757	2.58E-01	9.87E-02	6.104
Mode	NA	NA	NA	NA	NA	NA	NA
Std.Dev.	6.91E-03	12.306	17.0	8.276	5.29E-01	1.40E-01	7.480
Variance	4.77E-05	151.429	288.7	68.486	2.80E-01	1.95E-02	55.958
Kurtosis	2.35E+01	-0.812	-0.7	1.147	3.67E+00	4.75E+00	2.399
Skewness	4.63E+00	0.407	-0.4	1.432	1.87E+00	2.15E+00	1.511
Range	3.87E-02	42.033	63.0	29.142	2.24E+00	5.98E-01	30.861
Minimum	1.48E-03	9.830	20.7	0.718	1.24E-03	6.81E-03	0.411
Maximum	4.02E-02	51.864	83.6	29.860	2.24E+00	6.05E-01	31.292
Sum	1.73E-01	838.973	1564.0	265.877	1.40E+01	3.83E+00	213.173
Count	2.90E+01	29.000	29.0	29.000	2.90E+01	2.90E+01	29.000
C. L (0.95)	2.51E-03	4.479	6.2	3.012	1.93E-01	5.09E-02	2.723
% variation	0.80	523.43	535.35	747.00	58.24	14.79	761.25

Ped. Calc	He	CH4	H2O	N2	O2	Ar	CO2
Mean	2.73E-03	2.210	87.9	2.920	1.16E+00	6.36E-02	5.774
Std. Error	1.56E-03	1.330	8.0	1.761	8.42E-01	3.88E-02	4.419
Median	4.91E-04	0.834	98.0	0.216	6.67E-03	4.00E-03	0.943
Mode	NA	NA	NA	NA	NA	NA	NA
Std.Dev.	4.93E-03	4.207	25.4	5.569	2.66E+00	1.23E-01	13.975
Variance	2.43E-05	17.702	644.6	31.017	7.09E+00	1.50E-02	195.300
Kurtosis	3.14E+00	8.601	8.1	1.454	6.65E+00	1.41E+00	9.682
Skewness	2.01E+00	2.882	-2.8	1.778	2.57E+00	1.77E+00	3.096
Range	1.43E-02	13.766	81.3	13.996	8.23E+00	3.05E-01	45.072
Minimum	5.95E-05	0.107	18.2	0.031	6.80E-04	5.89E-04	0.247
Maximum	1.44E-02	13.872	99.5	14.028	8.23E+00	3.05E-01	45.319
Sum	2.73E-02	22.105	878.7	29.198	1.16E+01	6.36E-01	57.745
Count	1.00E+01	10.000	10.0	10.000	1.00E+01	1.00E+01	10.000
C. L (0.95)	3.06E-03	2.608	15.7	3.452	1.65E+00	7.60E-02	8.662
% variation	0.89	800.83	733.57	1062.31	612.54	23.61	3382.13

Act. Trav.	He	CH4	H2O	N2	O2	Ar	CO2
Mean	7.49E-05	0.019	99.8	0.158	3.91E-03	2.05E-03	0.043
Std. Error	3.73E-05	0.004	0.1	0.090	1.77E-03	1.03E-03	0.009
Median	2.87E-05	0.011	99.9	0.030	1.54E-03	6.06E-04	0.033
Mode	NA	NA	NA	NA	NA	NA	NA
Std.Dev.	1.58E-04	0.016	0.4	0.381	7.49E-03	4.38E-03	0.039
Variance	2.50E-08	0.000	0.2	0.145	5.61E-05	1.92E-05	0.002
Kurtosis	1.58E+01	-0.771	10.8	13.372	1.13E+01	1.25E+01	3.400
Skewness	3.91E+00	0.812	-3.2	3.572	3.27E+00	3.45E+00	1.870
Range	6.78E-04	0.047	1.7	1.586	3.11E-02	1.82E-02	0.153
Minimum	1.36E-05	0.001	98.3	0.008	1.83E-05	1.77E-04	0.004
Maximum	6.92E-04	0.048	100.0	1.595	3.11E-02	1.83E-02	0.157
Sum	1.35E-03	0.334	1795.9	2.846	7.03E-02	3.70E-02	0.770
Count	1.80E+01	18.000	18.0	18.000	1.80E+01	1.80E+01	18.000
C. L (0.95)	7.30E-05	0.007	0.2	0.176	3.46E-03	2.02E-03	0.018
% variation	0.03	1.31	0.17	92.01	1.44	0.93	3.55

Ant. Trav	He	CH4	H2O	N2	O2	Ar	CO2
Mean	2.31E-03	0.060	99.7	0.078	1.64E-02	1.36E-03	0.191
Std. Error	5.41E-04	0.015	0.1	0.017	2.21E-03	2.12E-04	0.035
Median	1.66E-03	0.046	99.8	0.052	1.45E-02	1.09E-03	0.148
Mode	NA	NA	NA	NA	NA	NA	NA
Std.Dev.	1.87E-03	0.053	0.2	0.058	7.64E-03	7.34E-04	0.122
Variance	3.51E-06	0.003	0.0	0.003	5.84E-05	5.38E-07	0.015
Kurtosis	-6.33E-01	7.819	-1.8	1.859	5.18E+00	3.19E+00	-0.876
Skewness	8.23E-01	2.653	-0.4	1.699	2.12E+00	1.78E+00	0.709
Range	5.47E-03	0.197	0.5	0.174	2.79E-02	2.63E-03	0.352
Minimum	2.45E-04	0.019	99.4	0.036	9.43E-03	5.89E-04	0.071
Maximum	5.71E-03	0.216	99.8	0.209	3.73E-02	3.22E-03	0.423
Sum	2.77E-02	0.716	1195.8	0.931	1.97E-01	1.63E-02	2.293
Count	1.20E+01	12.000	12.0	12.000	1.20E+01	1.20E+01	12.000
C. L (0.95)	1.06E-03	0.030	0.1	0.033	4.32E-03	4.15E-04	0.069
% variation	0.15	4.76	0.04	4.28	0.36	0.04	7.85

Phr. Calc.	He	CH4	H2O	N2	O2	Ar	CO2
Mean	1.31E-03	5.871	88.3	4.441	2.77E-01	8.44E-02	1.002
Std. Error	6.93E-04	5.643	10.7	4.044	2.52E-01	8.12E-02	0.699
Median	5.91E-04	0.265	98.8	0.446	1.52E-02	3.24E-03	0.369
Mode	NA	NA	NA	NA	NA	NA	NA
Std.Dev.	1.70E-03	13.822	26.3	9.906	6.18E-01	1.99E-01	1.712
Variance	2.88E-06	191.049	689.3	98.133	3.81E-01	3.95E-02	2.930
Kurtosis	5.27E+00	5.998	6.0	5.960	5.95E+00	5.99E+00	5.789
Skewness	2.27E+00	2.449	-2.4	2.439	2.44E+00	2.45E+00	2.393
Range	4.42E-03	34.049	65.1	24.630	1.53E+00	4.90E-01	4.455
Minimum	2.94E-04	0.036	34.8	0.013	9.19E-04	3.05E-04	0.023
Maximum	4.71E-03	34.084	99.9	24.643	1.54E+00	4.90E-01	4.478
Sum	7.87E-03	35.228	530.1	26.647	1.66E+00	5.06E-01	6.012
Count	6.00E+00	6.000	6.0	6.000	6.00E+00	6.00E+00	6.000
C. L (0.95)	1.36E-03	11.060	21.0	7.926	4.94E-01	1.59E-01	1.370
% variation	0.22	3253.92	780.26	2209.52	137.92	46.83	292.40

Vein Calc	He	CH4	H2O	N2	O2	Ar	CO2
Mean	2.68E-03	0.034	99.8	0.072	2.14E-02	1.37E-03	0.046
Std. Error	4.46E-04	0.003	0.0	0.008	1.92E-03	1.46E-04	0.009
Median	2.58E-03	0.034	99.8	0.072	1.97E-02	1.33E-03	0.035
Mode	NA	NA	NA	NA	NA	NA	NA
Std.Dev.	1.61E-03	0.011	0.1	0.029	6.94E-03	5.25E-04	0.032
Variance	2.59E-06	0.000	0.0	0.001	4.81E-05	2.76E-07	0.001
Kurtosis	-8.04E-01	-1.456	-1.0	-0.966	-8.27E-01	-1.18E+00	5.709
Skewness	5.70E-01	0.211	-0.1	0.236	1.34E-01	1.45E-01	2.363
Range	4.99E-03	0.031	0.2	0.095	2.33E-02	1.63E-03	0.116
Minimum	5.79E-04	0.020	99.7	0.028	9.98E-03	6.05E-04	0.021
Maximum	5.57E-03	0.051	99.9	0.123	3.32E-02	2.23E-03	0.138
Sum	3.48E-02	0.438	1297.7	0.938	2.78E-01	1.78E-02	0.599
Count	1.30E+01	13.000	13.0	13.000	1.30E+01	1.30E+01	13.000
C. L (0.95)	8.75E-04	0.006	0.0	0.016	3.77E-03	2.85E-04	0.017
% variation	0.10	0.35	0.00	1.16	0.22	0.02	2.25

LANL	He	CH4	H2O	N2	O2	Ar	CO2
Mean	7.46E-03	28.645	44.6	19.317	7.04E-01	1.72E-01	6.549
Std. Error	1.43E-03	3.104	4.3	3.225	1.87E-01	4.12E-02	1.159
Median	5.75E-03	29.573	41.9	15.339	2.36E-01	8.52E-02	5.201
Mode	NA	NA	NA	NA	NA	NA	NA
Std.Dev.	6.72E-03	14.560	20.3	15.129	8.77E-01	1.93E-01	5.436
Variance	4.52E-05	211.999	412.3	228.873	7.69E-01	3.74E-02	29.547
Kurtosis	3.11E+00	1.042	-0.7	0.956	4.19E+00	1.51E+00	-0.664
Skewness	1.77E+00	0.776	0.4	1.293	1.91E+00	1.59E+00	0.825
Range	2.70E-02	60.804	73.1	56.094	3.53E+00	6.78E-01	16.395
Minimum	7.17E-04	7.030	13.1	2.322	1.80E-02	1.56E-02	0.508
Maximum	2.77E-02	67.834	86.2	58.415	3.55E+00	6.94E-01	16.903
Sum	1.64E-01	630.180	981.7	424.975	1.55E+01	3.78E+00	144.082
Count	2.20E+01	22.000	22.0	22.000	2.20E+01	2.20E+01	22.000
C. L (0.95)	2.81E-03	6.084	8.5	6.322	3.66E-01	8.08E-02	2.271
% variation	0.61	740.10	924.04	1184.32	109.23	21.77	451.16

LANL-BN	He	CH4	H2O	N2	O2	Ar	CO2
Mean	6.27E-03	24.453	60.1	5.763	2.20E-01	5.38E-02	9.418
Std. Error	1.18E-03	3.248	4.9	0.452	6.77E-02	1.55E-02	2.464
Median	6.94E-03	23.451	60.2	5.610	1.80E-01	3.99E-02	10.035
Mode	NA	NA	NA	NA	NA	NA	NA
Std.Dev.	3.11E-03	8.594	13.1	1.196	1.79E-01	4.11E-02	6.520
Variance	9.67E-06	73.858	170.6	1.431	3.21E-02	1.69E-03	42.513
Kurtosis	9.03E-01	1.103	1.5	-0.717	4.01E+00	4.60E+00	-1.621
Skewness	7.21E-01	0.740	-0.7	0.563	1.88E+00	1.99E+00	0.143
Range	9.33E-03	26.972	41.6	3.335	5.31E-01	1.26E-01	17.027
Minimum	2.53E-03	12.923	36.3	4.322	6.49E-02	1.48E-02	1.466
Maximum	1.19E-02	39.896	77.9	7.657	5.96E-01	1.41E-01	18.493
Sum	4.39E-02	171.173	420.6	40.340	1.54E+00	3.76E-01	65.928
Count	7.00E+00	7.000	7.0	7.000	7.00E+00	7.00E+00	7.000
C. L (0.95)	2.30E-03	6.366	9.7	0.886	1.33E-01	3.04E-02	4.830
% variation	0.15	302.04	283.92	24.83	14.58	3.14	451.38

TABLE B5:
Statistical description of different carbonates (water-free).

Caliches	He	CH4	N2	O2	Ar	CO2
Mean	0.01	63.31	19.76	1.29	0.29	15.33
Std. Error	0.00	3.05	2.88	0.31	0.05	2.46
Median	0.01	59.24	12.57	0.48	0.23	10.39
Mode	NA	NA	NA	NA	NA	NA
Std.Dev.	0.01	16.42	15.53	1.67	0.27	13.22
Variance	0.00	269.62	241.07	2.78	0.07	174.86
Kurtosis	9.64	-0.93	-0.43	3.49	1.80	-0.71
Skewness	2.72	0.54	0.96	2.02	1.42	0.76
Range	0.05	56.43	52.95	6.27	1.05	41.67
Minimum	0.00	37.07	2.55	0.00	0.03	0.89
Maximum	0.06	93.50	55.50	6.27	1.08	42.56
Sum	0.38	1836.09	572.92	37.42	8.55	444.64
Count	29.00	29.00	29.00	29.00	29.00	29.00
C. L. (0.95)	0.00	5.98	5.65	0.61	0.10	4.81

PC	He	CH4	N2	O2	Ar	CO2
Mean	0.03	27.89	20.31	3.97	0.43	47.36
Std. Error	0.01	4.79	6.55	1.84	0.17	6.42
Median	0.02	24.45	10.77	0.54	0.18	48.64
Mode	NA	NA	NA	NA	NA	NA
Std.Dev.	0.03	15.16	20.70	5.82	0.55	20.31
Variance	0.00	229.82	428.57	33.87	0.30	412.61
Kurtosis	0.10	-1.02	1.23	-0.84	1.83	-0.81
Skewness	1.21	0.40	1.66	1.12	1.74	-0.49
Range	0.08	45.61	54.73	13.30	1.58	56.64
Minimum	0.01	6.58	6.81	0.15	0.05	14.97
Maximum	0.09	52.19	61.54	13.45	1.62	71.60
Sum	0.31	278.91	203.12	39.72	4.31	473.63
Count	10.00	10.00	10.00	10.00	10.00	10.00
C. L. (0.95)	0.02	9.40	12.83	3.61	0.34	12.59

Act. Trav.	He	CH4	N2	O2	Ar	CO2
Mean	0.05	16.43	46.51	2.09	0.77	34.15
Std. Error	0.01	2.28	4.92	0.35	0.05	4.07
Median	0.04	17.83	40.34	1.69	0.82	33.56
Mode	NA	NA	NA	NA	NA	NA
Std.Dev.	0.04	9.65	20.86	1.50	0.21	17.28
Variance	0.00	93.19	435.22	2.24	0.05	298.47
Kurtosis	1.00	-1.29	-0.18	-0.32	-0.59	-0.28
Skewness	1.08	-0.20	0.72	0.59	-0.50	0.15
Range	0.14	29.76	76.96	5.39	0.75	67.12
Minimum	0.00	1.56	15.85	0.03	0.32	3.04
Maximum	0.14	31.33	92.81	5.42	1.07	70.15
Sum	0.89	295.77	837.23	37.58	13.79	614.74
Count	18.00	18.00	18.00	18.00	18.00	18.00
C. L. (0.95)	0.02	4.46	9.64	0.69	0.10	7.98

Ant. Trav	He	CH4	N2	O2	Ar	CO2
Mean	1.05	17.57	22.22	5.35	0.43	53.39
Std. Error	0.30	2.44	1.99	0.52	0.05	3.83
Median	0.50	18.04	22.05	6.15	0.40	47.82
Mode	NA	NA	NA	NA	NA	NA
Std.Dev.	1.05	8.46	6.90	1.81	0.17	13.26
Variance	1.11	71.55	47.67	3.29	0.03	175.74
Kurtosis	-1.02	-0.65	1.21	-1.63	-0.36	-0.38
Skewness	0.74	0.41	0.43	-0.43	0.43	0.72
Range	2.92	27.34	27.07	4.83	0.55	44.05
Minimum	0.05	5.97	9.83	2.64	0.21	36.20
Maximum	2.97	33.31	36.90	7.47	0.76	80.25
Sum	12.59	210.81	266.63	64.16	5.19	640.62
Count	12.00	12.00	12.00	12.00	12.00	12.00
C. L. (0.95)	0.60	4.79	3.91	1.03	0.09	7.50

PC-CCG	He	CH4	N2	O2	Ar	CO2
Mean	0.26	32.01	32.27	3.64	0.38	31.45
Std. Error	0.21	5.72	9.73	1.74	0.10	9.20
Median	0.04	33.59	30.14	1.83	0.32	26.27
Mode	NA	NA	NA	NA	NA	NA
Std.Dev.	0.53	14.00	23.82	4.26	0.25	22.54
Variance	0.28	196.07	567.48	18.12	0.06	508.12
Kurtosis	5.89	-0.36	-1.60	1.72	-1.20	-0.39
Skewness	2.42	0.03	0.16	1.50	0.60	0.77
Range	1.32	39.51	61.40	11.15	0.64	60.19
Minimum	0.01	12.74	2.40	0.17	0.11	6.86
Maximum	1.33	52.25	63.81	11.32	0.75	67.05
Sum	1.55	192.06	193.60	21.82	2.29	188.68
Count	6.00	6.00	6.00	6.00	6.00	6.00
C. L. (0.95)	0.42	11.20	19.06	3.41	0.20	18.04

PC-VC	He	CH4	N2	O2	Ar	CO2
Mean	1.52	19.75	40.45	12.51	0.77	25.00
Std. Error	0.23	1.85	3.01	1.16	0.05	3.04
Median	1.27	17.75	40.46	13.09	0.79	22.30
Mode	NA	NA	NA	NA	NA	NA
Std.Dev.	0.85	6.66	10.86	4.19	0.19	10.97
Variance	0.72	44.33	118.00	17.56	0.04	120.33
Kurtosis	-0.35	0.28	-0.60	3.13	0.15	5.79
Skewness	0.61	0.96	0.16	1.22	0.58	2.13
Range	2.80	21.69	37.88	16.63	0.68	43.03
Minimum	0.44	12.18	21.64	6.69	0.49	13.40
Maximum	3.24	33.87	59.53	23.32	1.17	56.44
Sum	19.75	256.78	525.84	162.65	9.98	325.00
Count	13.00	13.00	13.00	13.00	13.00	13.00
C. L. (0.95)	0.46	3.62	5.91	2.28	0.10	5.96

LANL	He	CH4	N2	O2	Ar	CO2
Mean	0.01	54.15	32.84	1.11	0.27	11.62
Std. Error	0.00	4.21	3.82	0.24	0.05	1.53
Median	0.01	54.93	30.97	0.55	0.16	10.87
Mode	NA	NA	NA	NA	NA	NA
Std.Dev.	0.02	19.76	17.91	1.15	0.24	7.15
Variance	0.00	390.39	320.84	1.31	0.06	51.17
Kurtosis	5.14	-0.14	1.95	2.04	2.73	-0.96
Skewness	2.30	-0.71	1.13	1.42	1.76	0.10
Range	0.06	67.91	76.61	4.44	0.93	24.51
Minimum	0.00	10.15	7.74	0.04	0.07	0.70
Maximum	0.06	78.06	84.34	4.49	1.00	25.21
Sum	0.32	1191.25	722.48	24.42	5.90	255.63
Count	22.00	22.00	22.00	22.00	22.00	22.00
C. L. (0.95)	0.01	8.26	7.48	0.48	0.10	2.99

LANL-BN	He	CH4	N2	O2	Ar	CO2
Mean	0.02	61.60	15.77	0.71	0.17	21.74
Std. Error	0.00	3.91	2.65	0.34	0.08	4.83
Median	0.02	60.49	13.52	0.37	0.09	24.83
Mode	NA	NA	NA	NA	NA	NA
Std.Dev.	0.01	10.33	7.02	0.89	0.21	12.78
Variance	0.00	106.80	49.29	0.80	0.04	163.25
Kurtosis	2.33	0.43	6.45	6.36	6.80	-0.67
Skewness	1.24	-0.25	2.51	2.49	2.59	0.39
Range	0.02	31.56	19.87	2.55	0.59	35.85
Minimum	0.01	44.36	11.62	0.15	0.05	6.64
Maximum	0.03	75.92	31.49	2.70	0.64	42.49
Sum	0.11	431.23	110.37	4.94	1.17	152.18
Count	7.00	7.00	7.00	7.00	7.00	7.00
C. L. (0.95)	0.01	7.66	5.20	0.66	0.15	9.47

TABLE B6:
Data for ternary diagrams, from figures 32 to 39 and figure 41

Calliches

Sample #	Ar %	N2 %	He %
WB-01-94	51.16	24.00	24.85
WB-02-94	29.73	32.13	38.14
WB-03-94	37.46	37.00	25.54
WB-04-94	27.80	42.40	29.80
WB-05-94	42.49	36.08	21.44
WB-06-94	8.52	12.58	80.90
WB-07-94	31.11	33.73	35.16
WB-08-94	60.74	20.00	19.26
NC-01-94	65.31	30.04	4.65
NC-02-94	64.78	31.04	4.18
NC-03-94	58.35	32.61	9.04
NC-04-94	34.91	58.81	6.29
NC-05-94	58.00	36.53	5.47
NC-06-94	34.66	44.22	21.12
WR-01-94	47.65	35.01	17.34
WR-02-94	31.05	14.53	54.42
WR-03-94	20.88	28.47	50.66
WR-04-94	71.88	7.03	21.10
WR-05-94	20.71	49.64	29.65
WR-06-94	23.66	24.95	51.39
WR-07-94	46.21	33.86	19.92
WR-08-94	47.93	47.71	4.37
WR-09-94	43.43	39.34	17.24
LL-01-94	35.18	25.67	39.15
LC-01-94	52.07	14.65	33.27
LC-02-94	46.94	20.46	32.59
SAE-01-94	43.85	43.01	13.14
SAE-02-94	28.26	34.45	37.28
04-LR-93	36.03	18.92	45.05

Calliches

Sample #	Ar %	N2 %	O2 %
WB-01-94	61.52	28.86	9.62
WB-02-94	18.57	20.07	61.36
WB-03-94	43.04	42.51	14.45
WB-04-94	30.72	46.86	22.43
WB-05-94	35.44	30.07	34.49
WB-06-94	30.57	58.94	10.49
WB-07-94	32.21	34.92	32.87
WB-08-94	67.31	22.16	10.52
NC-01-94	67.82	31.20	0.99
NC-02-94	66.63	31.93	1.43
NC-03-94	61.48	34.36	4.16
NC-04-94	35.49	59.79	4.72
NC-05-94	57.12	35.97	6.91
NC-06-94	41.39	52.82	5.79
WR-01-94	33.64	24.72	41.64
WR-02-94	63.91	29.91	6.17
WR-03-94	37.27	50.83	11.90
WR-04-94	81.29	7.95	10.76
WR-05-94	7.58	18.11	74.33
WR-06-94	24.26	25.59	50.15
WR-07-94	19.47	14.26	66.27
WR-08-94	41.44	41.25	17.31
WR-09-94	44.93	40.70	14.37
LL-01-94	39.77	29.02	31.21
LC-01-94	73.55	20.70	5.75
LC-02-94	43.47	18.95	37.58
SAE-01-94	39.96	39.20	20.85
SAE-02-94	36.52	44.53	18.95
04-LR-93	65.31	34.31	0.38

Calliches

Sample #	Ar %	N2 %	CH4 %
WB-01-94	33.43	15.68	50.89
WB-02-94	15.21	16.44	68.35
WB-03-94	14.80	14.62	70.59
WB-04-94	6.88	10.49	82.63
WB-05-94	15.76	13.37	70.87
WB-06-94	5.30	10.22	84.47
WB-07-94	10.56	11.45	77.99
WB-08-94	31.23	10.28	58.48
NC-01-94	54.16	24.92	20.92
NC-02-94	49.32	23.64	27.04
NC-03-94	40.52	22.64	36.84
NC-04-94	19.00	32.01	48.99
NC-05-94	41.68	26.25	32.07
NC-06-94	16.22	20.69	63.09
WR-01-94	36.63	26.91	36.46
WR-02-94	10.39	4.86	84.74
WR-03-94	7.61	10.38	82.01
WR-04-94	33.19	3.25	63.56
WR-05-94	2.72	6.51	90.77
WR-06-94	4.22	4.45	91.33
WR-07-94	15.78	11.56	72.65
WR-08-94	37.59	37.42	24.99
WR-09-94	32.80	29.71	37.48
LL-01-94	27.25	19.88	52.87
LC-01-94	37.78	10.63	51.59
LC-02-94	26.78	11.68	61.54
SAE-01-94	25.47	24.99	49.54
SAE-02-94	6.94	8.46	84.59
04-LR-93	7.21	3.79	89.00

Active Travertine

Sample #	Ar %	N2 %	He %
as-01-94	44.50	38.71	16.79
as-02-94	36.28	6.46	57.26
as-03-94	54.67	38.01	7.32
sd-01-94	55.16	43.50	1.34
sd-02-94	44.70	20.72	34.57
lc-01-94	50.05	27.42	22.52
lc-02-94	48.67	33.80	19.53
lc-04-94	48.99	37.78	13.23
sd2-01-94	42.75	25.17	32.08
sd2-02-94	55.18	14.56	30.26
sd2-03-94	36.75	23.22	40.03
sd2-04-94	46.70	44.58	8.72
sd2-05-94	42.73	37.93	19.34
sd2-06-94	28.17	24.41	47.41
mhs-01-94	44.06	20.34	35.60
mhs-02-94	35.16	16.45	48.39
lh-01-94	41.52	24.03	34.45
lh-02-94	50.05	22.82	27.13

Active Travertine

Sample #	Ar %	N2 %	O2 %
as-01-94	51.43	44.74	3.83
as-02-94	62.92	11.21	25.87
as-03-94	53.54	37.22	9.24
sd-01-94	44.85	35.37	19.79
sd-02-94	59.22	27.45	13.33
lc-01-94	59.55	32.63	7.82
lc-02-94	57.19	41.42	1.39
lc-04-94	56.38	43.48	0.14
sd2-01-94	51.72	30.46	17.81
sd2-02-94	63.88	16.85	19.28
sd2-03-94	48.16	30.43	21.40
sd2-04-94	47.13	44.99	7.88
sd2-05-94	44.85	39.81	15.34
sd2-06-94	48.94	42.40	8.66
mhs-01-94	53.54	24.71	21.74
mhs-02-94	45.86	21.45	32.69
lh-01-94	53.67	31.06	15.27
lh-02-94	58.40	26.62	14.98

Active Travertine

Sample #	Ar %	N2 %	CH4 %
as-01-94	52.89	46.00	1.12
as-02-94	66.71	11.88	21.41
as-03-94	54.05	37.58	8.36
sd-01-94	53.90	42.51	3.59
sd-02-94	57.10	26.47	16.43
lc-01-94	55.40	30.36	14.24
lc-02-94	48.58	35.19	16.23
lc-04-94	53.79	41.48	4.72
sd2-01-94	58.99	33.57	9.44
sd2-02-94	66.61	17.57	15.82
sd2-03-94	53.91	34.06	12.03
sd2-04-94	49.09	46.86	4.05
sd2-05-94	50.26	44.61	5.13
sd2-06-94	52.19	45.22	2.59
mhs-01-94	51.21	23.64	25.15
mhs-02-94	54.82	25.65	19.53
lh-01-94	49.80	28.82	21.38
lh-02-94	56.93	25.95	17.11

Ancient Travertine

Sample #	Ar %	N2 %	He %
01-AM-93	5.14	3.25	91.61
02-AM-93	11.00	7.11	81.90
03-AM-93	25.38	18.44	56.18
04-AM-93	5.34	2.55	92.11
05-AM-93	19.87	15.28	65.05
NMT-01-94	2.49	0.60	96.91
NMT-02-94	2.35	1.12	96.53
NMT-03-94	2.43	1.26	96.31
NMT-04-94	16.20	10.53	73.27
NMT-05-94	3.97	1.89	94.14
NMT-06-94	2.05	0.75	97.20
NMT-07-94	15.42	9.41	75.17

Ancient Travertine

Sample #	Ar %	N2 %	O2 %
01-AM-93	30.93	19.53	49.55
02-AM-93	36.13	23.36	40.51
03-AM-93	32.79	23.83	43.39
04-AM-93	31.99	15.30	52.71
05-AM-93	39.58	30.74	29.68
NMT-01-94	44.94	10.90	44.15
NMT-02-94	33.88	16.15	49.98
NMT-03-94	32.65	16.90	50.45
NMT-04-94	35.59	23.14	41.28
NMT-05-94	39.13	18.67	42.21
NMT-06-94	39.10	14.22	46.68
NMT-07-94	32.84	19.93	47.44

Ancient Travertine

Sample #	Ar %	N2 %	CH4 %
01-AM-93	51.05	32.24	16.71
02-AM-93	53.24	34.41	12.34
03-AM-93	38.97	28.32	32.70
04-AM-93	56.53	27.04	16.43
05-AM-93	36.74	28.54	34.72
NMT-01-94	61.97	15.04	22.99
NMT-02-94	51.74	24.66	23.61
NMT-03-94	51.81	26.81	21.37
NMT-04-94	54.01	35.11	10.87
NMT-05-94	56.02	26.73	17.25
NMT-06-94	55.10	20.03	24.87
NMT-07-94	51.37	31.36	17.27

Pedogenic Calcrete

Sample #	Ar %	N2 %	He %
01-94-PC	24.03	31.72	44.25
02-94-PC	33.11	33.23	33.67
03-94-PC	39.33	20.94	39.73
04-94-PC	61.90	21.47	16.63
05-94-PC	23.98	41.06	34.95
06-94-PC	26.60	18.79	54.61
07-94-PC	19.73	6.99	73.28
01-LR-93	51.19	23.09	25.72
02-LR-93	58.85	26.12	17.04
05-LR-93	57.13	21.68	21.19

Pedogenic Calcrete

Sample #	Ar %	N2 %	O2 %
01-94-PC	35.44	46.76	17.80
02-94-PC	44.50	44.66	10.84
03-94-PC	60.68	32.31	7.01
04-94-PC	70.22	24.36	5.42
05-94-PC	32.30	55.31	12.40
06-94-PC	45.82	32.37	21.81
07-94-PC	57.60	20.42	21.98
01-LR-93	39.64	17.88	42.48
02-LR-93	24.07	11.06	64.87
05-LR-93	45.28	17.18	37.55

Pedogenic Calcrete

Sample #	Ar %	N2 %	CH4 %
01-94-PC	17.94	23.67	58.40
02-94-PC	14.98	15.04	69.98
03-94-PC	27.52	14.65	57.83
04-94-PC	42.32	14.68	43.00
05-94-PC	7.18	12.26	80.58
06-94-PC	25.10	17.73	57.18
07-94-PC	46.96	16.64	36.40
01-LR-93	63.95	28.84	7.21
02-LR-93	52.25	24.01	23.74
05-LR-93	70.42	26.72	2.86

TABLE B6:
Data for ternary diagrams, from figures 32 to 39 and figure 41, continue

Phreatic Calcrete (Calcite cemented gravels).

Sample #	Ar %	N2 %	He %
08-94-PC	39.87	34.69	25.64
09-94-PC	27.81	56.73	15.48
10-PC-94	62.54	31.44	6.02
LC-03-94	12.17	1.78	86.05
LC-04-94	16.48	20.32	63.22
LC-05-94	2.41	1.62	95.97

Phreatic Calcrete (Calcite cemented gravels).

Sample #	Ar %	N2 %	O2 %
08-94-PC	35.48	31.00	33.54
09-94-PC	28.92	58.99	12.09
10-PC-94	55.06	27.68	17.25
LC-03-94	80.05	11.71	8.24
LC-04-94	33.07	40.84	26.09
LC-05-94	19.76	13.31	66.93

Phreatic Calcrete (Calcite cemented grave

Sample #	Ar %	N2 %	CH4 %
08-94-PC	48.05	42.01	9.94
09-94-PC	26.96	54.98	18.06
10-PC-94	45.49	22.87	31.64
LC-03-94	33.57	4.91	61.52
LC-04-94	17.60	21.73	60.66
LC-05-94	35.22	23.73	41.05

Phreatic Calcrete (Vein Calcites).

Sample #	Ar %	N2 %	He %
UNK-01-93	7.27	5.41	87.32
UNK-02-93	8.88	6.30	84.83
MCA-01-94	8.57	4.67	86.76
MCA-02-94	4.00	1.54	94.46
MCA-03-94	6.77	4.16	89.07
MCA-04-94	2.44	1.36	96.20
Tower-01-94	13.87	10.18	75.95
Tower-02-94	5.15	3.66	91.19
NMBMG-02	3.48	0.86	95.69
NMBMG-04	3.41	2.40	94.20
NMBMG-05	3.79	1.64	94.57
NMBMG-06	3.88	1.69	94.43
TC-01-94	4.73	1.59	93.67

Phreatic Calcrete (Vein Calcites).

Sample #	Ar %	N2 %	O2 %
UNK-01-93	31.18	23.22	45.60
UNK-02-93	15.51	11.01	73.48
MCA-01-94	33.06	18.01	48.93
MCA-02-94	30.55	11.77	57.68
MCA-03-94	30.47	18.74	50.79
MCA-04-94	31.17	17.38	51.45
Tower-01-94	29.29	21.49	49.22
Tower-02-94	27.60	19.64	52.76
NMBMG-02	54.97	13.62	31.42
NMBMG-04	25.26	17.76	56.98
NMBMG-05	36.15	15.66	48.20
NMBMG-06	36.03	15.68	48.30
TC-01-94	40.99	13.77	45.24

Phreatic Calcrete (Vein Calcites).

Sample #	Ar %	N2 %	CH4 %
UNK-01-93	51.90	38.66	9.45
UNK-02-93	49.16	34.89	15.96
MCA-01-94	58.21	31.71	10.07
MCA-02-94	59.04	22.74	18.22
MCA-03-94	54.96	33.80	11.24
MCA-04-94	49.13	27.39	23.48
Tower-01-94	53.08	38.95	7.97
Tower-02-94	48.70	34.66	16.64
NMBMG-02	65.06	16.11	18.82
NMBMG-04	48.34	33.99	17.67
NMBMG-05	60.50	26.20	13.30
NMBMG-06	60.27	26.23	13.51
TC-01-94	65.09	21.88	13.03

Phreatic Calcrete (Calcite concretions in sand).

Sample #	Ar %	N2 %	He %
PM-01-94	49.28	32.47	18.26
PM-02-94	61.16	36.56	2.29

Phreatic Calcrete (Calcite concretions in sand).

Sample #	Ar %	N2 %	O2 %
PM-01-94	40.21	26.49	33.30
PM-02-94	40.27	24.07	35.65

Phreatic Calcrete (Calcite concretions in

Sample #	Ar %	N2 %	CH4 %
PM-01-94	28.00	18.44	53.56
PM-02-94	53.62	32.06	14.32

Carbonates from Los Alamos National Laboratory

Sample #	Ar %	N2 %	He %
1-AL-93	33.65	48.45	17.90
2-AL-93	23.13	18.57	58.31
3-AL-93	10.46	9.64	79.90
4-AL-93	37.45	50.66	11.89
5-AL-93	18.15	57.08	24.78
6-LA-93	53.82	44.97	1.21
7-LA-93	36.95	40.63	22.42
8-LA-93	24.58	56.64	18.79
9-LA-93	53.74	45.24	1.02
TA63(1-1)	15.18	62.53	22.29
TA63(1-2)	28.12	58.96	12.92
TA63(1-3)	27.77	59.83	12.40
TA63(1-4)	18.59	67.06	14.35
LANL-01-94	44.93	39.84	15.23
LANL-02-94	24.84	44.71	30.66
LANL-03-94	41.71	46.64	11.65
LANL-04-94	30.73	28.28	40.99
LANL-05-94	51.13	42.58	6.28
LANL-06-94	48.07	45.28	6.65
LANL-07-94	36.94	39.66	23.40
LANL-08-94	22.23	39.83	37.94
LANL-09-94	24.38	56.70	18.92
LAH-4-A	23.34	30.07	46.58
LAH-4-B	24.35	36.31	39.34
LAH-4-C	29.20	29.43	41.37
LAL-8898A	17.74	51.87	30.39
LAL-8898B	29.53	45.72	24.75
LAL-8898C	24.14	33.90	41.96
LAL8898-30	50.28	24.77	24.96

Carbonates from Los Alamos National Laboratory

Sample #	Ar %	N2 %	O2 %
1-AL-93	39.45	56.80	3.75
2-AL-93	46.38	37.24	16.37
3-AL-93	24.48	22.55	52.97
4-AL-93	39.37	53.27	7.36
5-AL-93	23.76	74.73	1.51
6-LA-93	50.86	42.50	6.64
7-LA-93	45.88	50.45	3.67
8-LA-93	29.01	66.86	4.13
9-LA-93	47.48	39.97	12.55
TA63(1-1)	14.88	61.29	23.83
TA63(1-2)	27.55	57.77	14.68
TA63(1-3)	30.38	65.45	4.17
TA63(1-4)	20.87	75.31	3.82
LANL-01-94	36.29	32.18	31.53
LANL-02-94	33.98	61.67	4.35
LANL-03-94	40.62	45.41	13.97
LANL-04-94	41.81	38.47	19.73
LANL-05-94	39.34	32.76	27.90
LANL-06-94	43.03	40.54	16.44
LANL-07-94	32.26	34.64	33.10
LANL-08-94	30.64	54.90	14.45
LANL-09-94	27.44	63.81	8.75
LAH-4-A	37.17	47.90	14.93
LAH-4-B	35.58	53.04	11.38
LAH-4-C	40.24	40.56	19.19
LAL-8898A	19.45	56.86	23.69
LAL-8898B	35.04	54.25	10.71
LAL-8898C	38.96	54.71	6.33
LAL8898-300	52.23	25.73	22.04

Carbonates from Los Alamos National Lab

Sample #	Ar %	N2 %	CH4 %
1-AL-93	21.04	30.30	48.66
2-AL-93	13.42	10.78	75.80
3-AL-93	9.18	8.45	82.37
4-AL-93	21.56	29.17	49.27
5-AL-93	6.77	21.31	71.92
6-LA-93	40.06	33.47	26.46
7-LA-93	10.21	11.23	78.55
8-LA-93	14.90	34.33	50.78
9-LA-93	51.46	43.32	5.21
TA63(1-1)	9.46	38.97	51.57
TA63(1-2)	11.79	24.72	63.49
TA63(1-3)	16.66	35.89	47.45
TA63(1-4)	10.23	36.89	52.88
LANL-01-94	18.84	16.71	64.45
LANL-02-94	15.16	27.51	57.33
LANL-03-94	31.40	35.10	33.50
LANL-04-94	33.28	30.62	36.10
LANL-05-94	45.82	38.16	16.03
LANL-06-94	44.61	42.03	13.36
LANL-07-94	21.01	22.58	56.42
LANL-08-94	8.77	15.71	75.51
LANL-09-94	9.55	22.22	68.23
LAH-4-A	11.11	14.31	74.58
LAH-4-B	11.35	16.92	71.73
LAH-4-C	13.78	13.89	72.33
LAL-8898A	5.05	14.78	80.17
LAL-8898B	9.94	15.39	74.67
LAL-8898C	13.82	19.40	66.78
LAL8898-30	41.53	20.46	38.01

Samples from Brent Newman

Sample #	Ar %	N2 %	He %
LAH-4-A	23.34	30.07	46.58
LAH-4-B	24.35	36.31	39.34
LAH-4-C	29.20	29.43	41.37
LAL-8898A	17.74	51.87	30.39
LAL-8898B	29.53	45.72	24.75
LAL-8898C	24.14	33.90	41.96
LAL8898-30	50.28	24.77	24.96

Samples from Brent Newman

Sample #	Ar %	N2 %	O2 %
LAH-4-A	37.17	47.90	14.93
LAH-4-B	35.58	53.04	11.38
LAH-4-C	40.24	40.56	19.19
LAL-8898A	19.45	56.86	23.69
LAL-8898B	35.04	54.25	10.71
LAL-8898C	38.96	54.71	6.33
LAL8898-300	52.23	25.73	22.04

Samples from Brent Newman

Sample #	Ar %	N2 %	CH4 %
LAH-4-A	11.11	14.31	74.58
LAH-4-B	11.35	16.92	71.73
LAH-4-C	13.78	13.89	72.33
LAL-8898A	5.05	14.78	80.17
LAL-8898B	9.94	15.39	74.67
LAL-8898C	13.82	19.40	66.78
LAL8898-30	41.53	20.46	38.01

Samples from Nevada Test Site

Sample #	Ar %	N2 %	He %
LANL-357	52.97	42.50	4.53
GTE-1	43.58	52.95	3.47
WS-5-SSL	48.07	41.05	10.89

Samples from Nevada Test Site

Sample #	Ar %	N2 %	O2 %
LANL-357	40.83	32.76	26.41
GTE-1	29.42	35.74	34.84
WS-5-SSL	36.18	30.89	32.93

Samples from Nevada Test Site

Sample #	Ar %	N2 %	CH4 %
LANL-357	45.75	36.70	17.55
GTE-1	39.88	48.44	11.68
WS-5-SSL	32.23	27.52	40.24

Carbonates from Reylieh, N.M.

Sample #	Ar %	N2 %	He %
ry-01-94	51.62	46.96	1.42
ry-02-94	54.66	12.96	32.38
ry-03-94	52.60	16.43	30.98

Carbonates from Reylieh, N.M.

Sample #	Ar %	N2 %	O2 %
ry-01-94	42.48	38.64	18.88
ry-02-94	55.79	13.23	30.97
ry-03-94	54.56	17.04	28.40

Carbonates from Reylieh, N.M.

Sample #	Ar %	N2 %	CH4 %
ry-01-94	47.38	43.10	9.52
ry-02-94	33.26	7.89	58.85
ry-03-94	34.16	10.67	55.18

TABLE B6:
Data for ternary diagrams, from figures 32 to 39 and figure 41, continue

Calliches

Sample #	Ar %	N2 %	C02 %
WB-01-94	34.63	16.24	49.13
WB-02-94	30.55	33.02	36.43
WB-03-94	27.21	26.88	45.91
WB-04-94	23.70	36.15	40.15
WB-05-94	16.98	14.41	68.61
WB-06-94	15.36	29.62	55.02
WB-07-94	18.69	20.26	61.05
WB-08-94	40.16	13.22	46.61
NC-01-94	65.44	30.10	4.45
NC-02-94	66.63	31.93	1.43
NC-03-94	57.77	32.28	9.95
NC-04-94	35.90	60.47	3.64
NC-05-94	58.74	35.74	7.52
NC-06-94	27.38	34.94	37.68
WR-01-94	54.19	39.82	6.00
WR-02-94	64.71	30.29	5.00
WR-03-94	37.97	51.78	10.26
WR-04-94	86.00	8.41	5.59
WR-05-94	19.88	47.64	32.48
WR-06-94	31.67	33.40	34.93
WR-07-94	53.34	39.08	7.58
WR-08-94	48.16	47.93	3.91
WR-09-94	48.44	43.88	7.69
LL-01-94	37.64	27.46	34.90
LC-01-94	45.80	12.89	41.31
LC-02-94	43.44	18.94	37.62
SAE-01-94	36.89	36.19	26.91
SAE-02-94	34.25	41.76	23.99
04-LR-93	10.82	5.68	83.50

Calliches

Sample #	Ar %	CH4 %	C02 %
WB-01-94	25.37	38.63	35.99
WB-02-94	14.96	67.21	17.83
WB-03-94	13.41	63.97	22.62
WB-04-94	6.80	81.68	11.52
WB-05-94	10.49	47.15	42.36
WB-06-94	4.88	77.67	17.46
WB-07-94	8.58	63.37	28.04
WB-08-94	24.79	46.43	28.78
NC-01-94	68.76	26.56	4.68
NC-02-94	63.71	34.92	1.37
NC-03-94	48.05	43.68	8.27
NC-04-94	27.18	70.07	2.75
NC-05-94	52.57	40.45	6.97
NC-06-94	15.96	62.08	21.96
WR-01-94	47.49	47.26	5.25
WR-02-94	10.83	88.33	0.84
WR-03-94	8.30	89.45	2.24
WR-04-94	33.56	64.26	2.18
WR-05-94	2.78	92.69	4.54
WR-06-94	4.21	91.15	4.64
WR-07-94	17.41	80.12	2.47
WR-08-94	57.27	38.08	4.65
WR-09-94	43.45	49.65	6.90
LL-01-94	25.85	50.17	23.98
LC-01-94	30.60	41.79	27.60
LC-02-94	24.02	55.18	20.80
SAE-01-94	27.21	52.94	19.85
SAE-02-94	7.20	87.75	5.04
04-LR-93	4.75	58.59	36.66

Calliches

Sample #	N2 %	CH4 %	C02 %
WB-01-94	13.75	44.65	41.60
WB-02-94	15.97	66.41	17.62
WB-03-94	13.27	64.07	22.66
WB-04-94	10.02	78.86	11.12
WB-05-94	9.04	47.91	43.05
WB-06-94	8.99	74.30	16.70
WB-07-94	9.24	62.92	27.84
WB-08-94	9.79	55.69	34.52
NC-01-94	50.31	42.25	7.44
NC-02-94	45.89	52.26	2.05
NC-03-94	34.07	55.43	10.50
NC-04-94	38.60	59.08	2.32
NC-05-94	41.11	50.23	8.66
NC-06-94	19.50	59.48	21.03
WR-01-94	39.92	54.07	6.01
WR-02-94	5.38	93.73	0.89
WR-03-94	10.99	86.83	2.18
WR-04-94	4.71	92.17	3.13
WR-05-94	8.40	89.23	4.37
WR-06-94	4.43	90.94	4.63
WR-07-94	13.38	84.03	2.59
WR-08-94	57.16	38.18	4.66
WR-09-94	41.04	51.77	7.19
LL-01-94	20.28	53.94	25.78
LC-01-94	11.04	53.58	35.38
LC-02-94	12.11	83.83	24.06
SAE-01-94	26.83	53.21	19.96
SAE-02-94	8.64	86.39	4.97
04-LR-93	2.55	59.94	37.51

Active Travertine

Sample #	Ar %	N2 %	C02 %
as-01-94	52.68	45.82	1.50
as-02-94	57.14	10.18	32.69
as-03-94	53.72	37.35	8.92
sd-01-94	49.72	39.21	11.06
sd-02-94	56.32	26.11	17.58
lc-01-94	43.08	23.60	33.32
lc-02-94	43.92	31.81	24.28
lc-04-94	53.46	41.23	5.31
sd2-01-94	54.62	32.17	13.21
sd2-02-94	56.48	14.90	28.63
sd2-03-94	53.82	34.01	12.17
sd2-04-94	40.31	38.48	21.21
sd2-05-94	31.61	28.06	40.33
sd2-06-94	24.46	21.19	54.35
mhs-01-94	49.38	22.79	27.83
mhs-02-94	53.28	24.93	21.79
lh-01-94	43.72	25.31	30.97
lh-02-94	46.37	21.14	32.49

Active Travertine

Sample #	Ar %	CH4 %	C02 %
as-01-94	95.28	2.01	2.71
as-02-94	52.83	16.96	30.22
as-03-94	75.71	11.72	12.57
sd-01-94	77.58	5.16	17.26
sd-02-94	62.51	17.98	19.51
lc-01-94	49.25	12.66	38.09
lc-02-94	53.00	17.71	29.29
lc-04-94	84.24	7.40	8.36
sd2-01-94	71.05	11.77	17.18
sd2-02-94	57.32	13.62	29.06
sd2-03-94	69.01	15.39	15.60
sd2-04-94	62.16	5.13	32.71
sd2-05-94	42.06	4.29	53.65
sd2-06-94	30.56	1.51	67.92
mhs-01-94	48.67	23.90	27.43
mhs-02-94	56.65	20.18	23.17
lh-01-94	46.78	20.08	33.14
lh-02-94	49.97	15.02	35.01

Active Travertine

Sample #	N2 %	CH4 %	C02 %
as-01-94	94.81	2.29	3.10
as-02-94	16.63	29.97	53.41
as-03-94	68.43	15.23	16.35
sd-01-94	73.18	6.17	20.65
sd-02-94	43.59	27.05	29.35
lc-01-94	34.71	16.28	49.00
lc-02-94	44.95	20.74	34.31
lc-04-94	80.48	9.16	10.36
sd2-01-94	59.11	16.63	24.27
sd2-02-94	26.16	23.56	50.28
sd2-03-94	58.45	20.63	20.91
sd2-04-94	61.06	5.28	33.66
sd2-05-94	39.18	4.50	56.32
sd2-06-94	27.61	1.58	70.81
mhs-01-94	30.44	32.39	37.17
mhs-02-94	37.94	28.89	33.16
lh-01-94	33.72	25.01	41.27
lh-02-94	31.29	20.63	48.08

Ancient Travertine

Sample #	Ar %	N2 %	C02 %
01-AM-93	30.93	19.53	49.55
02-AM-93	27.04	17.48	55.49
03-AM-93	20.99	15.26	63.75
04-AM-93	18.58	8.88	72.54
05-AM-93	35.67	27.71	36.63
NMT-01-94	55.66	13.50	30.84
NMT-02-94	42.03	20.03	37.93
NMT-03-94	38.10	19.72	42.19
NMT-04-94	41.15	26.75	32.09
NMT-05-94	45.70	21.80	32.50
NMT-06-94	45.11	16.40	38.48
NMT-07-94	27.26	16.64	56.10

Pedogenic Calcrete

Sample #	Ar %	N2 %	C02 %
01-94-PC	17.60	23.23	59.17
02-94-PC	16.57	16.63	66.79
03-94-PC	14.93	7.95	77.11
04-94-PC	32.76	11.36	55.88
05-94-PC	8.88	15.21	75.91
06-94-PC	11.11	7.85	81.05
07-94-PC	23.08	8.18	68.75
01-LR-93	63.65	28.71	7.64
02-LR-93	33.97	15.61	50.42
05-LR-93	67.45	25.59	6.96

Ancient Travertine

Sample #	Ar %	CH4 %	C02 %
01-AM-93	34.14	11.17	54.69
02-AM-93	30.45	7.06	62.49
03-AM-93	20.51	17.21	62.28
04-AM-93	19.25	5.59	75.16
05-AM-93	33.65	31.80	34.55
NMT-01-94	51.95	19.27	28.78
NMT-02-94	42.40	19.34	38.26
NMT-03-94	39.69	16.37	43.94
NMT-04-94	50.48	10.16	39.36
NMT-05-94	49.53	15.25	35.22
NMT-06-94	43.39	19.59	37.02
NMT-07-94	29.46	9.90	60.64

Pedogenic Calcrete

Sample #	Ar %	CH4 %	C02 %
01-94-PC	13.13	42.75	44.12
02-94-PC	10.31	48.15	41.54
03-94-PC	12.10	25.42	62.48
04-94-PC	26.87	27.30	45.83
05-94-PC	4.81	54.10	41.09
06-94-PC	9.46	21.53	69.01
07-94-PC	21.03	16.30	62.66
01-LR-93	81.12	9.15	9.73
02-LR-93	34.03	15.46	50.51
05-LR-93	87.43	3.55	9.02

Ancient Travertine

Sample #	N2 %	CH4 %	C02 %
01-AM-93	24.66	12.78	62.56
02-AM-93	22.06	7.91	70.03
03-AM-93	15.79	18.23	65.98
04-AM-93	10.23	8.22	83.55
05-AM-93	28.28	34.38	37.36
NMT-01-94	20.78	31.77	47.45
NMT-02-94	25.97	24.86	49.17
NMT-03-94	25.40	20.25	54.35
NMT-04-94	39.85	12.34	47.81
NMT-05-94	31.89	20.58	47.53
NMT-06-94	21.80	27.06	51.14
NMT-07-94	20.32	11.18	68.50

Pedogenic Calcrete

Sample #	N2 %	CH4 %	C02 %
01-94-PC	16.63	41.02	42.35
02-94-PC	10.34	48.13	41.53
03-94-PC	6.83	26.95	66.22
04-94-PC	11.30	33.11	55.59
05-94-PC	7.96	52.31	39.73
06-94-PC	6.87	22.15	70.98
07-94-PC	8.63	18.87	72.51
01-LR-93	65.97	16.49	17.54
02-LR-93	19.16	18.95	61.89
05-LR-93	72.52	7.76	19.73

TABLE B6:
Data for ternary diagrams, from figures 32 to 39 and figure 41, continue

Phreatic Calcrete (Calcite cemented gravels).

Sample #	Ar %	N2 %	C02 %
08-94-PC	43.25	37.81	18.94
09-94-PC	28.78	58.71	12.51
10-PC-94	62.73	31.54	5.73
LC-03-94	19.12	2.80	78.08
LC-04-94	14.81	18.28	66.91
LC-05-94	40.99	27.61	31.40

Phreatic Calcrete (Calcite cemented gravels).

Sample #	Ar %	CH4 %	C02 %
08-94-PC	60.80	12.58	26.62
09-94-PC	47.51	31.84	20.65
10-PC-94	55.97	38.92	5.11
LC-03-94	14.46	26.50	59.04
LC-04-94	11.15	38.44	50.41
LC-05-94	34.11	39.76	26.13

Phreatic Calcrete (Calcite cemented gravel

Sample #	N2 %	CH4 %	C02 %
08-94-PC	57.56	13.62	28.82
09-94-PC	64.87	21.31	13.82
10-PC-94	38.99	53.93	7.08
LC-03-94	2.41	30.23	67.36
LC-04-94	13.42	37.46	49.12
LC-05-94	25.86	44.74	29.40

Phreatic Calcrete (Vein Calcites).

Sample #	Ar %	N2 %	C02 %
UNK-01-93	48.56	36.17	15.26
UNK-02-93	45.17	32.06	22.77
MCA-01-94	57.29	31.21	11.50
MCA-02-94	59.40	22.88	17.72
MCA-03-94	58.20	34.56	9.25
MCA-04-94	52.58	29.32	18.10
Tower-01-94	52.66	38.64	8.70
Tower-02-94	45.49	32.37	22.15
NMBMG-02	68.02	16.85	15.13
NMBMG-04	48.18	33.88	17.93
NMBMG-05	61.32	26.56	12.12
NMBMG-06	53.47	23.27	23.26
TC-01-94	45.20	15.19	39.61

Phreatic Calcrete (Vein Calcites).

Sample #	Ar %	CH4 %	C02 %
UNK-01-93	68.83	12.17	21.01
UNK-02-93	54.68	17.75	27.58
MCA-01-94	72.79	12.60	14.62
MCA-02-94	62.23	19.21	18.56
MCA-03-94	73.04	14.94	12.02
MCA-04-94	54.88	26.23	18.89
Tower-01-94	76.03	11.41	12.56
Tower-02-94	54.69	18.68	26.63
NMBMG-02	68.15	19.14	14.71
NMBMG-04	57.55	21.03	21.42
NMBMG-05	70.54	15.51	13.95
NMBMG-06	60.27	13.51	26.22
TC-01-94	48.16	9.64	42.20

Phreatic Calcrete (Vein Calcites).

Sample #	N2 %	CH4 %	C02 %
UNK-01-93	60.01	14.67	25.32
UNK-02-93	48.14	21.10	32.76
MCA-01-94	59.30	18.84	21.86
MCA-02-94	38.82	31.11	30.07
MCA-03-94	62.50	20.78	16.72
MCA-04-94	40.41	34.65	24.95
Tower-01-94	69.94	14.31	15.75
Tower-02-94	48.20	22.18	31.61
NMBMG-02	32.62	38.10	29.28
NMBMG-04	48.81	25.37	25.83
NMBMG-05	50.92	25.84	23.24
NMBMG-06	39.77	20.45	39.75
TC-01-94	23.79	14.17	62.04

Phreatic Calcrete (Calcite concretions in sand).

Sample #	Ar %	N2 %	C02 %
PM-01-94	47.29	31.16	21.56
PM-02-94	59.82	35.64	4.74

Phreatic Calcrete (Calcite concretions in sand).

Sample #	Ar %	CH4 %	C02 %
PM-01-94	29.68	56.79	13.53
PM-02-94	74.26	19.83	5.91

Phreatic Calcrete (Calcite concretions in s

Sample #	N2 %	CH4 %	C02 %
PM-01-94	21.76	63.19	15.05
PM-02-94	63.30	28.28	8.42

Carbonates from Los Alamos National Laboratory

Sample #	Ar %	N2 %	C02 %
1-AL-93	29.65	42.69	27.66
2-AL-93	39.04	31.34	29.62
3-AL-93	27.03	24.89	48.08
4-AL-93	33.30	45.05	21.66
5-AL-93	21.71	68.28	10.00
6-LA-93	54.18	45.26	0.58
7-LA-93	31.82	34.99	33.19
8-LA-93	24.84	57.25	17.90
9-LA-93	53.75	45.25	1.00
TA63(1-1)	16.35	67.35	16.30
TA63(1-2)	22.96	48.14	28.91
TA63(1-3)	24.31	52.39	23.30
TA63(1-4)	20.47	73.86	5.67
LANL-01-94	44.09	39.09	16.82
LANL-02-94	29.84	54.16	16.00
LANL-03-94	36.80	41.15	22.05
LANL-04-94	38.23	35.18	26.59
LANL-05-94	46.51	38.73	14.76
LANL-06-94	43.93	41.38	14.69
LANL-07-94	46.68	50.12	3.21
LANL-08-94	29.43	52.72	17.86
LANL-09-94	20.41	47.46	32.13
LAH-4-A	20.21	26.04	53.75
LAH-4-B	17.65	26.31	56.04
LAH-4-C	22.89	23.07	54.05
LAL-8898A	16.96	49.58	33.46
LAL-8898B	25.77	39.89	34.34
LAL-8898C	14.22	19.97	65.82
LAL8898-30	62.64	30.86	6.50

Carbonates from Los Alamos National Laboratory

Sample #	Ar %	CH4 %	C02 %
1-AL-93	23.56	54.47	21.97
2-AL-93	13.50	76.25	10.25
3-AL-93	8.51	76.35	15.14
4-AL-93	25.41	58.07	16.52
5-AL-93	8.28	87.90	3.82
6-LA-93	59.83	39.53	0.64
7-LA-93	10.27	79.01	10.72
8-LA-93	19.50	66.46	14.05
9-LA-93	89.30	9.05	1.66
TA63(1-1)	13.43	73.19	13.39
TA63(1-2)	13.08	70.45	16.47
TA63(1-3)	20.81	59.26	19.94
TA63(1-4)	15.51	80.20	4.29
LANL-01-94	20.83	71.23	7.95
LANL-02-94	18.80	71.12	10.08
LANL-03-94	37.51	40.02	22.47
LANL-04-94	35.97	39.02	25.01
LANL-05-94	59.98	20.98	19.04
LANL-06-94	61.21	18.33	20.47
LANL-07-94	26.84	71.53	1.83
LANL-08-94	9.79	84.27	5.94
LANL-09-94	10.29	73.50	16.21
LAH-4-A	9.64	64.72	25.64
LAH-4-B	9.53	60.21	30.26
LAH-4-C	11.61	60.96	27.43
LAL-8898A	5.31	84.22	10.48
LAL-8898B	10.16	76.30	13.54
LAL-8898C	9.56	46.20	44.25
LAL8898-30	49.53	45.33	5.14

Carbonates from Los Alamos National Labo

Sample #	N2 %	CH4 %	C02 %
1-AL-93	30.73	49.36	19.91
2-AL-93	11.14	78.33	10.53
3-AL-93	7.89	76.87	15.24
4-AL-93	31.54	53.29	15.16
5-AL-93	22.12	74.64	3.24
6-LA-93	55.45	43.84	0.71
7-LA-93	11.18	78.21	10.61
8-LA-93	35.82	52.98	11.20
9-LA-93	87.54	10.53	1.93
TA63(1-1)	38.98	51.58	9.43
TA63(1-2)	23.99	61.61	14.41
TA63(1-3)	36.15	47.78	16.08
TA63(1-4)	39.84	57.10	3.06
LANL-01-94	18.91	72.95	8.14
LANL-02-94	29.59	61.67	8.74
LANL-03-94	40.16	38.33	21.52
LANL-04-94	34.08	40.17	25.75
LANL-05-94	55.52	23.32	21.16
LANL-06-94	59.78	19.00	21.22
LANL-07-94	28.05	70.15	1.80
LANL-08-94	16.28	78.21	5.51
LANL-09-94	21.06	64.67	14.26
LAH-4-A	12.08	62.97	24.95
LAH-4-B	13.57	57.52	28.91
LAH-4-C	11.70	60.90	27.40
LAL-8898A	14.08	76.41	9.51
LAL-8898B	14.90	72.28	12.82
LAL-8898C	12.92	44.48	42.60
LAL8898-300	32.59	60.55	6.87

Samples from Brent Newman

Sample #	Ar %	N2 %	C02 %
LAH-4-A	20.21	26.04	53.75
LAH-4-B	17.65	26.31	56.04
LAH-4-C	22.89	23.07	54.05
LAL-8898A	16.96	49.58	33.46
LAL-8898B	25.77	39.89	34.34
LAL-8898C	14.22	19.97	65.82
LAL8898-30	62.64	30.86	6.50

Samples from Brent Newman

Sample #	Ar %	CH4 %	C02 %
LAH-4-A	9.64	64.72	25.64
LAH-4-B	9.53	60.21	30.26
LAH-4-C	11.61	60.96	27.43
LAL-8898A	5.31	84.22	10.48
LAL-8898B	10.16	76.30	13.54
LAL-8898C	9.56	46.20	44.25
LAL8898-30	49.53	45.33	5.14

Samples from Brent Newman

Sample #	N2 %	CH4 %	C02 %
LAH-4-A	12.08	62.97	24.95
LAH-4-B	13.57	57.52	28.91
LAH-4-C	11.70	60.90	27.40
LAL-8898A	14.08	76.41	9.51
LAL-8898B	14.90	72.28	12.82
LAL-8898C	12.92	44.48	42.60
LAL8898-300	32.59	60.55	6.87

Samples from Nevada Test Site

Sample #	Ar %	N2 %	C02 %
LANL-357	48.04	38.54	13.42
GTE-1	43.05	52.30	4.65
WS-5-SSL	34.71	29.64	35.64

Samples from Nevada Test Site

Sample #	Ar %	CH4 %	C02 %
LANL-357	60.13	23.07	16.80
GTE-1	71.38	20.91	7.72
WS-5-SSL	30.53	38.12	31.35

Samples from Nevada Test Site

Sample #	N2 %	CH4 %	C02 %
LANL-357	54.75	26.18	19.06
GTE-1	75.18	18.13	6.69
WS-5-SSL	27.29	39.90	32.81

Carbonates from Reylieh, N.M.

Sample #	Ar %	N2 %	C02 %
ry-01-94	45.09	41.02	13.90
ry-02-94	79.54	18.86	1.60
ry-03-94	74.93	23.40	1.67

Carbonates from Reylieh, N.M.

Sample #	Ar %	CH4 %	C02 %
ry-01-94	66.27	13.31	20.43
ry-02-94	35.85	63.43	0.72
ry-03-94	37.91	61.24	0.84

Carbonates from Reylieh, N.M.

Sample #	N2 %	CH4 %	C02 %
ry-01-94	64.12	14.16	21.72
ry-02-94	11.70	87.30	0.99
ry-03-94	16.01	82.85	1.14

TABLE B6:
Data for ternary diagrams, from figures 32 to 39 and figure 41, continue

Calíches

Sample #	Ar %	CH4 %	CO2 %	N2 %	CH4 %	CO2 %
WB-01-94	25.37	38.83	35.99	13.75	44.65	41.60
WB-02-94	14.96	67.21	17.83	15.97	66.41	17.62
WB-03-94	13.41	63.97	22.62	13.27	64.07	22.66
WB-04-94	6.80	81.68	11.52	10.02	78.86	11.12
WB-05-94	10.49	47.15	42.36	9.04	47.91	43.05
WB-06-94	4.88	77.67	17.46	8.99	74.30	16.70
WB-07-94	8.58	63.37	28.04	9.24	62.92	27.84
WB-08-94	24.79	46.43	28.78	9.79	55.69	34.52
NC-01-94	68.76	26.56	4.68	50.31	42.25	7.44
NC-02-94	63.71	34.92	1.37	45.69	52.26	2.05
NC-03-94	48.05	43.68	8.27	34.07	55.43	10.50
NC-04-94	27.18	70.07	2.75	38.60	59.08	2.32
NC-05-94	52.57	40.45	6.97	41.11	50.23	8.66
NC-06-94	15.96	62.08	21.96	19.50	59.46	21.03
WR-01-94	47.49	47.26	5.25	39.92	54.07	6.01
WR-02-94	10.83	88.33	0.84	5.38	93.73	0.89
WR-03-94	8.30	89.45	2.24	10.99	86.83	2.18
WR-04-94	33.56	64.26	2.18	4.71	92.17	3.13
WR-05-94	2.78	92.69	4.54	6.40	89.23	4.37
WR-06-94	4.21	91.15	4.64	4.43	90.94	4.63
WR-07-94	17.41	80.12	2.47	13.38	84.03	2.59
WR-08-94	57.27	38.08	4.65	57.16	38.18	4.66
WR-09-94	43.45	49.65	6.90	41.04	51.77	7.19
LL-01-94	25.85	50.17	23.98	20.28	53.94	25.78
LC-01-94	30.60	41.79	27.60	11.04	53.58	35.38
LC-02-94	24.02	55.18	20.80	12.11	63.83	24.06
SAE-01-94	27.21	52.94	19.85	26.83	53.21	19.96
SAE-02-94	7.20	87.75	5.04	8.64	86.39	4.97
04-LR-93	4.75	58.59	36.66	2.55	59.94	37.51

Calíches

Sample #	H2O %	CH4 %	CO2 %	H2O %	CH4 %	He %
WB-01-94	1.35	51.07	47.58	1.96	74.33	23.71
WB-02-94	2.14	77.34	20.52	2.11	76.15	21.74
WB-03-94	0.30	73.65	26.05	0.36	87.19	12.46
WB-04-94	0.81	86.93	12.26	0.85	91.03	8.12
WB-05-94	0.40	52.46	47.14	0.68	89.30	10.02
WB-06-94	0.48	81.26	18.27	0.33	56.04	43.63
WB-07-94	2.53	67.57	29.90	3.14	84.00	12.86
WB-08-94	0.82	61.23	37.95	1.13	84.55	14.32
NC-01-94	1.57	83.68	14.74	1.56	83.12	15.32
NC-02-94	2.52	93.80	3.68	2.35	87.37	10.28
NC-03-94	2.61	81.89	15.51	2.65	83.18	14.17
NC-04-94	0.60	95.65	3.76	0.58	92.93	6.49
NC-05-94	0.61	84.78	14.61	0.64	88.51	10.85
NC-06-94	1.34	72.88	25.78	1.56	85.11	13.33
WR-01-94	6.86	83.82	9.32	5.66	69.08	25.26
WR-02-94	1.21	97.86	0.93	1.01	81.47	17.52
WR-03-94	1.50	96.09	2.41	1.26	80.59	18.15
WR-04-94	2.05	94.73	3.22	1.84	85.11	13.05
WR-05-94	1.54	93.86	4.59	1.55	94.40	4.05
WR-06-94	5.12	90.28	4.60	4.91	86.42	8.67
WR-07-94	1.93	95.13	2.94	1.83	89.77	8.41
WR-08-94	4.28	85.30	10.42	4.23	84.23	11.54
WR-09-94	3.50	84.73	11.77	2.97	72.02	25.01
LL-01-94	3.61	65.22	31.17	3.40	61.39	35.21
LC-01-94	2.84	58.52	38.65	3.20	65.95	30.86
LC-02-94	1.99	71.18	26.83	2.10	75.18	22.72
SAE-01-94	1.02	71.99	27.00	1.21	85.61	13.19
SAE-02-94	0.72	93.89	5.40	0.69	89.61	9.70
04-LR-93	1.32	60.70	37.98	1.93	89.04	9.02

Active Travertine

Sample #	Ar %	CH4 %	CO2 %	N2 %	CH4 %	CO2 %
as-01-94	95.28	2.01	2.71	94.61	2.29	3.10
as-02-94	52.83	16.96	30.22	16.63	29.97	53.41
as-03-94	75.71	11.72	12.57	68.43	15.23	16.35
sd-01-94	77.58	5.16	17.26	73.18	6.17	20.65
sd-02-94	62.51	17.98	19.51	43.59	27.05	29.35
lc-01-94	49.25	12.66	38.09	34.71	16.28	49.00
lc-02-94	53.00	17.71	29.29	44.95	20.74	34.31
lc-04-94	84.24	7.40	8.36	80.48	9.16	10.36
sd2-01-94	71.05	11.77	17.18	59.11	16.63	24.27
sd2-02-94	57.32	13.62	29.06	26.16	23.56	50.28
sd2-03-94	69.01	15.39	15.60	58.45	20.63	20.91
sd2-04-94	62.16	5.13	32.71	61.06	5.28	33.66
sd2-05-94	42.06	4.29	53.65	39.18	4.50	56.32
sd2-06-94	30.58	1.51	67.92	27.61	1.58	70.81
mhs-01-94	48.67	23.90	27.43	30.44	32.39	37.17
mhs-02-94	56.65	20.18	23.17	37.94	28.89	33.16
lh-01-94	46.78	20.08	33.14	33.72	25.01	41.27
lh-02-94	49.97	15.02	35.01	31.29	20.63	48.08

Active Travertine

Sample #	H2O %	CH4 %	CO2 %	H2O %	CH4 %	He %
as-01-94	91.54	3.60	4.86	57.37	2.26	40.37
as-02-94	91.17	3.18	5.66	82.91	2.89	14.20
as-03-94	90.85	4.41	4.73	91.70	4.45	3.85
sd-01-94	82.94	3.93	13.13	93.93	4.45	1.63
sd-02-94	95.95	1.94	2.11	93.06	1.88	5.06
lc-01-94	87.88	3.02	9.09	91.36	3.14	5.50
lc-02-94	95.79	1.59	2.63	96.40	1.60	2.00
lc-04-94	98.63	0.64	0.72	97.42	0.63	1.95
sd2-01-94	98.43	0.64	0.93	96.53	0.63	2.84
sd2-02-94	96.34	1.17	2.49	96.15	1.16	2.69
sd2-03-94	99.21	0.39	0.40	97.73	0.39	1.88
sd2-04-94	94.68	0.72	4.60	97.57	0.74	1.68
sd2-05-94	96.01	0.30	3.69	98.36	0.30	1.34
sd2-06-94	93.79	0.14	6.08	95.19	0.14	4.67
mhs-01-94	98.16	0.86	0.98	97.74	0.85	1.41
mhs-02-94	97.95	0.95	1.09	95.48	0.93	3.59
lh-01-94	97.75	0.85	1.40	97.52	0.85	1.63
lh-02-94	92.08	2.38	5.54	93.25	2.41	4.34

Ancient Travertine

Sample #	Ar %	CH4 %	CO2 %	N2 %	CH4 %	CO2 %
01-AM-93	34.14	11.17	54.69	24.66	12.78	62.56
02-AM-93	30.45	7.06	62.49	22.06	7.91	70.03
03-AM-93	20.51	17.21	62.28	15.79	18.23	65.98
04-AM-93	19.25	5.59	75.16	10.23	6.22	83.55
05-AM-93	33.65	31.80	34.55	28.26	34.38	37.36
NMT-01-94	51.95	19.27	28.78	20.78	31.77	47.45
NMT-02-94	42.40	19.34	38.26	25.97	24.86	49.17
NMT-03-94	39.69	16.37	43.94	25.40	20.25	54.35
NMT-04-94	50.48	10.16	39.36	39.85	12.34	47.81
NMT-05-94	49.53	15.25	35.22	31.89	20.58	47.53
NMT-06-94	43.39	19.59	37.02	21.80	27.06	51.14
NMT-07-94	29.46	9.90	60.64	20.32	11.18	68.50

Ancient Travertine

Sample #	H2O %	CH4 %	CO2 %	H2O %	CH4 %	He %
01-AM-93	89.78	1.73	8.48	48.30	0.93	50.77
02-AM-93	83.00	1.73	15.28	59.21	1.23	39.56
03-AM-93	69.90	8.52	23.59	74.67	6.96	18.37
04-AM-93	68.63	2.17	29.20	34.33	1.09	64.58
05-AM-93	68.78	14.96	16.26	50.54	10.99	38.47
NMT-01-94	88.05	4.79	7.16	14.75	0.80	84.44
NMT-02-94	90.31	3.25	6.44	23.36	0.84	75.79
NMT-03-94	86.70	3.61	9.69	19.85	0.83	79.32
NMT-04-94	75.91	4.94	19.15	39.55	2.58	57.87
NMT-05-94	90.04	3.01	6.95	27.71	0.93	71.37
NMT-06-94	87.18	4.44	8.39	15.66	0.80	83.54
NMT-07-94	71.93	3.94	24.13	54.07	2.96	42.97

Pedogenic Calcrete

Sample #	Ar %	CH4 %	CO2 %	N2 %	CH4 %	CO2 %
01-94-PC	13.13	42.75	44.12	16.63	41.02	42.35
02-94-PC	10.31	48.15	41.54	10.34	48.13	41.53
03-94-PC	12.10	25.42	62.48	6.83	26.95	66.22
04-94-PC	26.87	27.30	45.83	11.30	33.11	55.59
05-94-PC	4.81	54.10	41.09	7.96	52.31	39.73
06-94-PC	9.46	21.53	69.01	6.87	22.15	70.98
07-94-PC	21.03	16.30	62.66	8.63	18.87	72.51
01-LR-93	81.12	9.15	9.73	65.97	16.49	17.54
02-LR-93	34.03	15.46	50.51	19.16	18.95	61.89
05-LR-93	87.43	3.55	9.02	72.52	7.76	19.73

Pedogenic Calcrete

Sample #	H2O %	CH4 %	CO2 %	H2O %	CH4 %	He %
01-94-PC	67.17	16.16	16.68	72.64	17.47	9.88
02-94-PC	32.45	36.27	31.29	42.35	47.34	10.31
03-94-PC	69.94	8.69	21.36	84.45	10.50	5.05
04-94-PC	38.90	22.81	38.29	57.43	33.67	8.90
05-94-PC	30.88	39.28	29.83	41.04	52.20	6.76
06-94-PC	13.08	20.67	66.25	24.97	39.45	35.57
07-94-PC	56.84	8.91	34.25	52.41	8.22	39.38
01-LR-93	10.39	43.42	46.20	4.20	17.56	78.24
02-LR-93	0.31	23.36	76.33	0.79	59.78	39.44
05-LR-93	72.22	7.84	19.94	47.61	5.17	47.22

TABLE B6:
Data for ternary diagrams, from figures 32 to 39 and figure 41, continue

Phreatic Calcrete (Calcite cemented gravels).

Sample #	Ar %	CH4 %	C02 %	N2 %	CH4 %	C02 %
08-94-PC	60.80	12.58	26.62	57.56	13.62	28.82
09-94-PC	47.51	31.64	20.85	64.87	21.31	13.82
10-PC-94	55.97	38.92	5.11	38.99	53.93	7.08
LC-03-94	14.46	26.50	59.04	2.41	30.23	67.36
LC-04-94	11.15	38.44	50.41	13.42	37.46	49.12
LC-05-94	34.11	39.76	26.13	25.86	44.74	29.40

Phreatic Calcrete (Vein Calcites).

Sample #	Ar %	CH4 %	C02 %	N2 %	CH4 %	C02 %
UNK-01-93	66.83	12.17	21.01	60.01	14.67	25.32
UNK-02-93	54.68	17.75	27.56	46.14	21.10	32.76
MCA-01-94	72.79	12.60	14.62	59.30	18.84	21.86
MCA-02-94	62.23	19.21	18.56	38.82	31.11	30.07
MCA-03-94	73.04	14.94	12.02	62.50	20.78	16.72
MCA-04-94	54.88	26.23	18.89	40.41	34.65	24.95
Tower-01-94	76.03	11.41	12.56	69.94	14.31	15.75
Tower-02-94	54.69	18.68	26.63	46.20	22.18	31.61
NMBMG-02	66.15	19.14	14.71	32.62	36.10	29.28
NMBMG-04	57.55	21.03	21.42	48.81	25.37	25.83
NMBMG-05	70.54	15.51	13.95	50.92	25.84	23.24
NMBMG-06	60.27	13.51	26.22	39.77	20.48	39.75
TC-01-94	48.16	9.64	42.20	23.79	14.17	62.04

Phreatic Calcrete (Calcite concretions in sand).

Sample #	Ar %	CH4 %	C02 %	N2 %	CH4 %	C02 %
PM-01-94	29.68	56.79	13.53	21.76	63.19	15.05
PM-02-94	74.26	19.83	5.91	83.30	28.28	8.42

Carbonates from Los Alamos National Laboratory

Sample #	Ar %	CH4 %	C02 %	N2 %	CH4 %	C02 %
1-AL-93	23.58	54.47	21.97	30.73	49.36	19.91
2-AL-93	13.50	76.25	10.25	11.14	78.33	10.53
3-AL-93	8.51	76.35	15.14	7.89	76.87	15.24
4-AL-93	25.41	58.07	16.52	31.54	53.29	15.16
5-AL-93	8.28	87.90	3.82	22.12	74.64	3.24
6-LA-93	59.83	39.53	0.64	55.45	43.84	0.71
7-LA-93	10.27	79.01	10.72	11.18	78.21	10.61
8-LA-93	19.50	66.46	14.05	35.82	52.98	11.20
9-LA-93	89.30	9.05	1.66	87.54	10.53	1.93
TA63(1-1)	13.43	73.19	13.39	38.98	51.58	9.43
TA63(1-2)	13.08	70.45	16.47	23.99	61.61	14.41
TA63(1-3)	20.81	59.26	19.94	36.15	47.78	16.08
TA63(1-4)	15.51	80.20	4.29	39.84	57.10	3.06
LANL-01-94	20.83	71.23	7.95	18.91	72.95	8.14
LANL-02-94	18.80	71.12	10.08	29.59	61.67	8.74
LANL-03-94	37.51	40.02	22.47	40.16	38.33	21.52
LANL-04-94	35.97	39.02	25.01	34.08	40.17	25.75
LANL-05-94	59.98	20.98	19.04	55.52	23.32	21.16
LANL-06-94	61.21	18.33	20.47	59.78	19.00	21.22
LANL-07-94	26.64	71.53	1.83	28.05	70.15	1.80
LANL-08-94	9.79	84.27	5.94	16.28	78.21	5.51
LANL-09-94	10.29	73.50	16.21	21.06	64.67	14.26

Samples from Brent Newman

Sample #	Ar %	CH4 %	C02 %	N2 %	CH4 %	C02 %
LAH-4-A	9.64	64.72	25.64	12.08	62.97	24.95
LAH-4-B	9.53	60.21	30.26	13.57	57.52	28.91
LAH-4-C	11.61	60.96	27.43	11.70	60.90	27.40
LAL-8898A	5.31	84.22	10.48	14.08	76.41	9.51
LAL-8898B	10.16	76.30	13.54	14.90	72.28	12.82
LAL-8898C	9.56	46.20	44.25	12.92	44.48	42.60
LAL8898-30	49.53	45.33	5.14	32.59	60.55	6.87

Samples from Nevada Test Site

Sample #	Ar %	CH4 %	C02 %	N2 %	CH4 %	C02 %
LANL-357	60.13	23.07	16.80	54.75	26.18	19.06
GTE-1	71.38	20.91	7.72	75.18	18.13	6.69
WS-5-SSL	30.53	38.12	31.35	27.29	39.90	32.81

Carbonates from Reylieh, N.M.

Sample #	Ar %	CH4 %	C02 %	N2 %	CH4 %	C02 %
ry-01-94	66.27	13.31	20.43	64.12	14.16	21.72
ry-02-94	35.85	63.43	0.72	11.70	87.30	0.99
ry-03-94	37.91	61.24	0.84	16.01	82.85	1.14

Phreatic Calcrete (Calcite cemented gravels).

Sample #	H2O %	CH4 %	CO2 %	H2O %	CH4 %	He %
08-94-PC	64.24	11.48	24.28	57.58	10.29	32.13
09-94-PC	62.75	22.60	14.66	60.28	21.71	18.01
10-PC-94	0.89	87.60	11.51	0.89	87.07	12.04
LC-03-94	65.32	10.74	23.93	55.58	9.14	35.28
LC-04-94	50.81	21.28	27.91	53.04	22.21	24.75
LC-05-94	94.43	3.36	2.21	44.40	1.58	54.01

Phreatic Calcrete (Vein Calcites).

Sample #	H2O %	CH4 %	CO2 %	H2O %	CH4 %	He %
UNK-01-93	93.91	2.24	3.86	38.53	0.92	60.55
UNK-02-93	95.22	1.87	2.91	62.54	1.23	36.23
MCA-01-94	95.26	2.19	2.55	42.19	0.97	56.84
MCA-02-94	95.81	2.13	2.06	36.71	0.82	62.48
MCA-03-94	93.13	3.81	3.06	27.24	1.11	71.65
MCA-04-94	93.35	3.87	2.78	22.45	0.93	76.62
Tower-01-94	95.48	2.15	2.37	54.20	1.22	44.58
Tower-02-94	92.28	3.18	4.54	35.43	1.22	63.35
NMBMG-02	91.79	4.64	3.57	16.96	0.86	82.17
NMBMG-04	93.54	3.20	3.26	27.61	0.94	71.45
NMBMG-05	91.45	4.50	4.05	15.08	0.74	84.18
NMBMG-06	88.36	3.96	7.68	16.94	0.76	82.30
TC-01-94	85.48	2.70	11.82	24.08	0.76	75.16

Phreatic Calcrete (Calcite concretions in sand).

Sample #	H2O %	CH4 %	CO2 %	H2O %	CH4 %	He %
PM-01-94	1.87	79.25	18.88	1.93	82.16	15.91
PM-02-94	3.91	74.04	22.05	4.43	83.84	11.73

Carbonates from Los Alamos National Laboratory

Sample #	H2O %	CH4 %	CO2 %	H2O %	CH4 %	He %
1-AL-93	0.88	70.64	28.49	1.00	80.48	18.52
2-AL-93	0.92	87.34	11.74	0.73	68.63	30.65
3-AL-93	2.52	81.35	16.13	1.64	53.13	45.22
4-AL-93	2.60	75.82	21.58	2.93	85.24	11.84
5-AL-93	1.88	94.06	4.08	1.72	87.08	11.20
6-LA-93	0.85	97.56	1.58	0.84	95.89	3.27
7-LA-93	0.17	87.91	11.92	0.18	92.52	7.30
8-LA-93	2.86	80.19	16.95	2.83	79.37	17.80
9-LA-93	3.56	81.51	14.92	3.55	81.17	15.28
TA63(1-1)	0.96	83.73	15.31	0.89	78.07	21.03
TA63(1-2)	7.67	74.83	17.50	8.63	84.19	7.18
TA63(1-3)	5.36	70.82	23.83	6.14	81.14	12.72
TA63(1-4)	2.48	92.56	4.96	2.28	85.03	12.69
LANL-01-94	0.63	89.40	9.98	0.63	90.40	8.96
LANL-02-94	1.00	86.71	12.29	0.86	74.59	24.55
LANL-03-94	0.51	63.72	35.78	0.63	78.76	20.61
LANL-04-94	1.14	60.24	38.62	0.84	44.47	54.68
LANL-05-94	0.62	52.11	47.27	0.87	73.36	25.77
LANL-06-94	0.56	46.98	52.46	0.80	67.85	31.34
LANL-07-94	1.04	96.49	2.47	0.86	80.21	18.92
LANL-08-94	1.49	92.03	6.49	1.33	82.35	16.32
LANL-09-94	0.51	81.52	17.97	0.56	89.69	9.75

Samples from Brent Newman

Sample #	H2O %	CH4 %	CO2 %	H2O %	CH4 %	He %
LAH-4-A	0.65	71.16	28.19	0.70	76.55	22.76
LAH-4-B	2.13	65.14	32.74	2.53	77.62	19.85
LAH-4-C	1.40	68.00	30.59	1.60	77.49	20.92
LAL-8898A	2.55	86.66	10.78	2.59	87.92	9.49
LAL-8898B	1.75	83.45	14.80	1.85	88.30	9.85
LAL-8898C	1.47	50.33	48.20	2.11	72.00	25.89
LAL8898-30	5.14	85.20	9.67	3.76	62.40	33.84

Samples from Nevada Test Site

Sample #	H2O %	CH4 %	CO2 %	H2O %	CH4 %	He %
LANL-357	2.23	56.58	41.19	3.12	79.23	17.65
GTE-1	9.81	65.88	24.31	10.48	70.39	19.14
WS-5-SSL	1.85	53.85	44.29	2.83	82.25	14.92

Carbonates from Reylieh, N.M.

Sample #	H2O %	CH4 %	CO2 %	H2O %	CH4 %	He %
ry-01-94	98.45	0.61	0.94	99.30	0.62	0.08
ry-02-94	98.67	1.31	0.01	98.26	1.31	0.44
ry-03-94	98.78	1.21	0.02	98.36	1.20	0.44

This thesis is accepted on behalf of the faculty of the Institute by the following committee:

David R. Nemon
Adviser

Thomas L. Kilfoy

John W. Hawley

J. B. J. Harrison

May 8, 1995
Date